E&G

Eiszeitalter und Gegenwart
Quaternary Science Journal

planetearth®
Earth Sciences for Society

GEOZON

DEUQUA

Vol. 58
No 2
2009

CHANGING ENVIRONMENTS –
YESTERDAY, TODAY, TOMORROW

PROCEEDINGS OF THE DEUQUA 2008 IN VIENNA

GUEST EDITORS

Markus Fiebig, Christine Neugebauer-Maresch,
Martina Pacher, Jürgen Reitner and Verena Winiwarter

planetearth®
Earth Sciences for Society

GEOZON

E&G

Eiszeitalter und Gegenwart
Quaternary Science Journal

Preface

Special issue: Changing environments – Yesterday, Today, Tomorrow

This volume of the Quaternary Science Journal (Eiszeitalter & Gegenwart) contains five scientific articles, which were presented during the meeting of the German Quaternary Association (DEUQUA) in Vienna from the 31. of August to the 6. of September 2008.

Already during the meeting in Vienna a broad spectrum of regional and thematic contributions was displayed. And also the presented articles in this volume range regionally from the Baltic sea, over Northern Germany, Lower Austria up to Serbia and from marine Holocene sequences to Pleistocene cover sediments and continental loess.

We would like to thank the 25 authors and co-authors and the 12 reviewers for their valuable contributions to this volume!

Finally we would like to appreciate the special engagement of our graphic designer, Mrs. Helene Pfalz-Schwingenschlögl, and our native speaker Dr. Johanna Lomax at the Institut of Applied Geology at the University of Natural Resources and Applied Life Sciences Vienna. Without their support all the necessary changes would not have been possible. Thank's a lot!

Markus Fiebig
(for the organisation committee including Christine Neugebauer-Maresch, Martina Pacher, Jürgen Reitner und Verena Winiwarter; Vienna, Austria)

Vorwort

Sonderband: Veränderter Lebensraum – Gestern, Heute und Morgen

Dieser Band des Quaternary Science Journal (Eiszeitalter und Gegenwart) umfasst fünf wissenschaftliche Artikel, die bei der Hauptversammlung der Deutschen Quartärvereinigung e.V. (DEUQUA) in Wien vom 31. August bis 6. September 2008 erstmalig präsentiert wurden.

Schon während der Tagung zeigte sich ein sehr breites Spektrum an regionalen und thematischen Beiträgen. Und auch die hier vorgelegten Artikel reichen regional von der Ostsee über Norddeutschland und Niederösterreich bis nach Serbien und von marinen Sedimenten aus dem Holozän über eiszeitliche Deckschichten bis hin zu kontinentalem Löss.

Wir möchten den insgesamt 25 AutorInnen und Co-AutorInnen der Artikel sowie 12 ReviewerInnen sehr herzlich für Ihren wertvollen Beitrag zu diesem Band danken!

Schließlich sei erwähnt, dass ohne das besondere Engagement unserer Zeichnerin, Frau Helene Pfalz-Schwingenschlögl, und unserer Englisch-Muttersprachlerin Dr. Johanna Lomax am Institut für Angewandte Geologie der Universität für Bodenkultur Wien, die durchgeführten Verbesserungen an den Beiträgen nicht machbar gewesen wären. Vielen herzlichen Dank!

Markus Fiebig
(für das Organisationsteam bestehend aus Christine Neugebauer-Maresch, Martina Pacher, Jürgen Reitner und Verena Winiwarter; Wien, Österreich)
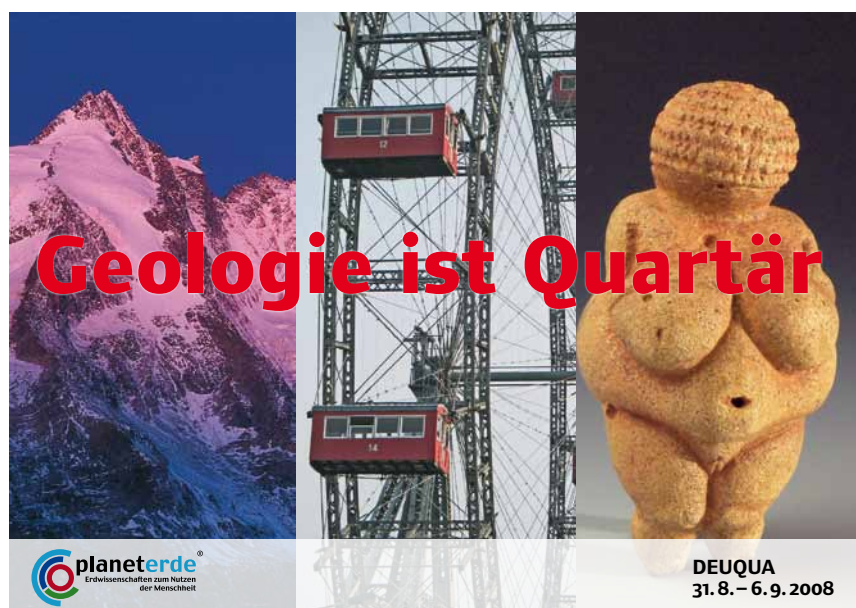
Invitation card of DEUQUA Conference 2008 in Vienna

Einladungs-Karte der DEUQUA-Tagung 2008 in Wien

Archäometrische Analysen von Lengyelkeramik aus Niederösterreich

Ângela Carneiro

Kurzfassung: Dieser Beitrag präsentiert die ersten Ergebnisse zur Untersuchung von Herstellungsprozessen (Rohstoffauswahl, Aufarbeitung und Herkunft sowie Maltechniken) von Keramik der Lengyelkultur aus der Siedlung von Michelstetten, die im Zentralweinviertel des norddanubischen Niederösterreich liegt und nach der Radiokarbon-Methode zwischen 4600 und 4360 a cal. BC datiert wurde. Unter Anwendung verschiedener archäometrischer Verfahren konnte die mineralogische Zusammensetzung von Lengyelkeramik und ihre Malpigmente sowie von Ton- und Lehmmaterialien, die als Rohstoffproben gedient haben, bestimmt werden. Neben einer genauen Charakterisierung der Herstellungssubstanzen prähistorischer Keramik von Michelstetten wurden unterschiedliche Erzeugungsvorgänge, wie Rohstoffauswahl, Art und Qualität der Materialaufbereitung, Brennverfahren und Maltechniken behandelt, genauso wie Herkunftsfragen diskutiert.

[Archaeometrical analysis of Lengyel pottery from Lower Austria]

Abstract: This study is about methods used in the production of prehistoric ceramic (origin and selection of raw materials, treatment of fabrics and painting techniques) based on several analysis of ceramic pottery from the site of Michelstetten in the North of Lower Austria dated between 4600–4360 a cal. BC. Using different archaeometrical methods it was possible to know the mineralogical composition of Lengyel pottery, her painting pigments and of the raw material collected near the site. Besides a specific characterisation of the clay materials used in the production of prehistoric pottery from Michelstetten, a number of pottery techniques like selection of raw material, type and quality of fabrics, firing methods and painting techniques will be explained and discussed here as well as questions about the origin of the raw materials.

Keywords: *production of neolithic ceramic, Lengyel Culture, Lower Austria*

Adress of author: A. **Carneiro**, Fundação para a Ciência e a Tecnologia, Portugal. E-Mail: Angela.Carneiro07@gmail.com

1 Einleitung

Um Auswahl, Art der Aufarbeitung und Herkunft verwendeter Rohstoffe sowie angewendete Brennverfahren und Maltechniken an Lengyelkeramik der Siedlung von Michelstetten (Niederösterreich, 4600–4360 a cal. BC) näher zu kennen, wurden zuerst verschiedene archäologische Untersuchungen an ca. 6.000 Gefäßeinheiten durchgeführt. Danach wurden aus einer gezielten Keramikauswahl 37 Keramikproben aus Michelstetten und 22 Ton- und Lehmmaterialien als Rohstoffproben aus der Umgebung der Siedlung von Michelstetten, unter Anwendung von petrographischen und Schwermineralanalysen zur mineralogischen Bestimmung und zu Herkunftsfragen prähistorischer Keramik und Tonrohstoffen untersucht. Schließlich wurden Röntgendiffraktometrie und Polarisationsmikroskopie zum Erkennen der chemischen Zusammensetzung der Malpigmente an 16 weiteren Lengyelkeramikproben aus Michelstetten angewendet.

Die naturwissenschaftlichen Analysen wurden am Institut für Konservierungswissenschaften und Restaurierung der Universität für angewandte Kunst Wien mit finanzieller Unterstützung der Hochschuljubiläumsstiftung der Stadt Wien durchgeführt.

Lengyelkeramik wird nach dem Eponym-Fundort *Lengyel* in Südwestungarn genannt, der am Ende des 19. Jahrhunderts von M. Wosinsky (1888) entdeckt und ausgegraben wurde. Fundstellen mit derartiger Keramik sind, vor allem im heutigen Südmähren, Westslowakei, Westungarn und Niederösterreich, häufig. Nach der ¹⁴C-Methode wird sie heute zwischen 4800 und 4200 a cal. BC datiert. Die Lengyelkeramik von Michelstetten weist nicht nur anhand ihrer Eigenschaften, sondern auch aufgrund ihrer absoluten Datierung, jüngere Züge auf. Charakteristisch für die Lengyelkeramik ist die auf die Gefäßoberflächen nach dem Brennen aufgetragene Bemalung, auch Kaltbemalung genannt. Die am häufigsten verwendeten Farben sind rot, weiß und gelb, die monochrom oder polychrom, oft kombiniert mit Knubben und/oder Ritzverzierungen, auf die äußeren und inneren Keramikoberflächen aufgetragen wurden. Darüber hinaus macht das häufig feine Aussehen ihrer keramischen Masse und unverwechselbaren Formen, das Interesse an ihrer Erforschung, insbesondere in der Kernregion, seit Ende des 19. Jahrhunderts, aus. Dennoch sind Untersuchungen zu den Herstellungstechniken von Lengyelkeramik mit Hilfe naturwissenschaftlicher Verfahren bis heute doch selten geblieben. Der jetzige Beitrag stellt selbst die ersten Ergebnisse derartiger Analysen, durchgeführt an Lengyelkeramik der Siedlung von Michelstetten, dar.

2 Geografie und Geologie der Fundstelle

In der Abbildung 1 ist der Raum um Michelstetten dargestellt. Geologisch gehört er zur Waschbergzone, die sich nördlich von Stockerau bis nördlich von Drasenhofen in SW-NO Richtung ausdehnt und das westliche vom östlichen Weinviertel trennt. In der leicht welligen Landschaft ragen
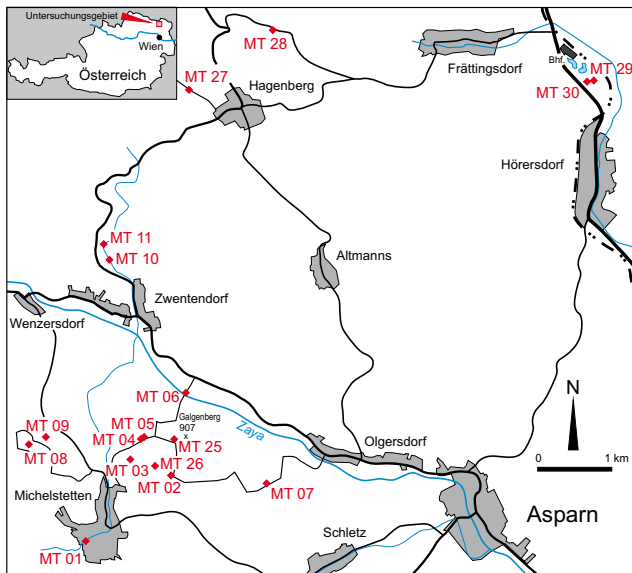
Abb. 1: Lage der prähistorischen Fundstelle von Michelstetten (roter Punkt) und der Umgebung mit Kennzeichnung der Stellen, in denen die Rohstoffproben entnommen wurden. Ausschnitt, umgezeichnet aus der Österreichischen Karte, Blatt 24 (Mistelbach), Maßstab 1: 50 000. (© BEV 2009, T2009/56720)

Fig. 1: Location (red dot) of the prehistorical find spot of Michelstetten and the surroundings with the places, where raw material samples were extracted (detailed map based on the Austrian Map, sheet 24 (Mistelbach), scale 1: 50 000. (© BEV 2009, T2009/56720)

diese Kalkberge hervor, die daher als Klippenzone bezeichnet werden. Sie wurden während der tertiären Bildung der Waschbergzone vom Untergrund abgetrennt und hochgeschürft. Die Leiser Berge, wo die prähistorische Fundstelle von Michelstetten an ihrem nördlichsten Ausläufer liegt, sind eine dieser Erhebungen. Wie Grill (1968: 29–30) erfasst hat, besteht die Waschbergzone aus Jura- und Kreideablagerungen des Mesozoikums, die sandige Sedimente, Tonmergel, Tegel und lokal verbreitete Schotter, Konglomerate und Kalke in abwechselnder Abfolge enthalten. Ein reiches Spektrum maritimer Mikro- und Makrofossilien lässt ihren marinen Ursprung erkennen. Die Klentnitzer Schichten, welche großteils die Leiser Berge bilden, schließen eine vielfältige fossile Meeresfauna, wie Muscheln, Ammoniten, Belemniten und Foraminiferen ein (Thenius 1983: 42). Ebenfalls mariner Herkunft sind die weichen Sedimente der Michelstettener Formation, die dem oberen Oligozän und dem unteren Miozän zuzuordnen sind und auch viele Mikrofossilien enthalten (Wessely 2006: 75). Meeresmikrofossilien finden sich zum Teil in der behandelten Lengyelkeramik wieder.

3 Ausgangssituation der archäometrischen Untersuchungen

Die Auswahl der archäometrisch untersuchten Keramikproben ergab sich aus der Auswahl von 2–3 Gefäßfragmenten jeweils aus einer der 15 Materialtypen, die aus der vorher vorgenommenen archäologischen Bestimmung des Keramikfabrikats mit Hilfe einer Lupe bei 8-facher Vergrößerung resultieren. Als Kriterien für die archäologische Beschreibung der Materialgruppen wurden Art und Aussehen, sowie die Qualität der Bearbeitung der plastischen Masse, das Verhältnis zwischen Menge und Größe der mineralischen Einschlüs-

se, sowie ihre Verteilung, ihre Form und die Eigenschaft, die die einzelnen Materialgruppen am stärksten kennzeichnet, berücksichtigt (Carneiro 2002: 23–27).

Die Vielfalt der Korngröße der Tongruppen und ihre differenzierte Quantität führte zur Berücksichtigung aller vorhandenen Einschlussgrößen mit ihren Häufigkeiten, anstatt die häufigste Größe der Gesteine, wie es in der Archäologie üblich ist, aufzunehmen. Beispielsweise besitzt die Materialgruppe 1 pro cm² gleichzeitig über 20 Partikel, die kleiner als 0,1 mm sind, 10 bis 20 Partikel, die von 0,1 bis 0,5 mm groß sind und weniger als 5 Einschlüsse, die zwischen 0,5 und 1,0 mm groß sind.

Weiters hat sich während der Aufnahme der Materialgruppen bald erwiesen, dass eine Bestimmung der Partikel unnötig war, weil erstens die erkennbaren Einschlüsse – Quarz, Quarzit, Feldspat und Glimmer – in allen Tongruppen vorhanden sind und zweitens die Inklusionen, die Rückschlüsse auf die Tonzusammensetzung zulassen, genauer mittels Dünnschliffanalysen erfassbar sind. Deswegen wurden sie nicht ausführlich beschrieben, aber vermerkt, wenn sie in besonderen Verhältnissen zu bestimmten Materialgruppen standen.

Die Merkmale der Materialgruppen werden ausführlich in der Tabelle 1 dargestellt.

Hier wird nur kurz auf sie eingegangen. Die Grundmasse zur Keramikherstellung fast aller Materialgruppen hat ein feines lehmiges Aussehen, auch wenn sie mit vielen und großen Einschlüssen durchsetzt ist. Die 15 Materialtypen unterscheiden sich voneinander am deutlichsten durch die Größe und die Menge ihrer Partikeln. Mit der Ausnahme der Materialgruppen 1, 4 und 5 fallen alle anderen in den Bereich der grobkörnigen Materialgruppen, wobei einige weniger grob (2, 3, 6, 8, 11, 12, 13) als andere (7, 9, 10, 14, 15) sind. Außerdem besitzen einige Materialgruppen entweder mehr Glimmer (4, 11) oder Sand (7, 10, 14, 15) als die übrigen. Eine andere verbreitete Eigenschaft, die in allen Tongruppen beobachtet wurde, ist das Vorhandensein von Einschlüssen wie Kalk, Eisenoxyden, Meeresmikrofossilien und Tonbällchen. Manchmal treten mehrere Arten dieser Partikeln in einem Gefäß auf.

4 Ergebnisse der archäometrischen Analysen

4.1 Die Keramikproben

Die Keramikproben der naturwissenschaftlichen Analysen wurden als Mi01/01 bis Mi37/01 nummeriert und werden im Textteil als Mi01, 2, 3 … simplifiziert erwähnt.

Nach den petrographischen und schwermineralischen Untersuchungen wurden die prähistorischen Keramikproben aufgrund der Unterschiede in der texturellen und mineralogischen Zusammensetzung in 20 unterschiedliche Keramiktypen von A bis T und im Brenngrad in 5 Varianten (Bh, C1, D1, Eh, F1) eingeteilt (Abb. 2–4).

Die Korrelation der Gruppierung A–T mit der Nummerierung der Keramikproben ist, wie folgt: A: Mi01, Mi30; B: Mi02, Mi03, Mi15; Bh: Mi06; C: Mi34; C1: Mi05; D: Mi19, Mi33; D1: Mi18; E: Mi26, Mi29; Eh: Mi07, Mi14; F: Mi10, Mi21, Mi23–Mi25, Mi35; F1: Mi11; G: Mi17, Mi22; H: Mi20; I: Mi36; J: Mi04; K: Mi16; L: Mi28; M: Mi31; N: Mi37; O: Mi32; P: Mi27; Q: Mi12; R: Mi09; S: Mi13; T: Mi08.

Material-gruppen	Art / Aussehen der plastischen Elemente der keramischen Masse	Bearbeitung der plastischen Elemente der keramischen Masse	Größe (mm) und Menge (pro cm^2) der Einschlüsse	Verteilung der Einschlüsse	Form der Einschlüsse	Besondere Merkmale
1	lehmartig, sehr fein, dicht, homogen, wie geschlämmt	gut	<0,1 zu >20 0,1-0,5 zu 10-20 0,5-1,0 zu <5	gleichmäßig	gerundet und kantig	
2	lehmartig, fein, etwas locker, homogen	gut	<0,1 zu 10-20 0,1-1,0 zu 5-10 1,0-2,0 zu <5	ungleichmäßig	gerundet und kantig	
3	lehmartig, fein, etwas locker, homogen	± gut	<0,1 zu 10-20 0,1-1,0 zu >20 1,0-2,0 zu 5-10 >2,0 zu <5	± gleichmäßig	gerundet und kantig	
4	lehmartig, sehr fein, dicht, homogen, wie geschlämmt	sehr gut	<0,1-0,5 zu >20	gleichmäßig	gerundet und kantig	viel und klein, Glimmer
5	lehmartig, sehr fein, dicht, homogen, wie geschlämmt	gut	<0,1 zu 10-20 0,1-0,5 zu 5-10	gleichmäßig	gerundet	
6	lehmartig, fein, sehr dicht, homogen	gut	<0,1 zu >20 0,1-0,5 zu 10-20 0,5-1,0 zu <5	gleichmäßig	gerundet und kantig	
7	lehmartig, grob, etwas locker, homogen	gut	<0,1-1,0 zu >20	gleichmäßig	gerundet und kantig	viel Sand
8	lehmartig, fein, etwas locker, homogen	± gut	<0,1 zu >20 0,1-1,0 zu 5-10 1,0-2,0 zu <5	ungleichmäßig	gerundet und kantig	etwas pflanzliches Material
9	lehmartig, fein, etwas locker, homogen	± gut	<0,1-2,0 zu >20 2,0->3,0 zu 5-10	± gleichmäßig	gerundet	
10	lehmartig, fein, etwas locker, homogen	gut	<0,1-1,0 zu >20 1,0-2,0 zu <5	gleichmäßig	gerundet und kantig	sehr viel Sand
11	sandartig, sehr fein, dicht, homogen	± gut	<0,1 zu >20 0,5-1,0 zu 5-10 1,0-2,0 zu <5	± gleichmäßig	gerundet und kantig	viel klein und groß, Glimmer
12	lehmartig, fein, etwas locker, homogen	schlecht	<0,1 zu >20 0,5-2,0 zu 5-10	ungleichmäßig	gerundet und kantig	einige Eisenoxide und viele Tonbällchen
13	lehmartig, sehr fein, dicht, homogen, wie geschlämmt	± gut	0,1-0,5 zu >20 0,5-2,0 zu 5-10	ungleichmäßig	gerundet	etwas pflanzliches Material
14	lehmartig, sehr fein, dicht, homogen	gut	<0,1-1,0 zu >20 1,0-2,0 zu <5	sehr gleichmäßig	gerundet und kantig	sehr viel Sand
15	lehmartig, fein, etwas locker, homogen	± gut	<0,1-2,0 zu >20 2,0-3,0 zu 5-10	± gleichmäßig	gerundet und kantig	

Die Grundmasse fast aller Keramiktypen hat ein feines Aussehen (besonders Mi08, 17, 22, 27, 36, 37), wobei einige glimmerig (Mi01, 9, 11−13, 20, 28, 30−32, 37), andere kalkhaltig (Mi04, 7, 10, 11, 14, 18−26, 29, 33, 36, 37) oder kalkarm (Mi02, 3, 6, 15, 16, 28, 31) bis kalkfrei (Mi08, 9, 12, 13, 27, 32), andere noch karbonhaltig (Mi01, 30) sind.

Der durchschnittliche Anteil an nicht-plastischen Elementen ist unterschiedlich und kann in drei Kategorien gruppiert werden: zwischen 16−19 % (Mi05, 7, 14, 17, 22, 26, 29, 34), zwischen 26−33 % (Mi04, 10−13, 18−21, 23−25, 28, 31−33) und zwischen 36−46 % (Mi01-3, 6, 8, 9, 15, 16, 27, 30, 36, 37). Die mittlere Größe der nicht-plastischen Elemente, in natürlicher

Form in den Rohstoffen vorhanden, ist recht variabel und kann als etwas feiner, zwischen 0,03−0,05 mm (Mi02, 3, 6, 15, 16, 18−20, 27, 33, 36), weniger fein, zwischen 0,06−0,09 mm (Mi01, 4, 5, 7, 14, 17, 22, 26, 28, 29, 30, 34), grob, zwischen 0,10−0,17 mm (Mi08, 10, 11, 13, 21, 23−25, 31, 37) und sehr grob, zwischen 0,20−0,30 mm (Mi09, 12, 32) angesprochen werden. Sie bestehen hauptsächlich aus monokristallinen Quarzen und/oder Muskovit in unterschiedlicher Menge, manchmal untergeordnet auch noch aus Karbonaten (Mi01, 30), Alkalifeldspaten (Mi016) und oxidiertem Glaukonit (Mi04).

Die Keramik einiger Proben hat neben den nicht-plastischen Elementen, die in der Grundmasse natürlich vorkom-

men können, auch noch gröbere Partikel, die andere mineralogische Zusammensetzung und schlechteren Abrundungsgrad aufweisen. Der mittlere Wert ihrer Korngröße verteilt sich in einer Skala von 0,7–2,4 mm (Mi01, 30), 0,8–3,16 mm (Mi02, 3, 6, 15), 0,83–2,36 mm (Mi16), 0,8–3,68 mm (Mi18, 19, 33), über 1–2,12 mm: (Mi27) bis 1,36–4,4 mm (Mi20). Dieser Teil der Keramik scheint künstlich, meist durch den Zusatz von grobem Sand (poly- und monokristallinen Quarzen), gemagert worden zu sein.

Anderer Teil der Keramik wurde noch mit Ton/Siltsteinklastern bzw. „Schamottbröckchen" (Mi04, 10–12, 18, 19, 21, 23–25, 33) und/oder Pflanzenfasern (Mi01, 7, 10, 11, 14, 18, 19, 21, 23–26, 29, 30, 33) gemagert.

Das Vorhandensein von echtem Schamott scheint sich durch die teilweise sehr eckigen und scharfkantigen, siltigen Bröckchen auszuzeichnen, die gebrannter Keramik gleichen. Solch scharfkantige Brüche sind normalerweise bei Alttonbröckchen (eingetrocknete und wieder zugesetzte Tonbröckchen oder natürliche verfestigte Tonsteinklaster) nicht zu erwarten. Etwa 25 % des Magerungsanteils der Keramikproben F (Mi10, 21, 23–25, 35) besteht aus solchen Partikeln, die bis 4,2 mm lang sein können. Bei Keramikprobe Mi11 ist ihr Anteil wesentlich reduziert (6 %), dennoch signifikant.

Die organischen Magerungsmaterialien bestanden ursprünglich (v. a. bei Keramikproben Mi07, 14, 26, 29) aus länglichen, feinen Pflanzenfasern, die im Dünnschliff eine

bis zu 3,5 mm Länge erreichen konnten und jetzt als Pseudomorphosen in Form länglicher schmaler Poren vorliegen.

Die Sortierung der Körner ist in der Regel bimodal (Mi01–07, 14–20, 22, 26–30, 33, 34, 36), wobei manche Keramikrohstoffe teilweise ziemlich inhomogen (schlecht aufbereitet) zu sein scheinen (Mi08–13, 21, 23–25, 31, 32, 35, 37). Solche Proben lassen sich nicht nur durch eine größere Probenserie voneinander eindeutig abgrenzen, sondern deuten ebenfalls auf wenig Sorgfalt in der Aufarbeitung der Keramikrohstoffe hin. Ein weiterer Nachweis schlechter Tonaufarbeitung können die nicht resorbierten, eingestreuten Tonbröckchen mancher Proben darstellen, die häufig eine hellere oder dunklere Farbe als die der Grundmasse zeigen (Mi01, 10, 11, 20, 21, 23–25, 30).

Die Matrix der Proben ist großteils kalkhaltig (siehe oben) bzw. sind Kalkeinschlüsse teilweise mit bloßem Auge noch sichtbar. Das Vorhandensein dieses Calciumkarbonats deutet auf Brenntemperaturen der Keramik unter 800° C hin, da sich ab solchen Brenntemperaturen die Calciumkarbonate zersetzen und daher nicht mehr direkt bestimmbar sind. Darüber hinaus berichtet HENNICKE (1989: 17), dass unabhängig von der Ofenart, Keramik mit Brandtemperaturen ab 600°C erhaltbar und witterungsbeständig ist. Infolgedessen konnte die Keramik von Michelstetten bei 600 und unter 800° C gebrannt worden sein.
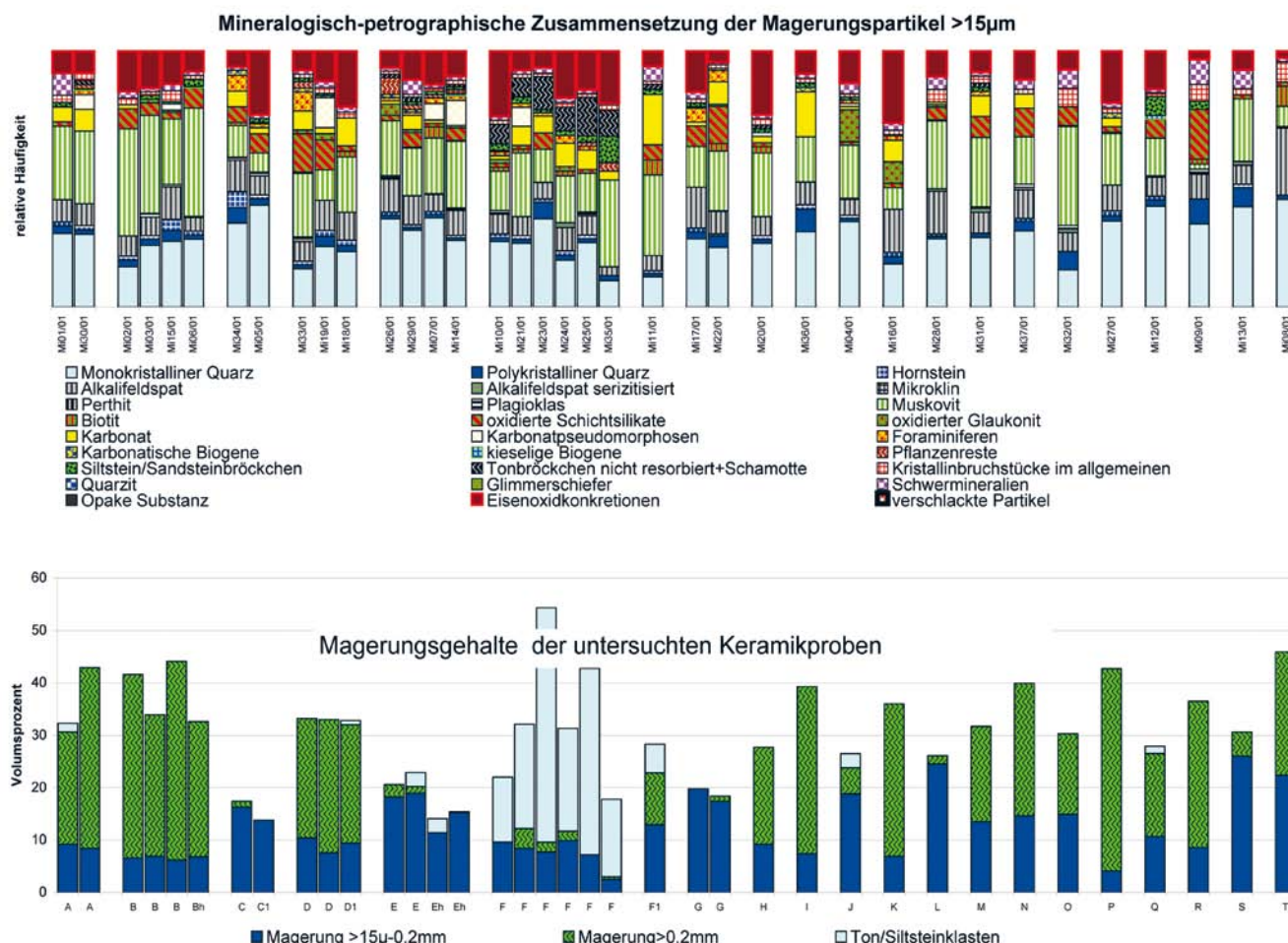

Abb. 2: Mineralogisch-petrographische Zusammensetzung der Magerungspartikel der Keramikproben (>15 µm).

Fig. 2: Mineralogic-petrographic composition of temper particles of the ceramic samples (>15 µm).

Zusammensetzung der groben Magerungspartikel (> 0.2 mm) in den Keramikproben (ohne Schamottepartikel)

Legend:
- □ Monokristalliner Quarz
- ■ Polykristalliner Quarz
- ▨ Hornstein
- ▨ Feldspäte
- ▦ Kristallinbruchstücke
- ■ Bioklasten
- ■ Kalkstein
- ▨ Sandstein/Siltstein
- ■ Tonklasten
- ▨ Glimmer
- ■ Glaukonit oxidiert
- ▨ Schwermineralien
- ▥ Plagioklas
- ▦ Quarzit
- ■ Glimmerschiefer
- ■ Eisenoxydkonkretionen
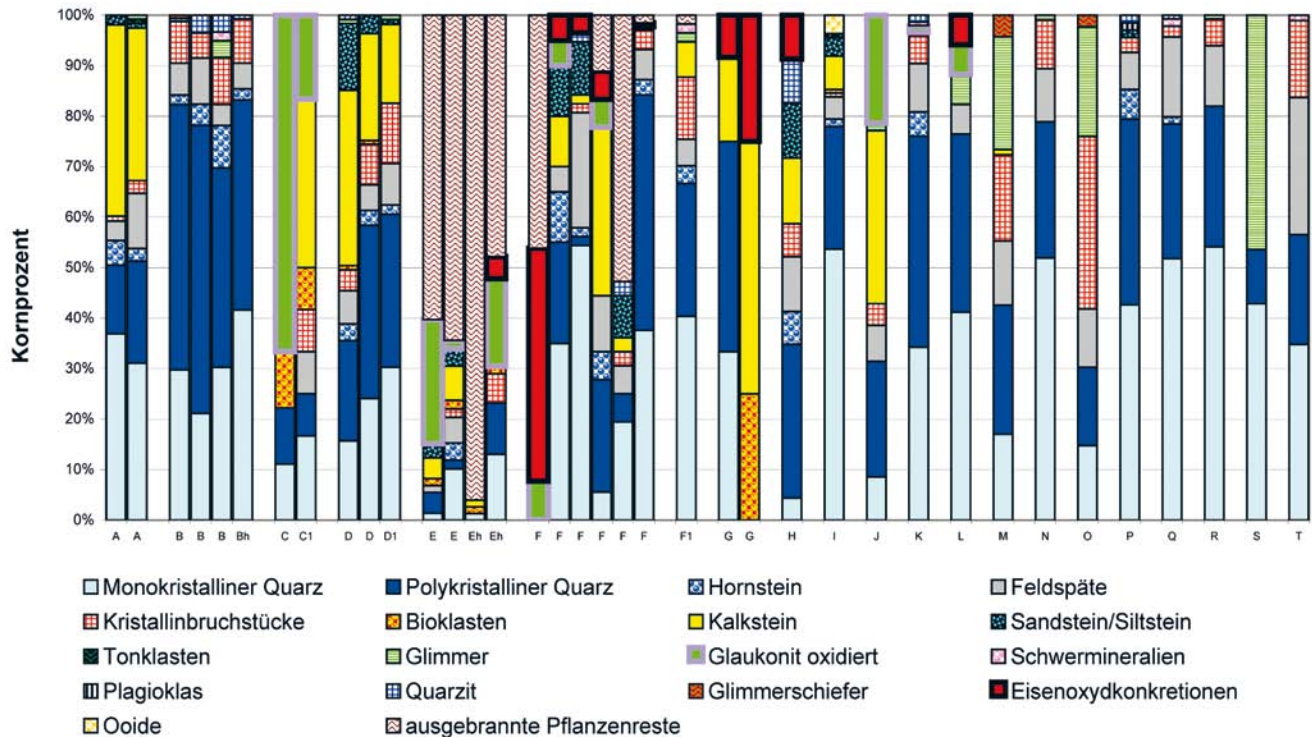- ▨ Ooide
- ▨ ausgebrannte Pflanzenreste

Abb. 3: Mineralogisch-petrographische Zusammensetzung der groben Magerungspartikel (>2,0 mm) der Keramikproben ohne Schamottepartikel.

Fig. 3: Mineralogic-petrographic composition of coarse temper particles (>2.0 mm) of the ceramic samples (> 2.0 mm) without fireclay particles.

In fast allen Keramikproben treten Eisenoxidkonkretionen in der Grundmasse häufig (Mi02–07, 10–12, 14–29, 33–37) oder untergeordnet (Mi08, 09, 13, 31, 32) auf, was für eine allgemeine Verwendung eisenhaltiger Rohstoffe spricht. Andererseits deuten Beobachtungen der Keramik von Michelstetten – wie abwechselnde Farbe der Keramikoberflächen von rot über beige und braun bis grau und schwarz und die Farbübergänge des Scherbenbruches von rot zu orange oder braun von den Gefäßoberflächen in Richtung Kern, meist mit braunen bzw. grauen Kernfarben – auf schwache und unregelmäßige Brenntemperaturen hin. Solche Farbnuancen entstehen am häufigsten beim Keramikbrennen unter Verwendung offener Brennanlagen, wie einfacher Meiler und Feldöfen. Bei offenen Brennanlagen besteht die Gasatmosphäre während des Brandes aus einer Mischung von Luft und Gasen, die bei der Verbrennung des Heizmaterials unter abwechselnder Windrichtung entsteht. Dadurch kann sich die oxidierende Brennatmosphäre nicht lang halten, bzw. wechselt die oxidierende und reduzierende Atmosphäre ab, wie es schon Noll (1991: 86) in seinen Keramikbrennexperimenten merkte. Unter solchen Brennbedienungen neigt die reduzierende Atmosphäre zu überwiegen und die Keramik zeigt häufig dunklere Farbtöne. Da die Oberflächen der Keramik von Michelstetten im Allgemeinen oxidierende Brennfarben (rot, orange, braun, beige) bei dunkleren Kernen aufweisen, konnte die rote Färbung ihrer Oberflächen erst in der Endphase des Brennvorganges entstanden sein, die anschließend durch das häufige Vorhandensein eisenhaltigen Herstellungsmaterials, die die rote Farbe betonen, verstärkt werden konnte. Tatsächlich ist es bekannt, dass die Farbe des Eisens sich schon bei Temperaturen ab 250° C und in einem schwach oxidierenden Milieu ändern kann: W. Noll (1991: 90). Andererseits zeigen Keramikbrennexperimente in offenen Anlagen, dass Sauerstoff erst nach der Verbrennung des Brennmaterials, während der Abkühlungsphase, dann in einer gasfreien Brennatmosphäre, die Keramik erreichen kann (Noll 1991: 88). Unter Verwendung offener Brennanlagen bei der Herstellung der Keramik von Michelstetten wären die Brenntemperaturen der oxidierenden Endphase noch hoch genug, damit chemische Verbindungen mit den Eisenoxiden an den Oberflächen entstanden, wodurch sie, und nicht mehr ihr Kern, rot gefärbt würden.

4.2 Die Rohstoffproben

Zur Ergänzung der wissenschaftlichen Untersuchungen und zur Charakterisierung lokal verfügbarer Rohstoffe wurden 22 Rohstoffproben aus einem Bereich von etwa 100 km² (Lat. 21°60'00' N bis 28°00'00' N, Long. 34°00'00' E bis 38°00'00' E) entnommen, wobei die meisten aus der näheren Umgebung von Michelstetten stammen (Abb. 1). Sie wurden als MT01–MT11 und MT20–MT30 kennzeichnet (Abb. 5) und im nachfolgenden Text als Rohstoffproben MT01, 02, 03 ... bezeichnet.

In Michelstetten kommen auf engstem Raum zahlreiche Formationen unterschiedlichen geologischen Alters vor (Quartär bis Oberjura), die zusätzlich noch teilweise tektonisch verschuppt worden sind und als Rohstofflieferanten in Frage kommen. Es wurde versucht, möglichst von allen geologischen Formationen, die dort als Rohstoffquellen in Frage kommen, Proben zu bekommen.

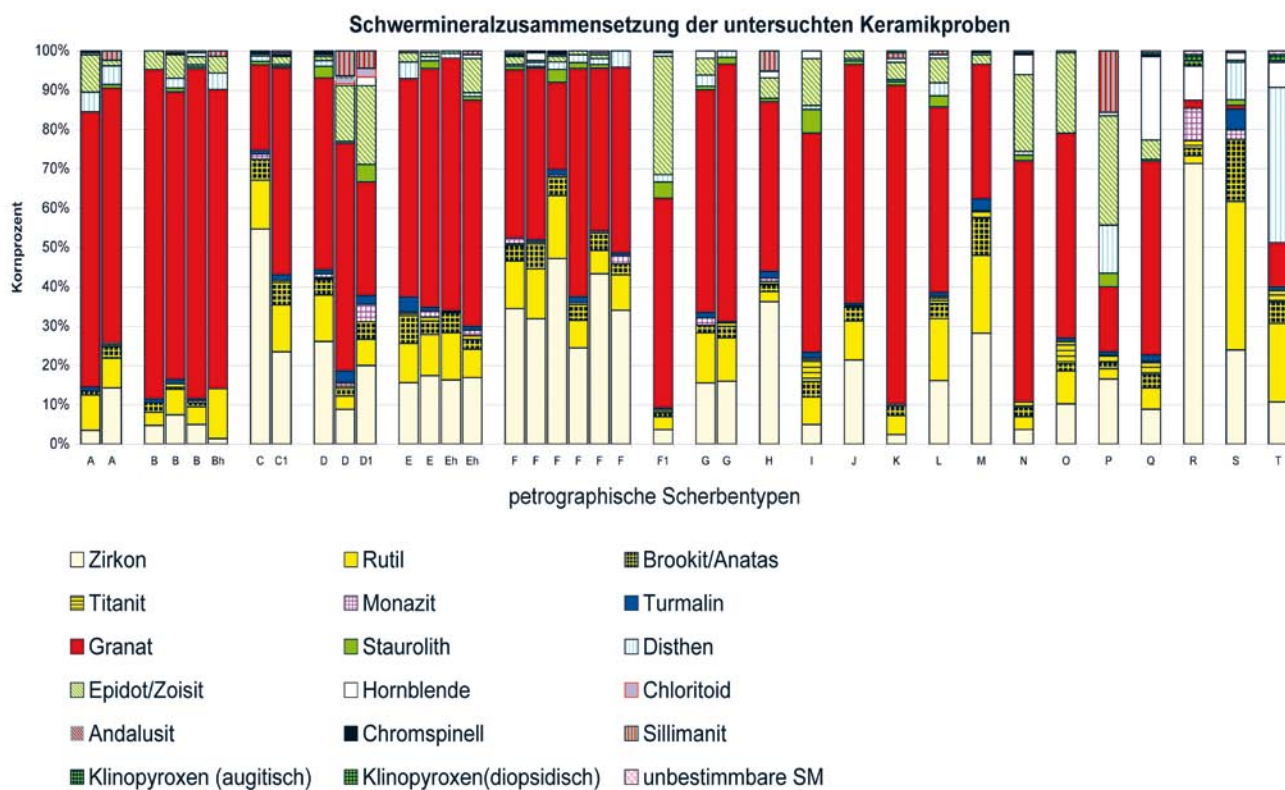Die Lehm- und Tonproben wurden nach Absieben der

Schwermineralzusammensetzung der untersuchten Keramikproben

Abb. 4: Schwermineralzusammensetzung der Keramikproben.

Fig. 4: Heavy mineral composition of ceramic samples.

Partikel gröber als 2 mm im Labor zu kleinen Ziegelchen geformt und bei 750° C gebrannt. Diese Ziegel wurden dann gleich wie die Keramik untersucht – Dünnschliff und bei genügender Probemenge (>5g) auch Schwermineralanalysen (Abb. 5). Während die Tonrohstoffe und Lehmvorkommen relativ vollständig untersucht werden konnten, sind Proben gröberer Sande, die als künstliches Magerungsmaterial in einiger Keramik vorkommen, möglicherweise nicht ausreichend berücksichtigt worden.

Aufgrund der teilweise schlechten Aufschlussverhältnisse konnten häufig nur sehr oberflächennahe und verunreinigte Proben entnommen werden. Diese Proben stellen daher häufig „Mischproben" mehrerer geologischer Formationen dar. Eine klare stratigraphische Ansprache dieser Proben ist dann schwierig. Gerade diese Proben eignen sich häufig als Vergleich bzw. entsprechen sie manchmal sogar direkt den verwendeten Keramikrohstoffen. Das lässt darauf schließen, dass die Töpfer der Lengyelkeramik aus Michelstetten oft oberflächennahe Rohstoffe und infolgedessen mit weniger Aufwand ausgesucht haben.

Proben folgender Formationen wurden für Vergleichszwecke untersucht und nach der aktuellen Nomenklatur bzw. nach der Nummerierung der Geologischen Karte für Niederösterreich 2002 parallelisiert. Diese steht in Klammern am Ende der Anführung einzelner geologischen Schichten (Schnabel, Krenmayr & Roetzel 2002: 5–6, 20–30; Wessely 2006: 41–75).

MT01, 06, 20, 21, 29, 30: Quartäre Lösslehme von allgemeinen Ausschneidungen (19);

MT07: sandiger Lehm der Hollabrunn-Mistelbach-Formation des Pannoniums aus dem oberen Miozän (111, Molassezone)

MT22–24: Marine Tontegel des Badeniums aus dem mittleren Miozän (113, Molassezone)

MT10, 11, 27, 28: Schieferige Tonmergel der Zdanice/Hustopece-Formation, von Eggenburgium bis Ottnangium, aus dem unteren Miozän (147, östl. Teil der Waschbergzone)

MT08, 09: Marine Tone bis sandige Mergel der Michelstetten-Formation des Egeriums aus dem oberen Oligozän und dem unteren Miozän, vermutlich mit Pannonsand oder Löss vermischt (149, Außenrand der Waschbergzone)

MT04, 26: Mergel, Mergelkalke und Oolithe der Klentnitzer-Formation des Oxfordiums und des Tithoniums aus dem Senon (158, Waschbergzone)

MT02, 03: Umgelagerte, zum Teil verunreinigte Kreidesedimente aus dem Senon und dem Paläozän (genauere geologische Zuordnung nicht möglich)

MT05: Tegel aus dem Senon (genauere geologische Zuordnung nicht möglich)

MT25: Oberflächenmischprobe des Senons und des Quartärs (genauere geologische Zuordnung nicht möglich).

4.3 Herkunftsmäßig interpretierte Keramikproben

Nach den naturwissenschaftlichen Untersuchungen scheint ein Großteil der beprobten prähistorischen Keramik mit Rohstoffen, die in der Nähe der Fundstelle entnommen wurden, hergestellt worden sein. Generell kann gesagt werden, dass praktisch sämtliche, lokal vorkommende Rohstoffe, wie quartäre Lehme, jung- und alttertiäre bis oberkretazische Tonmergel, verwendet worden sind. Es ist auch Keramik

Rohstoffproben
Mineralogisch-petrographische Zusammensetzung der natürlichen Magerungspartikel > 15µm

Schwermineralanalysen
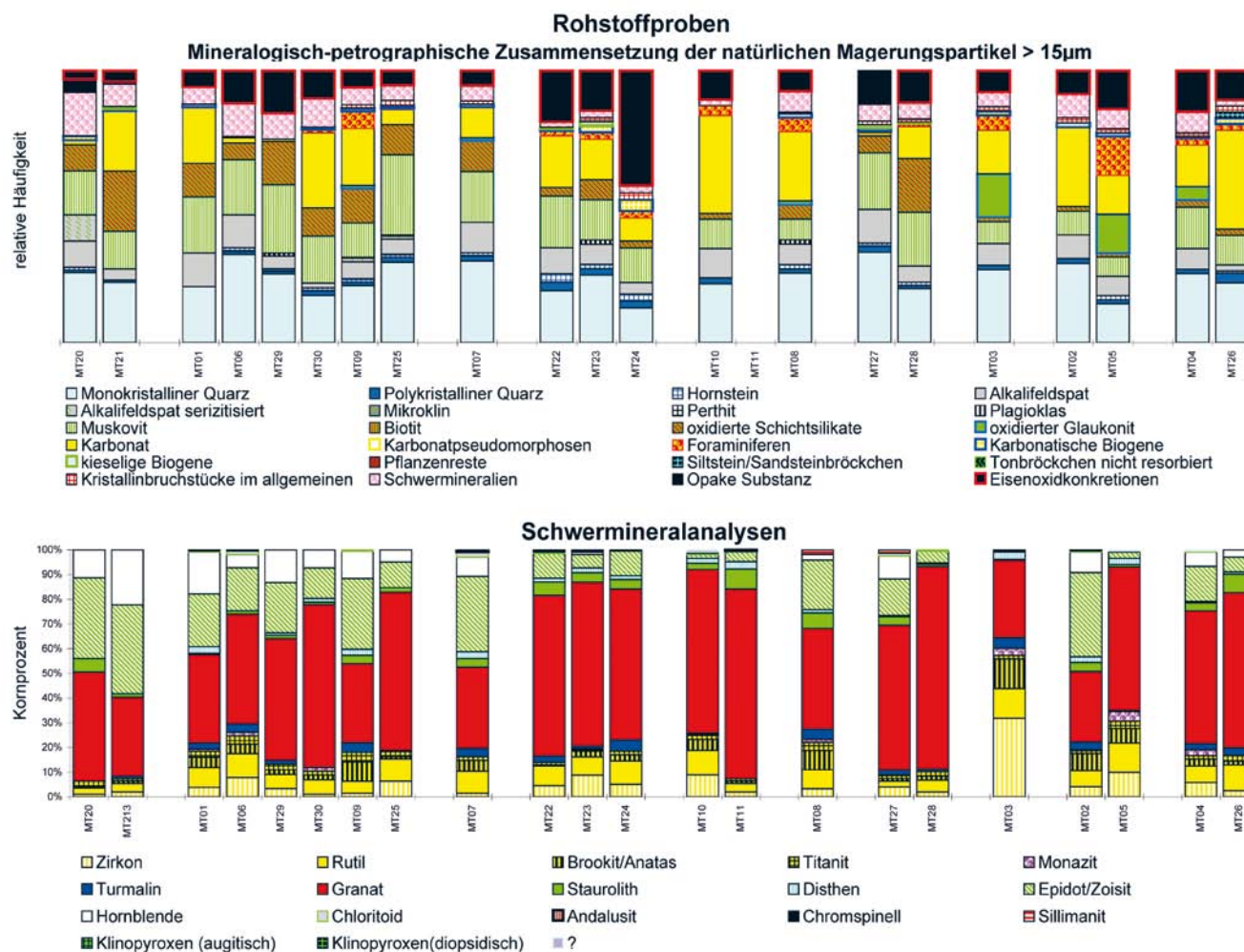
Abb. 5: Mineralogisch-petrographische Zusammensetzung und Schwermineralzusammensetzung der Magerungspartikel der Rohstoffproben (>15 µm).

Fig. 5: Mineralogic-petrographic and heavy mineral composition of temper particles of raw material samples (>15 µm).

vorhanden, die mit nicht lokalen Rohstoffen erzeugt wurde. Bei dieser wird ihr Ursprungsgebiet nur angedeutet, weil keine weiteren Untersuchungen zur Erschließung ihrer genaueren Herkunft gemacht worden sind. Das Material anderer Keramikproben konnte schwer mit den erfassten lokalen Rohstoffen in Verbindung gebracht werden. Bei diesen kann es sich um Keramik handeln, die entweder aus mehreren lokalen Materialien bestehen, also Mischproben darstellen, deren Herkunft nicht leicht nachgewiesen werden kann oder mit nicht-lokalen Rohstoffen hergestellt wurden.

Keramikproben, die die geologischen Formationen der Umgebung der prähistorischen Fundstelle von Michelstetten entsprechen, sind:

Mi02, 03, 06, 15: entkalkte Tone aus dem Schieferigen Tonmergel (Zdanice-Hustopece-Formation) oder des Pannon.

Mi04, 05, 07, 10, 14, 18, 19, 20?, 21, 23–26, 29, 33–35: senone Tonmergel.

Mi28: wahrscheinlich entkalkter, lokaler, (quartärer?) Rohstoff oder Senonmergel.

Mi11: vermutlich ein etwas anders zusammengesetzter Tonmergel, der möglicherweise durch quartäres Material verunreinigt worden ist.

Mi16: mariner Tonmergel des Senon.

Mi31: stark sandiger, tertiärer Tonmergel mit marinen Mikrofossilien.

Mi17, 22: mariner, neogener oder senoner, nicht künstlich gemagerter Tonmergel.

Mi37: quartärer, lokaler Lehm.

Folgende Probe lässt sich derzeit am ehesten mit der geologischen Formation eines von Michelstetten etwas entfernten Gebiets vergleichen:

Mi36: mariner Tonmergel, gemagert mit einem flachmarinen Sand bzw. Kalksandstein (Kalkooide).

Kalkooide kommen besonders häufig in Flachwasserablagerungen des Sarmat vor, wie laut geologischer Karte im nächstgelegenen Vorkommen von Sarmatsedimenten bei Hauskirchen, das ca. 24 km NO von Michelstetten entfernt liegt. Möglicherweise können solche Sedimente aber auch in anderen Ablagerungen auftreten. In den aufgesammelten Rohstoffen in der Umgebung von Michelstetten konnten solche oxidführenden Sande jedenfalls bisher nicht gefunden werden.

Keramikproben, deren Rohstoffherkunft derzeit ungewiss bleibt, sind:

Mi01,30: ein unmittelbar lokal anstehender Rohstoff mit derartig gut gerundeten Karbonatpartikeln ist derzeit lokal nicht bekannt. Es ist theoretisch auch möglich, dass die Proben mit Tonmergel marinen Ursprungs (Foraminiferen) und Sanden der schieferigen Tonmergel erzeugt worden sind. In diesem

Fall würde es sie sich um Mischproben aus lokalen Rohstoffen handeln.

Mi12: relativ untypisch ausgebildet, hauptsächlich durch relativ hohen Hornblendegehalt gekennzeichnet. Es liegt nahe, dass diese Hornblendekörner mit dem sandigen Magerungsmaterial in die Proben gekommen sind. Hornblende ist eher typisch für ganz junge Sedimente, quartäre Lehme oder Verwitterungslehme. Eine weitere Interpretation ist aber bei dieser Einzelprobe derzeit nicht möglich.

Mi27: ist im Dünnschliff den Proben Mi02, 03, 06 und 15 sehr ähnlich, aber mit einer völlig unterschiedlichen Schwermineralzusammensetzung, wobei nur eine relativ geringe Anzahl von Schwermineralien untersucht werden konnte. Das Vorhandensein von Epidotvormacht mit reichlich Sillimanit und Disthen lässt diese Einzelprobe ohne vergleichbare Herkunft der Rohstoffe erscheinen.

Eine lokale Herkunft der verwendeten Rohstoffe folgender Keramikproben ist aufgrund der schwermineralogischen Zusammensetzung auszuschließen. Leider lassen sich mögliche Herkunfsorte der nicht lokalen Keramikproben mangels an Vergleichsproben derzeit nicht näher eingrenzen.

Mi08: ist im Dünnschliff hauptsächlich durch den hohen Gehalt an feinkörnigen Feldspatkörnern, sowie an sehr charakteristischen Gesteinsbruchstückchen und Quarz-Perthitaggregaten gekennzeichnet. Das Schwermineralspektrum weicht durch die Disthen- und Rutilvormachten völlig von den lokal bekannten Rohstoffen ab. Vermutlich wurde die Probe, wie auch Probe Mi09, aus Verwitterungslehmen, wie sie in Kristallingebieten der Böhmischen Masse über hochmetamorphen Kristallingesteinen (z.B. Granulit) vorkommen können, erzeugt.

Mi09: ist im Dünnschliff durch einen auffällig erhöhten Gehalt an dunklen, z. T. oxidierten Glimmern (Biotit) gekennzeichnet. Das Schwermineralspektrum zeichnet sich durch massive Zirkonvormachten aus. Auffällig ist auch noch das Auftreten von Monazit, Hornblende und Klinopyroxen.

Mi13: ist im Dünnschliff hauptsächlich durch den hohen Glimmergehalt gekennzeichnet. Vermutlich wurde sie aus Verwitterungslehmen, wie sie in Kristallingebieten der Böhmischen Masse vorkommen können, erzeugt.

Mi32: hat eine Magerung mit einem extrem hohen Anteil an Kristallinbruchstücken (Glimmerschiefer und Gneisfragmente). Lokal konnten solche Rohstoffe bisher aber nicht gefunden werden.

4.4 Untersuchungen der Überzüge und Malmischungen

8.8 % der Keramik aus Michelstetten weist Reste von Kaltbemalung (Abb. 6) auf.

Neben der Kaltbemalung wurde hochglänzend monochrome, rote oder schwarze polierte Keramik hergestellt, die aufgrund ihrer Ähnlichkeit mit der römischen Ware als „unechte Terra Sigillata" und „unechte Terra Nigra" Keramik bezeichnet wurde (PALLIARDI 1914: 9). Die schwarze hochpolierte Keramik (Abb. 7) könnte mit Hilfe reduzierender Brennverfahren, eventuell unter Verwendung zusätzlicher organischer Stoffe (wie Asche, Holzkohle und Tierfett) in der Keramikmasse erzeugt werden, wie es Experimente durch KOVARNÍK (1983–84: 166–167) anführten.

Die Untersuchungen der Keramik von Michelstetten belegen, dass es sich bei der roten, hochpolierten Keramik, um rote Überzüge handelt, wie sie im Querschnitt mancher Gefäße genauer zu beobachten sind (Abb. 8).

Die archäologische Analyse ihrer Oberflächen ergibt, dass sie sowohl in dünnem Anstrich, wie Malfarben, als auch in flüssigen bis dickeren Überzügen auf die fertigen, ungebrannten Gefäße aufgetragen wurden.

16 Analysen der Malfarben an 11 bemalten Gefäßen von Michelstetten wurden mittels Röntgendiffraktometrie und Polarisationsmikroskopie durchgeführt und als MIP 01 bis MIP 11 bezeichnet (Tab. 2).

Es handelt sich dabei um die mineralogische Zusammensetzung und die farbgebende Substanz der Malmischungen und Überzüge zu bestimmen. Die Ergebnisse der mineralogischen Farbzusammensetzung sind einheitlich:

Die **weiße Farbe** besteht immer aus zerriebenem, feinkörnigem und grobkörnigem Kalzit (MIP 01, 03, 04a, 06a, 8–10, 11a).

Die **rote Farbe** wurde aus verschiedenen Mischungen zusammengesetzt: eine Gemenge aus feinkörnigem Hämatit, Eisenoxiden, Quarz und Muskovit (MIP 02, 06b, 11b); eine Mischung aus feinkörnigen Eisenoxiden mit Quarz und Tonmineralien (MIP 04b); eine Vermengung aus feinkörnigen Eisenoxiden und Ton, verunreinigt mit Quarz (MIP 05b) oder aus Eisenoxiden mit Tonsubstanz (MIP 07b) vermischt.

Die **gelbe Farbe** setzt sich aus einer feinkörnigen Mischung von Kalkspatpulver, etwas Quarz und gelben Eisensulfaten zusammen (MIP 05a). Die geringe Probemenge der einzigen Analyse erlaubt keine schlüssigen Aussagen zum

Abb. 6: Farbkombinationen der bemalten Keramik – gelbrot, weiß und rotweiß.

Fig. 6: Colour combinations of the painted ceramics – yellow red, white and red white.

Abb. 7: Auswahl charakteristischer Lengyelkeramik mit einem Exemplar der „unechten Terra Nigra" Keramik (rechts, oben).

Fig. 7: Selection of characteristic Lengyel ceramics with an exemplar of "artificial Terra Nigra" ceramic (top right).

Gehalt der gelben Farbe. Übrigens ist sie das einzige Beispiel gelber Malfarbe unter der Keramik von Michelstetten und für die Lengyelkeramik im Allgemeinen in diesem Zeitraum unüblich.

Weitere Ergebnisse zur Farbstoffauswahl der Lengyeltöpfer von Keramik anderer Funstellen erweitern etwas die bisherigen Kenntnisse. Die gelbe Pigmentierung der kalt bemalten Keramik der Lengyelkultur im südmährischen und ostösterreichischen Raum scheint vor allem während der Frühstufe (um etwa 4700–4600 vor Chr.) verwendet worden sein und allein auf dem Mineral Jarosit in reiner Form zurückzuführen sein (Kovarník 1989: 157; Doneus 2001: 44). Die weiße Farbe besteht in Kamegg (Niederösterreich) größtenteils aus Kaolinit (Doneus 2001: 44). In Mähren gibt es derzeit keine mineralogische Bestimmung des weißen Pigmentes. Es wird vermutet, dass es sich um Dolomit, Kaolin oder Kreide

handeln könnte (Kovarník 1989: 151). Die rote Farbe scheint in Kamegg, Falkenstein (Niederösterreich) und Südmähren ausschließlich aus Hämatit zu bestehen (Draždák 1973–74: 79; Neugebauer-Maresch 1981: 86; Doneus 2001: 44), genauso wie das rote farbgebende Mineral der Keramik aus Michelstetten.

In Michelstetten ähnelt die chemische Zusammensetzung der roten Malfarben kaltbemalter Keramik dem Gemenge der roten Keramiküberzüge. Das heißt, sowohl die Malfarben der Kaltbemalung als auch die Mischung der Überzüge wurden nach demselben Rezept vorbereitet, wobei manche Überzüge nur etwas dicker waren. Überzüge sind meiner Auffassung nach als Bemalungstechnik anzusehen. Die Besonderheit der Überzüge in Bezug auf die herkömmliche Kaltbemalung ist, dass Überzüge vor dem Brand, und nicht nach dem Brand, auf die Gefäßoberflächen aufgetragen wurden und das Feuer

Tab. 2: Mineralogische Zusammensetzung der Malfarben und Überzüge bemalter Gefäße.

Table 2: Mineralogical composition of the colours and coatings on painted vessels.

| Prb.Nr.	Inv.Nr.	Farbe	Zusammensetzung
MIP 01	683	weiss	Mischung aus zerriebenem, feinkörnigem und grobkörnigem Kalzit
MIP 02	1439	rot	Gemenge aus feinkörnigem Hämatit, Eisenoxiden, Quarz und Muskovit
MIP 03	1880	weiss	Mischung aus zerriebenem, feinkörnigem und grobkörnigem Kalzit
MIP 04a	1880	weiss	Mischung aus zerriebenem, feinkörnigem und grobkörnigem Kalzit
MIP 04b	2468	rot	Feinkörnige Eisenoxide mit Quarz und Tonmineralen vermengt
MIP 05a	5847	gelb	Gemenge aus feinkörnigem Kalzit, Eisen(hydro)xiden und Ton mit Quarz verunreinigt
MIP 05b	5847	rot	Mischung aus feinkörnigen Eisenoxiden und Ton mit Quarz verunreinigt
MIP 06a	5768	weiss	Gemenge aus zerriebenem, feinkörnigem und grobkörnigem Kalzit
MIP 06b	5768	rot	Mischung aus feinkörnigem Hämatit, Eisenoxiden, Quarz und Muskovit
MIP 07a	4676	weiss	Mischung aus feinkörnigem, zerriebenem und grobkörnigem Kalzit
MIP 07b	4676	rot	Mischung aus Eisenoxiden mit Tonsubstanz
MIP 08	4834	weiss	Gemenge aus zerriebenem, feinkörnigem und grobkörnigem Kalzit
MIP 09	4831	weiss	Gemenge aus zerriebenem, feinkörnigem und grobkörnigem Kalzit
MIP 10	4722	weiss	Gemenge aus zerriebenem, feinkörnigem und grobkörnigem Kalzit
MIP 11a	5378	weiss	Mischung aus zerriebenem, feinkörnigem und grobkörnigem Kalzit
MIP 11b	5378	rot	Mischung aus feinkörnigem Hämatit, Eisenoxiden, Quarz und Muskovit
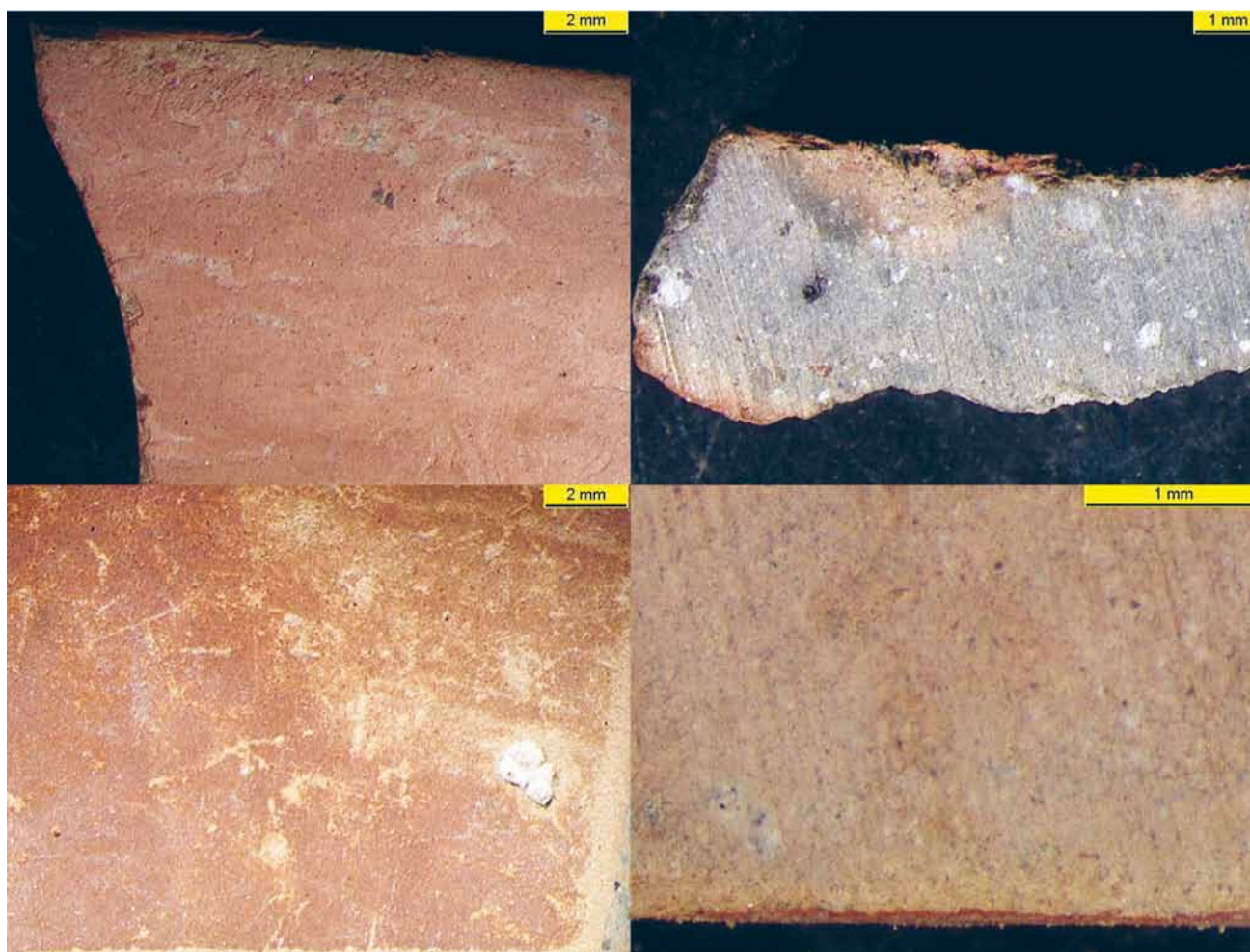
Abb. 8: Detail der Oberflächen außen (links) und im Querschnitt (rechts) der „unechten Terra Sigillata" Keramik.

Fig. 8: Detail of the surface (left) and cross-section (right) of the "artificial Terra Sigillata"

als Malfixierungsmittel, als Alternativ zur Anwendung organischer und anorganischer Fixierungssubstanzen der Kaltbemalung, bewusst verwendet worden ist. Die Kaltbemalung ist für die Lengyelkeramik seit dem Anfang ihres Auftretens (um 4800 vor Chr.) und für ihre gesamte Dauer sehr kennzeichnend, während die Überzüge erst in einer eingehenden Phase der Produktion von Lengyelkeramik hergestellt worden sind. Nach den Keramikuntersuchungen von Michelstetten konnte festgestellt werden, dass das Auftreten der Herstellungstechnik der sogenannten „unechten Terra Sigillata" Keramik zumindest ab 4600 vor Chr. nachgewiesen werden kann (Carneiro 2002: 37, 38, 123–130).

Interessant dabei ist, dass obwohl Überzüge wischfester sind und damit eine vorteilhafte Veränderung gegenüber der gebräuchlichen Maltechnologie der Lengyelkeramik darstellen, sie diese nicht ersetzt haben bzw. weitläufig viel weniger oft verwendet worden sind und nur auf die rote (möglicherweise z. Teil auch auf die schwarze) Farbe beschränkt sind. Die Kaltbemalung wurde unter Verwendung verschiedener Farben, neben der Erzeugung roter Überzüge, bis zur Endherstellung von Lengyelkeramik weiter angewendet. Darunter wurde die rote Farbe am häufigsten gebraucht. Für solchen Gebrauch konnten mehrere Argumente diskutiert werden. Als plausibler erscheint es mir, dass während die chemische Zusammensetzung von Hämatit (rote Farbe) erst bei 550° C, ohne eine wesentliche Farbumwandlung zu er-

leben, verändert wird, dagegen Jarosit bei 350–400° C und Gips bzw. Calciumsulfate bei 200° C schon veränderbar sind (Noll 1991: 187), wodurch die Haltbarkeit von Keramik mit weißen und gelben Überzügen und die gewünschte Färbung gefährdet würde. Andererseits, obwohl die Kaltbemalung weniger anhaltend als die mit Überzügen ist, stellt sie doch eine schnellere und einfacher herstellbare Technik dar, womit eine bunte, motivreiche Keramik erzeugt werden konnte, die den Zweck ihrer Hersteller/Benutzer erfüllt hat. Die Herstellung von hochglänzend polierter Keramik in den roten und schwarzen Farben könnte mit ihrem Gebrauch in bestimmten Situationen zusammenhängen. Dafür spricht auch im Allgemeinen die gute Ausführung ihrer Gefäße (meist aus weniger groben Herstellungsmaterialien, sorgfältig geformt und behandelt) und die Auswahl ihrer Formen, die zu einer betonten Profilierung neigen (Schüsseln mit ausladendem, gebogenem Oberteil; Töpfe und Flaschen aus weniger gewöhnlichen Formen).

Literaturverzeichnis

Carneiro, Â. (2002): Studien zur Spätlengyelzeit am Beispiel von Keramik von Michelstetten (Niederösterreich). – Unpubliziert Dissertation der Universität Wien. – 560 S.; Wien.

Doneus, M. (2001): Die Keramik der mittelneolitischen Kreisgrabenanlage von Kamegg, Niederösterreich. Ein Beitrag zur Chronologie der Stufe MOG I der Lengyel-Kultur. – Mitteilungen der prähistorischen Kommission, 46: 146 S.

Draždák, K. (1973-74): Mineralogische Analyse des roten und gelben Farbstoffes der neolithischen Keramik (MBK) aus Těšetice-Kyjovice, Bez. Znaim. – Sborník Prací Filosofické Fakulty Brnenské Univerzity, E 18–19: 69–79.

Grill, R. (1968): Erläuterungen zur geologischen Karte des nordöstlichen Weinviertels und zu Blatt Gänserndorf. – Geologische Bundesanstalt Wien – 155 S.; Wien (Verlag der Geologischen Bundesanstalt).

Hennicke, H. (1989): Rohstoffaufbereitung, Formgebung und Trocknen. – In: Schneider, G.: Naturwissenschaftliche Kriterien und Verfahren zur Beschreibung von Keramik, – Acta Praehistorica et Archaeologica, 21: 15–18 S.(Anhang).

Kovarník, J. (1983-84): Zur Technologie der neolithischen Keramik. – Mitteilungen der österreichischen Arbeitsgemeinschaft für Ur- und Frühgeschichte, 33–34/1: 151–169 S.

Kovarník, J. (1989): Die Anwendung von mineralischen Farbstoffen im Neolithikum. – In: Rulf, J. (ed.): Bylany Seminar 1987. Collected papers: 149–160; Praha (Archeologický ústav).

Krenmayr, H.-G. & Schnabel, W. (2002): Quartär – Ober – Pliozän (T1). –In: Schnabel, W. (ed.): Legende und Kürzerläuterung der Geologischen Karte von Niederösterreich 1:200.000, Geologische Bundesanstalt: 20–23 S.; Wien.

Neugebauer-Maresch, C. (1981): Archäologisches Fundmaterial aus den jungsteinzeitlichen Befestigungsanlagen Falkenstein-Schanzboden, NÖ. – Unpublizierte Dissertation der Universität Wien. – 255 S.; Wien.

Noll, W. (1991): Alte Keramiken und ihre Pigmente: Studien zu Material und Technologie. – 334 S.; Stuttgart (E. Schweizerbart'sche Verlagsbuchhandlung).

Palliardi, J. (1914): Die relative Chronologie der jüngeren Steinzeit in Mähren. – Wiener Prähistorischen Zeitschrift, 1: 1–24.

Roetzel, R. & Schnabel, W. (2002): Molasse, Waschbergzone, Paläogen und Neogen auf der Böhmischen Masse, in W. Schnabel (red.), Legende und Kürzerläuterung der Geologischen Karte von Niederösterreich 1:200.000, Geologische Bundesanstalt, 23–30 S.; Wien.

Schnabel,W., Krenmayr, H.-G. & Roetzel R. (2002): Geologie der Österreichischen Bundesländer, Niederösterreich. – Geologische Bundesanstalt, 2 Farbkarten und Erläuterungsbericht: 20–30.

Thenius, E. (1983): Niederösterreich im Wandel der Zeiten. Die Entwicklung der vorzeitlichen Tier- und Pflanzenwelt von Niederösterreich. – Katalog des Niederösterreichischen-Landesmuseums, NF 144: 156 S.

Wessely, G. (2006): Geologie der österreichischen Bundesländer, Niederösterreich. – Geologische Bundesanstalt, 416 S.; Wien.

Wosinsky, M. (1888): Das prähistorische Schanzwerk von Lengyel. Seine Erbauer und Bewohner. Heft 1: 221 S.; Budapest.

Pedological and geochemical investigations at the "Red Outcrop" of Langenlois (Lower Austria)

Edith Haslinger, Libuše Smolíková, Pavel Havlíček, Reinhard Roetzel, Maria Heinrich, Oldřich Holásek, Michal Vachek, Franz Ottner

Abstract: In an outcrop of loess-paleosol sequences over amphibolite, six soil profiles (Lois 1 to Lois 6) were sampled and analysed for pedological, mineralogical, and geochemical characteristics. A second outcrop (Lois 7) was investigated for soil micromorphology. Two soil profiles (Lois 1 and 2) have developed over amphibolites, two over an amphibolite/marble-body (Lois 5 and 6) and three polycyclic paleosol profiles with several fossil horizons have no visible underlying bedrock (Lois 3, 4 and 7). In the profiles Lois 1–4 and Lois 7 intense carbonate illuviations occur. These high amounts of carbonate cannot result from recent pedogenesis, but are interpreted as being derived from carbonate-rich sediments (loess) overlying the present outcrop in the past which were eroded. Furthermore, a layer of calc-sinter was found in the profile Lois 2. It is assumed, that this sinter could come from the weathering of the marble which can be found in the profile Lois 6. The sinter layer seems to inhibit the exchange of chemical elements between rock and soil in the profiles Lois 1 and 2, which is emphasized by the geochemical results. The clay cutans on aggregates in the fossil horizons also indicate that the clay eluviation has already taken place in former periods. Furthermore, weakly developed stagnic properties can be found in the fossil horizons. The paleosol profiles show several polycyclic sedimentation stages and thus several generations of fossil horizons. The results of the soil micromorphological analysis allow for an age classification of the soil profiles in the "Red Outcrop" and can thus be placed in Middle to Lower Pleistocene or older.

[Bodenkundliche und geochemische Untersuchungen am „Roten Aufschluss" in Langenlois (Niederösterreich)]

Kurzfassung: In einem Aufschluss von Löss-Paläoboden-Sequenzen über Rehberger Amphibolit NW von Langenlois wurden sechs Bodenprofile (Lois 1 bis Lois 6) beprobt und pedologisch, mineralogisch und geochemisch analysiert. Am Profil Lois 7 wurden bodenmikromorphologische Untersuchungen durchgeführt. Zwei Bodenprofile (Lois 1 und 2) haben sich über Amphibolit entwickelt, zwei über einer Amphibolit/Marmor-Wechsellagerung (Lois 5 und 6) und drei Bodenprofile sind Sequenzen von polyzyklischen Paläoböden mit fossilen Bodenhorizonten ohne unterlagerndes kristallines Gestein (Lois 3, 4 und 7). In den Profilen Lois 1–4 und Lois 7 konnten intensive Karbonatanreicherungen beobachtet werden. Diese hohen Mengen an Karbonat können nicht Produkt einer rezenten Bodenbildung sein, sondern sprechen für eine Infiltration von ursprünglich das Profil überlagernden kalzitreichen Sedimenten (Löss), die erodiert wurden. Zudem wurde in Profil Lois 2 ein Kalksinter angetroffen. Dieser Kalksinter könnte aus der Verwitterung der im Profil Lois 6 aufgeschlossenen Marmorlagen stammen. Die Kalksinter-Schicht scheint die Stoffflüsse zwischen unterliegendem Gestein und Solum in den Profilen Lois 1 und 2 mehr oder weniger zu unterbinden, was auch durch die Ergebnisse der geochemischen Analytik unterstrichen wird.

In den fossilen Horizonten wurden auch ältere Anzeichen von Tonverlagerung in Form von Tonkutanen über den Aggregaten und darüber hinaus leichte Pseudovergleyungserscheinungen angetroffen. Die mächtigen Profile ohne aufgeschlossenes Grundgebirge (Lois 3, 4 und 7) weisen mehrere polyzyklische Sedimentationsphasen und dadurch mehrere Generationen von fossilen Horizonten auf. Aufgrund der bodenmikromorphologischen Analyse können die Böden vom „Roten Aufschluss" altersmäßig im unteren bis mittleren Pleistozän oder älter angesiedelt werden.

Keywords: *Loess, Paleosol, Micromorphology, Amphibolite, Langenlois*

Addresses of authors: E. Haslinger, Austrian Institute of Technology, Sustainable Building Technologies, Giefinggasse 2, A-1210 Vienna, Austria, on behalf of the Geological Survey of Austria. E-Mail: edith.haslinger@ait.ac.at; **L. Smolíková,** Přírodovědecká fakulta Univerzity Karlovy, Ústav geologie a paleontologie Albertov 6, 12843 Praha 2, Czech Republic; **P. Havlíček, O. Holásek,** Česká geologická služba, Klárov 3, 11821 Praha 1, Czech Republic. E-Mail: pavel.havlicek@geology.cz, oldrich.holasek@geology.cz; **Reinhard Roetzel, Maria Heinrich,** Geological Survey of Austria, Neulinggasse 38, A-1030 Vienna, Austria. E-Mail: maria.heinrich@geologie.ac.at, reinhard.roetzel@geologie.ac.at; **M. Vachek,** Ministerstvo zemědělství – Pozemkový úřad Hodonín, Koupelní 19, 69501 Hodonín, Czech Republic. E-Mail: Michal.Vachek@mze.cz; **F. Ottner,** University of Natural Resources and Applied Life Sciences, Institute of Applied Geology, Peter-Jordan-Straße 70, A-1190 Vienna, Austria. E-Mail: franz.ottner@boku.ac.at

1 Introduction

In the summer of 2007 a new vineyard was established NW of Langenlois at the so-called 'Schenkenbichl-Hill' (Fig. 1 and 2, Coordinates: R: 49808, H: 5371937; Allotment 4975). The opportunity was taken to investigate an outcrop which is fresh and uncovered by vegetation in a geologically and historically distinct and interesting landscape. At the U-shaped outcrop with a height up to 5 m, a loess/paleosol/colluvi-um-sequence on a dome-shaped amphibolite with layers of marble was investigated. The loess/colluvium-sediments were deposited in the Early to Middle Pleistocene, according to the results of Smolíková, Havlíček, Holásek and Vachek, which are described in the chapter "Profile Lois 7". However, a Pliocene age of the sediments cannot be excluded. Such very old pedocomplexes at the SE-margin of the Bohemian Massif and especially in the area around Krems and Langenlois were described several times (Fink et al. 1976; Havlíček
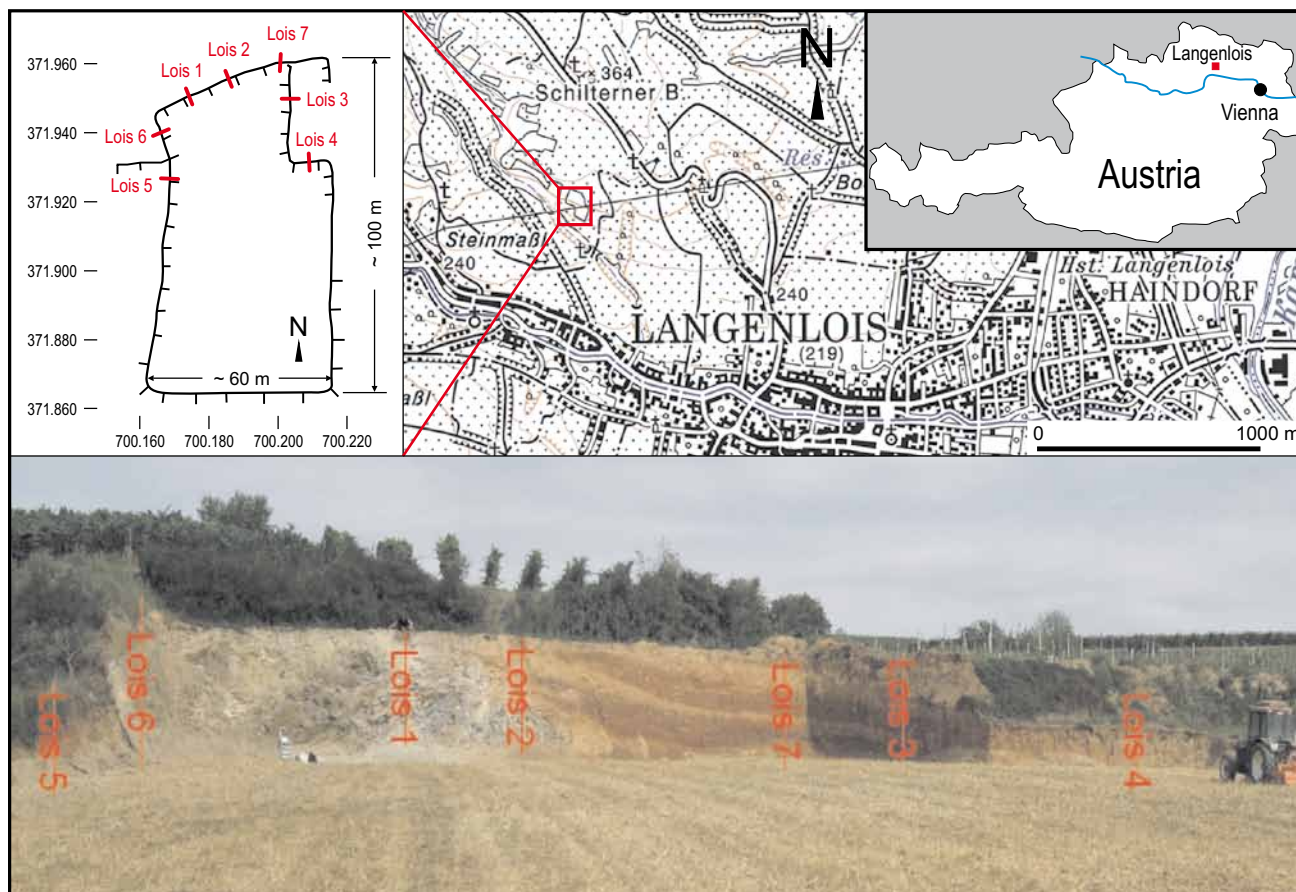
Fig. 1: Location of the outcrop (red circle) on a detail of the topographic map 1:50000 (© BEV – 2008, reproduced with permission of the BEV – Bundesamt für Eich- und Vermessungswesen Vienna, T2008/51914.), Overview of the outcrop with the sampled profiles Lois 1 to 7 and ground plot with coordinates (MGI_Austria_GK_M34; Projection: Transverse_Mercator) and positions of the profiles.

Abb. 1: Lage des Aufschlusses (roter Kreis) auf einem Ausschnitt der topographischen Karte 1:50000 (© BEV – 2008, Vervielfältigt mit Genehmigung des BEV – Bundesamtes für Eich- und Vermessungswesen in Wien, T2008/51914.), Übersicht über den Aufschluss mit den aufgenommenen Profilen Lois 1 bis Lois 7 und Grundriss und Koordinaten (BMN M34) des Aufschlusses und Positionen der aufgenommenen Profile.

et al. 1998; Havlíček et al. 2005; Havlíček et al. 2006). Due to the position of the area in the triangle between the SE-margin of the Bohemian Massif in the West, the river Danube in the South, and the river Kamp in the NE, these Lower Pleistocene to Pliocene sediments were protected from erosion. Young aeolian sediments, which covered the Middle to Upper Pleistocene sediments, additionally contributed to reduce the erosion.

The sediments are known in this area, for example from the 'Schießstätte' in Krems (Fink et al. 1976; Kovanda et al. 1995; Frank & Rabeder 1996b; Rabeder 1981), of the former brickyard 'Hammerer' in Langenlois (Fink et al. 1976; Jaburová 2009) or from outcrops in the hollow ways around Langenlois (Havlíček & Holásek 1998; Smolíková 1997, 1998; Havlíček et al. 2005; Smolíková & Havlíček 2007; Jaburová 2009). The sediments of the "Red Outcrop" are also comparable to the Plio-Pleistocene sediments of Stranzendorf (Fink et al. 1976; Kovanda et al. 1995; Frank & Rabeder 1996b; Döppes & Rabeder 1997; Rabeder 1981) or to soil sediments of the Middle Pleistocene in Neudegg (Frank & Rabeder 1996a; Döppes & Rabeder 1997; Havlíček et al. 2004).

According to Fuchs et al. (1984), the amphibolite on the Schenkenbichl-Hill belongs to the 'Rehberg-Formation'. The amphibolites are predominantly layered amphibolites, sometimes also gabbro-amphibolites, and locally associated with serpentinite and marble. The amphibolites occur in the shape of elongated bodies in the area around Langenlois, which is dominated by paragneisses. The petrology and geochemistry of the 'Rehberg'-amphibolite was thoroughly investigated in the doctoral thesis of Hödl (1985). The petrographic description of the 'Rehberg'-amphibolites can be found in Matura (1989). Höck (in Steininger 1999) points to the comparability of the sequence to ophiolites, which can be regarded as remains of the oceanic crust. In the 'Red Outcrop', no macroscopically visible fossils could be found in the examined profiles, therefore there was no further investigation in this respect.

In this study, the reconstruction of the landscape's history and the single pedogenetic processes in the outcrop was carried out for the first time with detailed geochemical and soil micromorphological analyses.

2 Methods

Field

Seven profiles (Lois 1–7) were investigated (Fig. 1):
Lois 1 and **Lois 2** on weathered amphibolite
Lois 3 and **4** in the loess/paleosol/colluvium-sequence
Lois 5 in a disturbed soil on amphibolite/marble with backfill material on top

Lois 6 on weathered amphibolite/marble, partially disturbed with backfill material on top

The profiles Lois 1–6 were pedogenetically described and composite samples (ca. 1 kg) were taken from the genetical horizons. Two samples per horizon were taken from layers with a depth of more than 50 cm.

The profile **Lois 7** has to be considered separately, since it was sampled only for the analysis of soil micromorphology and climatic stratigraphy. The laboratory analyses, which are described in the following, therefore refer only to the profiles Lois 1–6, with the exception of the description of the micromorphology method.

Laboratory

Drying and Sieving

Half of the samples were dried at 40 ℃ until constant weight, in order to simulate air drying. The other samples were stored cool and dark as retain samples. The dried samples were sieved to 2 mm to obtain the fine soil fraction. A representative portion of each sample was milled in a Netzsch-agate mortar.

Dry weight and loss on ignition

The samples were dried/heated at 105, 430 and 1000 ℃. After each drying/heating step the loss on drying/ignition was calculated.

Particle size analysis after wet sieving

100 g of the air-dried samples were wet-sieved with mesh-sizes 2000, 1000, 500, 250, 125, 63 and 32 μm. The particle size distribution of the fraction < 32 μm was determined with a sedigraph (Micromeritics, Sedigraph 5100 ET).

pH in H_2O and $CaCl_2$

The determination of the pH-values was carried out according to the Austrian Standard (ÖNORM) L 1083 (ON 2006).
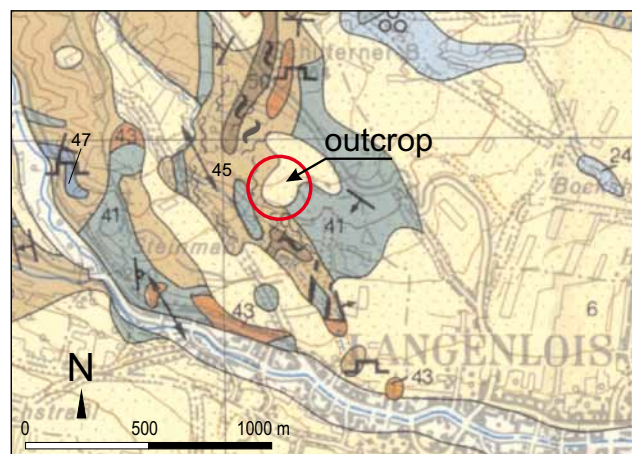
C/S-Analysis (LECO)

For each sample, 2 x 200 mg milled powder was weighed in tempered LECO-crucibles. The contents of C_{tot} and S_{tot} was determined in a LECO 200IS.

Content of organic matter

For each sample, 2 x 500 mg milled powder was weighed in tempered LECO-crucibles and wetted with H_2O deion. 3 x 2 M HCl were then percolated through the samples in order to dissolve the carbonate (C_{anorg}). In the next step, the samples were rinsed 10 times with H_2O deion. to remove the free Cl^--ions, since they interfere with the analysis. The C_{org}-content of the samples was measured in a LECO 200IS. The content of C_{anorg} was calculated by subtraction of the measured contents of organic carbon from the measured content of total carbon ($C_{tot} - C_{org}$). The analyses were carried out on two replicate samples.

Pedogenic oxides in dithionite and oxalate extract

The dithionite-extraction was carried out at room temperature according to the method of HOLMGREN (1967). The oxalate extraction was carried out according to the methods of TAMM (1932) and SCHWERTMANN (1964).

Fig. 2: Location of the outcrop (red circle) on a detail of the geological map 1:50000, Sheet 38 – Krems (FUCHS et al. 1984).

Abb. 2: Lage des Aufschlusses (roter Kreis) auf einem Ausschnitt der geologischen Karte 1:50000, Blatt 38 – Krems (FUCHS et al., 1984).

Total mineral content

The mineral phases were determined qualitatively and semi-quantitatively by X-ray diffraction in a Philips-XPert MPD Vertical Goniometer PW 3050 with the following measuring conditions: Measuring angle 2°–65° 2 Θ, Cu-Kα-ceramic tube, automatic equatorial divergence, receiving slit 0.3 mm, continuous scan, step size 0.02°, 40 kV, 40 mA, measuring time 1 s/step, measuring program X'Pert Data Collector. The peak areas of the main reflections were determined with the X'pert-Data Viewer-Programme. Afterwards, the mineralogical composition of the samples was determined according to the method of SCHULTZ (1964) with correction factors.

Clay mineral analysis (fraction < 2 μm)

The samples were dispersed with 15 % H_2O_2. After the reaction reached its equilibrium, the excess H_2O_2 was removed and the samples were treated in an ultrasonic bath for 15 minutes. The 2 μm-fraction was separated by centrifugation. Afterwards, 400 ml of the clay suspension of each sample was mixed with 100 ml 4 N KCl-solution or 4 N $MgCl_2$-solution, respectively, and shaken in a horizontal shaker for 24 h. The samples were prepared using the suction-on-ceramic-plate method. After X-ray diffraction, the K- and Mg-treated samples were treated with ethylene glycol and measured again. The Mg-treated samples were treated afterwards with glycerine for the distinction between smectite and vermiculite. The K-treated samples were treated with DMSO (Dimethyl sulfoxide) for the distinction between chlorite and kaolinite. Finally, the Mg-treated samples were tempered at 300℃ und afterwards at 550° for 2 h for the determination of primary

and secondary chlorite. The X-ray diffractometry for the clay samples was carried out in the same manner as for the total mineral composition. The correction factors were taken from Riedmüller (1978).

Determination of major and trace elements
4 g of the milled samples was mixed with 0.9 g wax (Merck, Hoechst Wax C Micropowder) in a planetary mill (Retsch MM200). The tablets were pressed with a Specac press. The analysis of major and trace elements was carried out by X-ray fluorescence (XRF) in a Spectro XLAB 2000.

Scanning electron microscopy (SEM) and microanalysis (EDX)
The SEM-analyses of the rock samples were carried out after C-sputtering on a Vega Tescan (CamScan, USA). The image capturing was carried out with the digital image capturing system analySIS (Soft Imaging Systems). The energy dispersive X-ray analysis (EDX) was carried out on a Link ISIS 200/300 (Oxford Instruments).

Soil micromorphological examinations on soil thin sections
The soil micromorphological analyses and description were carried out by Libuše Smolíková of the Karls-University in Prague.

Soil systematics
The determination of the soil types and their genetic horizons was carried out according to the Austrian Soil Classification System (Nestroy et al. 2000). However, in Table 1, there is a reference to the corresponding soil types according to *World Reference Base for Soil Resources* (WRB; IUSS Working Group WRB, 2006).

3 Results

The results of soil systematics, chemistry and physics, the mineralogical and geochemical analyses of the profiles Lois 1 to Lois 6, as well as the soil micromorphological analyses of Lois 7, are now shown and discussed. The chapters are divided into the sections 'Soil physical and chemical parameters', 'Mineralogy' and 'Geochemistry' for each profile. The soil micromorphological analyses of profile Lois 7 are discussed separately.

In Table 1 the soil descriptions as well as the most important soil chemical and physical parameters of the profiles Lois 1 to 6 are shown.

Profile Lois 1

Soil physical and chemical parameters
The examination of the chemical parameters of profile Lois 1 show that the pH-values in the whole profiles show no dynamics at all, with values between 7.2 and 7.5. The content of organic C is very low and decreases from 0.74 % in the uppermost (Ap-)horizon to 0.21 % in the lowermost (C-) horizon (Tab. 1). The pedogenic oxides decrease as well from top to bottom. The share of the pedogenic Fe compared to total Fe decreases from 7 to 4 %. The share of amorphous (active) Fe is low, which is a sign of low pedogenetical activity (Tab. 2). The texture of Lois 1 is relatively uniform through-

out the profile. The gravel content (> 2 mm) is between 19 and 30 %, the sand content increases from 34 to up to 49 % through the soil profile. The silt and clay contents decrease from top to bottom (silt from 24 to 17 %, clay from 15 to 5 %) (Tab. 1). The soil texture of profile Lois 1 is loamy sand to sandy loam. The soil profile shows no significant dynamic behaviour and slow pedogenetical processes.

Mineralogy
The thin section of the rock sample (240 cm) shows that the amphibolite is very rich in hornblende with plagioclase and quartz as accessories. The quartz primarily occurs in lenses, which is typical for the 'Rehberg'-amphibolite. Chlorite could be identified as accessory by XRD. In the sample G1/2 (382 cm), the amphibolite shows alternate layering of finer and coarser grains. The feldspar occurs in small crystals. Clinozoisite, rutile and titanite as well as a chlorite vein could also be identified. The rock sample G1/3 (440 cm) is significantly coarser than the other two rock samples with paler amphiboles. The thin section also shows clinopyroxene and garnet. In addition, zoisite and chlorite could be identified as accessories by XRD.

The mineralogical analyses of the soil samples of profile Lois 1 show a predominance of quartz, calcite and hornblende (Tab. 3). The quartz content decreases from 26 to 3 % from top to bottom. Calcite shows a reverse behaviour. The content of hornblende is very constant throughout the soil profile (18–34 %). The feldspars are dominated by plagioclase with contents between 11–14 %. The sheet silicate content is low (up to 10 % in the Ap-horizon). Noticeable is the high content of calcite in the soil profile. The calcite covers the solum as well as the amphibolite and occurs as a thick, purely white crust which can be easily removed by hand from the fresh and only slightly weathered amphibolites. The, in places, intense carbonate enrichment can also be observed in the other soil profiles. These high amounts of carbonate cannot be derived from recent pedogenetical processes, but suggest an infiltration from eroded calcite-rich sediments (loess), which originally overlaid the soil profile. Furthermore, an occurrence of calc-sinter was found in profile Lois 2. This calc-sinter could be a weathering product from the marble of profile Lois 6. This hypothesis is also supported by the morphology of the outcrop. The outcrop slightly descends from the western flank (profiles Lois 5 and 6) towards the other soil profiles. Therefore, it is possible that weathering-induced calcite-rich solutions ran off laterally and then precipitated in the form of calc-sinter in the profiles on the northern and eastern flank of the outcrop (Lois 1–4). However, it is possible that both processes – decalcification of superimposed loess and precipitation of calcite-rich weathering products – were active in the 'Red Outcrop'. The calc-sinter layer apparently hinders material flows between the host rock and the solum, which is supported by the geochemical analyses.

The clay mineral composition is dominated by smectite with contents between 49 % in the uppermost horizon to 65 % in the lowermost horizon (Tab. 3). Illite shows a reverse distribution with 31 % in the uppermost and 12 % in the lowermost horizon. Kaolinite and chlorite occur only in small amounts (maximum contents: kaolinite 15 %, chlorite 16 %), whereas the chlorite only occurs as primary (detritary) chlorite.

Table 1: Soil description and most important soil chemical and physical parameters of profiles Lois 1 to Lois 6.

Tab. 1: Ergebnisse der Bodenbeschreibung sowie der wichtigsten bodenchemischen und -physikalischen Parameter der Profile Lois 1 bis 6.

Profile	Sample no.	Soil type (ASCS; WRB)	Horizon depth	Horizon	soil colour (moist)	soil colour (dry)	Structure	Horizon transition/ boundary	Roots	% >2 mm	% Sand	% Silt	% Clay	pH H₂O	pH CaCl₂	C_org (%)
Lois 1	Lois 1/1	Karbonathaltige Braunerde aus grobklastischem Material - Haplic Calcisol	0 - 40	Ap	10YR/4/3	10YR/5,5/4	sab, gr	a, s	R3	26,3	33,7	24,7	15,4	7,5	7,2	0,74
	Lois 1/2		40 - 70	BwCv	10YR/5/3	10YR/6/2	sab	a, w	R1	19,0	44,7	24,1	12,2	7,7	7,3	0,48
	Lois 1/3		70 - 120	Cv	2,5Y/6/3,5	2,5Y/7/2,5	sab	a, w	R1	26,2	49,5	18,4	5,9	7,9	7,3	0,30
	Lois 1/4		120 - 140	C	2,5Y/6/3	2,5Y/7/3	sab	a, w	R1	30,1	47,1	17,1	5,7	7,9	7,5	0,21
Lois 2	Lois 2/1	Karbonathaltige Reliktbraunerde über Amphibolit - Endopetric Calcisol (Chromic)	0 - 45/50	Ap	10YR/4/3	10YR/6/3	ab, gr	a, s	R3	24,5	29,9	25,4	20,1	7,6	7,2	0,91
	Lois 2/2		45/50 - 170/180	Brel1	7,5YR/4,5/6	7,5YR/6/6	sab, gr	a, w	R2	6,1	17,2	33,3	43,5	7,8	7,5	0,22
	Lois 2/3			Brel1	7,5YR/4,5/6	7,5YR/6/6	sab, gr	g, w	R2	4,2	17,2	31,1	47,5	7,9	7,5	0,15
	Lois 2/4		170/180 - 220/230	Brel2	7,5YR/4/6	7,5YR/4/6	ab	g, w	R1	11,0	17,7	23,1	48,2	8,0	7,6	0,19
	Lois 2/5		220/230 - 310/340	BrelCv	7,5YR/4/6	7,5YR/4/6	ab	a, w	R1	14,0	23,3	20,0	42,6	8,0	7,6	0,18
	Lois 2/6			BrelCv	7,5YR/4/6	7,5YR/5/6	ab	a, w	R1	24,4	40,1	19,1	16,4	8,1	7,7	0,12
Lois 3	Lois 3/1	Karbonathaltige Parabraunerde aus reliktärem Lockersediment - Stagnic Hypercalcic Luvisol (Chromic)	0 - 25/30	Ap	10YR/3/2	10YR/4/3	ab, sab	a, s	R3	10,3	31,0	37,0	21,7	7,6	7,1	1,78
	Lois 3/2		25/30 - 60	Bh	10YR/4/3	7,5YR/5/4	sab, gr	a, w	R2	4,1	20,9	33,9	41,1	7,8	7,3	0,57
	Lois 3/3		60 - 120/130	B(t)	7,5YR/4/4	7,5YR/5/6	sab, gr	a, w	R1	1,4	11,4	32,3	54,9	7,8	7,4	0,33
	Lois 3/4			B(t)	7,5YR/4/6	7,5YR/6/6	sab, gr	a, w	R1	3,3	10,4	38,1	48,2	8,0	7,5	0,19
	Lois 3/5		120/130 - 190/200	Brel1	7,5YR/4,5/4	7,5YR/6/4	ab	g, w	R0	1,8	11,7	39,1	47,4	8,1	7,7	0,13
	Lois 3/6			Brel1	7,5YR/4/4	7,5YR/6/4	ab	g, w	R0	2,7	14,0	36,4	46,9	8,2	7,7	0,10
	Lois 3/7		190/200 - 290/300	Brel2	7,5YR/4/6	7,5YR/5/6	ab	g, w	R0	6,4	9,5	27,6	56,5	8,0	7,8	0,20
	Lois 3/8			Brel2	5YR/4,5/6	5YR/5/6	ab	g, w	R0	6,9	10,9	24,9	57,3	8,2	7,8	0,15
	Lois 3/9		290 - 409	Brel3	7,5YR/6/6	7,5YR/6/6	ab	g, w	R0	23,7	24,7	14,8	36,8	8,3	8,0	0,21
	Lois 3/10		409 - 460	Brel4	7,5YR/4/5	7,5YR/4/4	ab	g, w	R0	3,8	9,3	6,1	80,8	8,1	7,8	0,17
Lois 4	Lois 4/1	Karbonath. Parabraunerde aus reliktärem Lockersediment - Stagnic Hypercalcic Luvisol (Chromic)	0 - 20/25	Ap	10YR/4/3	10YR/5/4	gr	a, s	R3	7,2	23,3	32,2	37,3	7,6	7,2	1,01
	Lois 4/2		20/25 - 90/95	Brel1	5YR/4/6	5YR/5/6	ab	g, w	R1	2,3	10,1	25,0	62,6	7,8	7,4	0,25
	Lois 4/3		90/95 - 140	Brel2	7,5YR/5/6	7,5YR/6/6	ab	g, w	R1	9,9	33,8	24,1	32,2	8,1	7,6	0,13
Lois 5	Lois 5/1	Schüttungs- (Planie-)boden über skelettreicher karbonathaltiger Reliktbraunerde - Technic Cambisol (Chromic, Hypoepiskeletic)	30 - 0	Y	10YR/4/2	10YR/5/3,5				24,7	38,7	23,6	13,0	7,8	7,5	0,52
	Lois 5/2		0 - 15	Ap	10YR/4/3	10YR/4,5/3	sab, gr	a, s	R2	19,7	36,2	24,7	19,4	7,5	7,2	0,73
	Lois 5/3		15 - 120	BrelCv1	7,5YR/4/6	7,5YR/6/6	ab	g, s	R1	42,9	30,3	11,6	15,2	7,8	7,3	0,18
	Lois 5/4		120 - 200	BrelCv2	7,5YR/4/6	5YR/5/6	ab	g, s	R1	30,5	28,5	17,6	23,5	7,9	7,5	0,11
Lois 6	Lois 6/1	Schüttungs- (Planie-)boden über karbonathaltigem Grobmaterial- Rohboden - Technic Leptosol (Hypoepiskeletic)	+250 - 150	Y	10YR/4/3	10YR/5/3				18,1	42,0	26,7	13,2	7,5	7,2	0,84
	Lois 6/2		+150 - 0	YCv	10YR/4/3	10YR/5,5/3				25,5	37,5	23,0	14,0	7,7	7,5	0,56
	Lois 6/3		0 - 40	Cv1	2,5Y/6/3	2,5Y/7/2	sg	g, w	R0	54,9	32,5	8,8	3,8	7,8	7,6	0,36
	Lois 6/4		40 - 80	Cv2	2,5Y/4/3	2,5Y/6/3	sg	g, w	R0	45,1	43,0	10,1	1,8	8,2	7,6	0,40
	Lois 6/5		80 - 130	Cv3	2,5Y/4/3	2,5Y/6/4	sg	g, w	R0	29,4	52,6	15,6	2,4	8,2	7,6	0,10
	Lois 6/6		130 - 230	Cv4	2,5Y/4/4	2,5Y/6/4	sg	g, w	R0	52,6	31,7	13,2	2,5	7,9	7,6	0,15
	Lois 6/7		230 - 400	Cv5	2,5Y/5/4	2,5Y/6/4	sg	g, w	R0	25,3	48,8	18,7	7,3	8,1	7,7	0,23

Structure: sab = subangular blocky, ab = angular blocky, gr = granular, sg = single grain structure
Distinctness and topography of horizon boundaries: a = abrupt, g = gradual, s = smooth, w = wavy
Roots: R0 = none, R1 = few, R2 = moderate, R3 = many

ASCS = Austrian Soil Classification System; WRB = World Reference Base for Soil Resources

Table 2: Dithionite- and oxalate extractable fraction of the pedogenic oxides of profiles Lois 1 to 6.

Tab. 2: Dithionit- und oxalatlösliche Fraktion der pedogenen Oxide der Profile Lois 1 bis 6.

Profile	Horizon[1]/Depth	Fe_o (g/kg)	Al_o (g/kg)	Mn_o (g/kg)	Fe_d (g/kg)	Al_d (g/kg)	Mn_d (g/kg)	Fe_t (g/kg)	Fe_d/Fe_t	Fe_o/Fe_d
Lois 1	Ap - 40 cm	0,47	0,32	0,23	2,97	0,12	0,16	47,90	0,06	0,16
	BwCv - 70 cm	0,29	0,20	0,16	2,82	0,11	0,11	42,94	0,07	0,10
	Cv - 120 cm	0,11	0,09	0,05	2,51	0,08	0,04	48,16	0,05	0,04
	C - 140 cm	0,08	0,08	0,07	1,34	0,01	0,05	35,59	0,04	0,06
Lois 2	Ap - 25 cm	0,45	0,33	0,29	2,88	0,15	0,18	42,33	0,07	0,16
	Brel1 - 100 cm	0,27	0,28	0,31	2,29	0,11	0,19	33,53	0,07	0,12
	Brel1 - 170 cm	0,27	0,29	0,45	1,96	0,13	0,25	34,69	0,06	0,14
	Brel2 - 220 cm	0,30	0,33	0,46	2,91	0,19	0,32	49,72	0,06	0,10
	BrelCv - 270 cm	0,36	0,44	0,42	2,75	0,20	0,25	50,08	0,05	0,13
	BrelCv - 310 cm	0,35	0,50	0,28	2,37	0,17	0,15	55,43	0,04	0,15
Lois 3	Ap - 30 cm	0,68	0,56	0,38	2,87	0,18	0,19	38,40	0,07	0,24
	Bh - 60 cm	0,63	0,65	0,30	3,13	0,24	0,16	39,26	0,08	0,20
	B(t) - 90 cm	0,85	0,91	0,22	3,90	0,31	0,13	41,55	0,09	0,22
	B(t) - 120 cm	0,47	0,51	0,27	3,44	0,22	0,16	37,63	0,09	0,14
	Brel1 - 150 cm	0,32	0,28	0,24	2,21	0,11	0,13	30,26	0,07	0,14
	Brel1 - 190 cm	0,34	0,24	0,26	2,30	0,11	0,17	29,06	0,08	0,15
	Brel2 - 240 cm	0,67	0,47	0,23	3,65	0,24	0,16	41,84	0,09	0,18
	Brel2 - 290 cm	0,64	0,48	0,10	4,87	0,03	0,07	46,78	0,10	0,13
	Brel3 - 409 cm	1,01	0,60	0,88	2,85	1,21	0,41	62,40	0,05	0,35
	Brel4 - 460 cm	1,16	1,02	0,29	4,46	1,45	0,16	35,07	0,13	0,26
Lois 4	Ap - 20 cm	0,78	0,52	0,26	2,78	0,15	0,15	37,54	0,07	0,28
	Brel1 - 90 cm	0,80	0,59	0,07	4,83	0,33	0,05	45,84	0,11	0,17
	Brel2 - 140 cm	0,62	0,39	0,32	2,09	0,12	0,39	25,42	0,08	0,30
Lois 5	Y - +30 - 0 cm	0,51	0,31	0,20	5,55	0,13	0,16	54,04	0,10	0,09
	Ap - 15 cm	0,73	0,42	0,32	3,36	0,17	0,18	53,62	0,06	0,22
	BrelCv1 - 120 cm	0,44	0,31	0,46	5,23	0,29	0,31	61,24	0,09	0,08
	BrelCv2 - 200 cm	0,54	0,28	0,42	5,55	0,29	0,29	63,51	0,09	0,10
Lois 6	Y - +250 - 150 cm	0,73	0,40	0,27	3,36	0,17	0,17	51,11	0,07	0,22
	YCv - +150 - 0 cm	0,68	0,44	0,21	3,49	0,15	0,12	60,13	0,06	0,20
	Cv1 - 40 cm	0,19	0,16	0,10	6,10	0,06	0,11	69,44	0,09	0,03
	Cv2 - 80 cm	0,25	0,21	0,17	3,63	0,03	0,12	71,48	0,05	0,07
	Cv3 - 130 cm	0,09	0,10	0,07	2,76	0,06	0,06	61,57	0,04	0,03
	Cv4 - 230 cm	0,10	0,10	0,08	3,12	0,07	0,09	84,52	0,04	0,03
	Cv5 - 400 cm	0,47	0,18	0,26	3,21	0,02	0,14	36,60	0,09	0,15

[1] According to Austrian Soil Classification System

Profile	Horizon[1]/Depth	Qu	K-Fsp	Plag	Calc	Sh.si.	Hbl	Acc	Verm	Smec	Illite	Kao	Chl
Lois 1	Ap - 40 cm	26	4	13	27	10	20		2	48	31	15	4
	BwCv - 70 cm	14	2	11	45	8	22		1	47	28	15	9
	Cv - 120 cm	3	0	14	43	3	36		Sp	55	17	12	16
	C - 140 cm	4	0	12	49	7	27		Sp	65	12	13	10
	G 1/1 - 240 cm	0	0	4	0	0	96	Zoi, Chl					
	G 1/2 - 382 cm	0	0	4	0	0	96	Zoi, Chl, Rut, Tit					
	G 1/3 - 440 cm	4	0	3	0	0	92	Zoi, Chl, Pyx, Gr					
Lois 2	Ap - 25 cm	32	2	13	28	9	16		3	48	30	12	8
	Brel1 - 100 cm	22	2	4	41	20	11		5	43	39	9	4
	Brel1 - 170 cm	32	2	5	38	21	2		8	47	37	6	2
	Brel2 - 220 cm	31	2	2	7	56	1		7	49	41	3	1
	BrelCv - 270 cm	22	2	2	13	52	9		0	51	47	2	0
	BrelCv - 310 cm	7	0	6	6	50	30		8	67	22	2	0
	G 2/1 - 280 cm	4	0	3	0	0	93	Zoi, Chl, Gr, Tit					
	G 2/2 - 382 cm	0	0	4	96	0	0	Hbl					
Lois 3	Ap - 30 cm	49	6	9	6	23	6		6	46	30	15	3
	Bh - 60 cm	51	4	12	6	24	2		3	40	37	18	2
	B(t) - 90 cm	51	3	6	1	39	0		7	38	18	38	0
	B(t) - 120 cm	49	3	6	13	29	0		9	38	21	31	0
	Brel1 - 150 cm	36	3	5	32	21	3		9	47	17	25	2
	Brel1 - 190 cm	48	3	5	17	27	0		8	41	23	26	1
	Brel2 - 240 cm	45	3	3	6	43	0		5	39	27	29	0
	Brel2 - 290 cm	34	2	3	11	50	0		9	24	29	38	0
	Brel3 - 409 cm	40	2	2	31	25	0		4	56	32	8	0
	Brel4 - 460 cm	17	2	0	2	80	0		5	55	36	4	0
Lois 4	Ap - 20 cm	43	4	9	9	25	11		0	39	36	25	Sp
	Brel1 - 90 cm	46	6	3	3	41	0		0	36	43	21	0
	Brel2 - 140 cm	62	2	1	13	21	0		0	55	35	10	Sp
Lois 5	Y - +30 - 0 cm	24	3	13	28	15	17		5	73	9	7	6
	Ap - 15 cm	30	2	15	19	14	20		8	56	20	9	7
	BrelCv1 - 120 cm	19	2	17	22	31	9		7	73	13	5	2
	BrelCv2 - 200 cm	33	2	11	2	45	8		9	54	26	7	4
Lois 6	Y - +250 - 150 cm	36	3	17	7	19	19		7	29	37	16	11
	YCv - +150 - 0 cm	26	3	15	17	17	23		9	54	17	0	20
	Cv1 - 40 cm	5	1	8	51	5	31		0	90	0	0	10
	Cv2 - 80 cm	12	2	15	36	9	26		0	87	0	0	13
	Cv3 - 130 cm	5	2	8	52	19	14		0	89	0	0	11
	Cv4 - 230 cm	52	3	6	20	12	7		0	97	0	0	3
	Cv5 - 400 cm	16	3	11	37	19	15		0	60	13	14	13
	G 6/1 - 330 cm	16	18	5	59	0	2				13		

Column headers of the table: Soil mineralogical composition | Clay minerals in the < 2 μm

[1] According to Austrian Soil Classification System

Qu = Quartz, **K-Fsp** = Kali Feldspar, **Plag** = Plagioclase, **Kalz** = Calzite, **Sh.si** = Sheet silicate, **Hbl** = Hornblende,
Akc = Akcessories, **Chl** = Chlorite, **Gr** = Garnet, **Pyx** = Pyroxene, **Rut** = Rutile, **Tit** = Titanite, **Zoi** = Zoisite
Verm = Vermiculite, **Smek** = Smectite, **Kao** = Kaolinite, **Chl** = Chlorite

Table 3: Soil mineralogical and clay mineralogical composition of the rock and soil samples of the profiles Lois 1 to 6 in %.

Tab. 3: Gesamt- und tonmineralogische Zusammensetzung der Gesteins- und Bodenproben der Profile Lois 1 bis 6 in %.

Table 4: Major and trace elements in the soil profiles and the sampled rocks of the profiles Lois 1 to 6 in % (major elements) and ppm (trace elements); (H_2O^- = loss on drying at 105 ℃; H_2O^+ = LOI-H_2O^--CO_2-Hydroxide-Phosphate-Sulfide).

Tab 4: Gehalt an Haupt- und Spurenelementen in den Horizonten und den entnommenen Gesteinen der Profile Lois 1 bis 6 in % (Hauptelemente) und ppm (Spurenelemente); (H_2O^- = Trocknungsverlust bei 105 ℃; H_2O^+ = GV-H_2O^--CO_2-Hydroxide-Phosphate-Sulfide).

Profile	Horizon[1]/Depth	SiO_2	TiO_2	Al_2O_3	Fe_2O_3	MnO	MgO	CaO	Na_2O	K_2O	H_2O^-	P_2O_5	CO_2	SO_3	(H_2O^+)[2]	Σ	Ba	Co	Cr	Cs	Cu	Ni	Pb	Rb	Sr	V	Y	Zn	Zr	Σ
Lois 1	Ap - 40 cm	46,5	0,80	12,23	6,85	0,14	3,69	13,63	1,45	1,57	1,69	0,35	10,77	0,14	0,10	99,90	138	12	103	5	64	51	23	64	311	152	25	112	137	1494
	BwCv - 70 cm	35,0	0,50	8,63	6,14	0,10	3,56	24,27	1,15	0,89	1,51	0,23	17,53	0,12	0,20	99,84	283	17	97	2	91	59	19	43	368	155	16	70	80	1299
	Cv - 120 cm	29,5	0,31	6,57	6,89	0,08	4,25	29,71	0,93	0,30	1,16	0,11	19,53	0,11	0,60	100,03	220	23	164	<1,5	82	79	6	14	449	189	9	45	24	1303
	C - 140 cm	29,0	0,31	6,55	5,09	0,08	3,80	31,49	0,93	0,33	1,13	0,10	20,46	0,11	0,60	100,00	213	21	244	<1,5	76	124	7	16	438	122	9	45	35	1365
	G 1/1 - 240 cm	48,0	0,54	15,37	8,48	0,12	10,51	12,05	2,28	0,20	0,37	0,04	0,26	0,00	1,50	99,72	129	18	776	3	81	102	2	7	294	317	9	55	18	1811
	G 1/2 - 382 cm	47,5	0,59	15,24	7,64	0,12	11,07	13,35	2,88	0,25	0,24	0,03	0,27	0,01	1,00	100,18	56	14	496	<1,5	34	40	4	7	331	405	10	57	19	1472
	G 1/3 - 440 cm	44,0	0,39	17,25	11,06	0,13	10,40	10,50	2,84	0,29	0,59	0,05	0,12	0,01	2,30	99,99	128	28	322	<1,5	284	195	2	10	321	265	7	60	15	1636
Lois 2	Ap - 25 cm	48,0	0,76	12,86	6,05	0,14	3,15	12,02	1,65	1,75	1,84	0,34	11,33	0,10	0,10	100,14	354	13	100	<1,5	127	47	27	77	262	135	27	104	164	1436
	Brel1 - 100 cm	40,0	0,54	12,00	4,79	0,12	2,43	18,58	0,97	1,91	2,28	0,28	13,61	0,04	2,30	99,84	375	9	79	<1,5	52	43	20	87	184	99	25	88	162	1224
	Brel1 - 170 cm	44,0	0,57	12,43	4,96	0,16	2,72	15,07	1,07	2,14	2,77	0,28	11,32	0,04	2,50	100,03	403	10	83	<1,5	54	45	23	97	192	112	27	103	159	1305
	Brel2 - 220 cm	52,0	0,67	16,73	7,11	0,17	2,91	4,21	1,32	2,83	4,56	0,12	3,29	0,03	4,00	99,95	413	9	118	3	65	57	25	130	140	153	22	151	137	1422
	BrelCv - 270 cm	47,0	0,59	16,74	7,16	0,17	3,49	7,23	1,15	2,45	4,59	0,13	4,28	0,03	5,30	100,32	364	9	141	2	68	72	19	113	203	142	19	133	109	1394
	BrelCv - 310 cm	47,0	0,50	19,24	7,93	0,13	3,90	6,71	1,37	1,82	5,35	0,11	1,90	0,02	4,15	100,32	254	10	327	<1,5	61	86	13	81	254	179	26	109	54	1454
	G 2/1 - 280 cm	46,5	0,42	20,11	7,21	0,10	7,26	11,05	2,36	0,43	1,74	0,50	0,45	0,01	1,90	100,03	332	15	450	<1,5	49	85	3	14	1051	162	14	51	17	2244
	G 2/2 - 382 cm	3,1	0,04	1,25	0,61	0,01	1,12	51,00	<0,15	0,04	1,87	0,14	39,98	0,14	0,45	99,74	351	3	41	4	24	13	3	4	480	<10	2	16	<1	937
Lois 3	Ap - 30 cm	52,5	0,71	15,22	5,49	0,14	2,38	4,32	1,71	2,22	2,78	0,33	11,97	0,25	0,10	100,11	389	11	118	4	128	49	27	100	131	116	33	97	226	1428
	Bh - 60 cm	56,5	0,76	16,98	5,61	0,12	2,33	3,77	1,63	2,27	2,87	0,17	4,94	0,09	1,90	99,94	393	10	96	3	45	47	23	106	110	108	35	87	289	1353
	B(t) - 90 cm	57,5	0,81	19,04	5,94	0,08	2,13	1,29	1,73	2,42	3,59	0,08	1,65	0,08	3,70	100,05	425	10	101	3	42	44	25	120	93	120	35	89	329	1435
	B(t) - 120 cm	54,0	0,78	17,52	5,58	0,09	2,25	5,04	1,55	2,26	2,71	0,09	4,51	0,05	3,60	99,84	407	10	94	3	40	43	24	119	100	108	38	85	330	1401
	Brel1 - 150 cm	47,5	0,72	14,36	4,33	0,08	2,32	12,58	1,37	2,02	2,26	0,14	9,32	0,06	3,00	100,03	382	8	76	2	37	37	21	104	143	88	35	72	302	1304
	Brel1 - 190 cm	54,5	0,84	15,32	4,15	0,10	2,45	7,72	1,64	2,17	2,27	0,16	5,88	0,06	3,00	100,25	404	10	82	3	33	32	27	107	142	86	37	72	376	1410
	Brel2 - 240 cm	54,5	0,85	19,90	5,98	0,08	2,36	1,98	1,46	2,44	3,62	0,08	1,73	0,06	4,90	99,93	404	9	98	6	46	38	26	136	89	129	30	99	313	1421
	Brel2 - 290 cm	49,0	0,80	20,68	6,69	0,08	2,89	3,46	1,46	2,27	3,94	0,13	3,07	0,03	5,30	99,77	350	7	114	3	50	47	26	126	105	144	24	101	238	1334
	Brel3 - 409 cm	47,0	0,73	19,92	8,92	0,09	3,49	0,40	1,34	2,75	3,39	0,17	8,52	0,01	3,20	99,92	345	10	158	2	79	78	20	142	105	176	51	163	113	1442
	Brel4 - 460 cm	48,0	0,75	13,43	5,01	0,16	2,75	10,95	1,21	1,83	6,64	0,17	0,72	0,03	8,50	100,12	366	11	97	<1,5	50	45	20	93	169	114	27	89	185	1266
Lois 4	Ap - 20 cm	53,0	0,75	15,76	5,37	0,14	2,46	5,62	1,51	2,17	2,74	0,26	9,84	0,12	0,10	99,82	361	10	118	4	140	52	26	100	123	121	32	90	281	1458
	Brel1 - 90 cm	52,5	0,83	21,05	6,55	0,04	2,41	1,88	1,40	2,31	4,03	0,10	1,81	0,01	5,15	100,08	371	9	113	5	46	44	24	134	85	138	23	97	271	1360
	Brel2 - 140 cm	63,5	0,89	11,70	3,63	0,19	1,92	6,15	1,39	1,67	2,41	0,12	4,38	0,04	2,10	100,08	355	12	114	4	38	33	25	75	131	87	28	63	280	1246
Lois 5	Y - +30 - 0 cm	48,0	0,94	12,38	7,73	0,15	3,73	12,38	1,72	1,36	2,01	0,31	8,19	0,10	0,75	99,81	333	13	182	6	74	50	23	86	276	186	26	101	133	1439
	Ap - 15 cm	48,5	0,89	14,50	7,67	0,17	3,60	9,52	1,46	1,68	2,35	0,40	8,91	0,21	0,10	99,95	394	16	131	<1,5	132	60	24	73	228	197	26	111	161	1552
	BrelCv1 - 120 cm	44,5	0,82	16,00	8,76	0,17	3,32	9,99	1,60	1,72	3,50	0,32	5,96	0,09	3,10	99,85	476	23	130	2	77	72	15	88	194	202	28	133	123	1558
	BrelCv2 - 200 cm	52,0	0,85	18,10	9,08	0,17	3,43	3,16	1,78	2,10	4,35	0,19	1,29	0,07	3,80	100,22	473	17	123	5	77	71	17	104	178	202	28	135	142	1571
Lois 6	Y - +250 - 150 cm	30,0	0,91	6,61	9,93	0,13	4,29	27,08	0,70	0,28	1,95	0,22	17,40	0,18	0,30	99,97	387	15	140	3	108	59	25	75	223	172	28	105	172	1511
	YCv - +150 - 0 cm	39,0	0,89	10,13	10,22	0,17	5,15	18,70	1,52	0,33	2,25	0,27	10,40	0,05	0,55	99,63	329	18	152	11	71	57	28	55	273	202	27	108	144	1475
	Cv1 - 40 cm	30,0	1,36	9,73	8,80	0,15	4,19	25,33	0,78	0,69	2,77	0,18	14,40	0,05	1,80	99,73	211	27	34	<1,5	78	35	5	12	327	224	12	66	37	1067
	Cv2 - 80 cm	38,5	0,88	9,68	12,08	0,19	5,67	16,74	0,78	0,46	2,77	0,15	8,33	0,05	3,40	99,69	197	23	58	<1,5	88	88	7	18	508	260	23	76	77	1381
	Cv3 - 130 cm	56,0	0,84	8,32	5,23	0,10	2,77	12,24	1,81	0,98	1,56	0,21	7,17	0,08	2,77	100,08	152	14	29	<1,5	32	19	8	40	389	173	21	62	62	1000
	Cv4 - 230 cm	53,5	1,41	13,76	8,30	0,11	3,32	11,42	2,27	2,39	0,83	0,40	1,57	0,01	0,60	99,89	181	15	35	<1,5	41	31	10	34	200	203	26	99	72	939
	Cv5 - 400 cm	30,0	0,91	6,61	9,93	0,13	4,29	27,08	0,70	0,28	1,95	0,22	17,40	0,18	0,30	99,97	214	12	54	<1,5	47	45	12	39	267	76	22	48	162	997
	G 6/1 - 330 cm	39,0	0,89	10,13	10,22	0,17	5,15	18,70	1,52	0,33	2,25	0,27	10,40	0,05	0,55	99,63	660	11	98	2	48	38	8	80	526	173	20	58	104	1824

[1] According to Austrian Soil Classification System
[2] LOI = Loss on ignition (1000° C)

Geochemistry

In the doctoral thesis of Hödl (1985), seven samples of 'Rehberg'-amphibolite (loc. typ.) were examined by microanalysis. The contents in the rock sample of Lois 1 are in good accordance with the reported contents of major elements, where the trace elements show some deviations. The higher values of Cr, Cu, Ni and Sr of the Lois 1 samples, however, agree with the contents of the amphibolites from the 'Buschandlwandzug', which are also published as well in the dissertation of Hödl (1985) (Tab. 4). The elevated contents of K, P, and Cu in the uppermost (Ap-)horizon of profile Lois 1 are a consequence of the agricultural use (Tab. 4). The Ca-contents reflect the high amounts of calcite. The results of the geochemical analyses emphasize the missing flows between rock and soil, which may be due to the c alc-sinter layer, as discussed in the Mineralogy section.

Profile Lois 2

Soil physical and chemical parameters

The examination of the chemical parameters of profile Lois 2 showed that the pH-value shows no dynamic behaviour (comparable to profile Lois 1) with values between 7.2 and 7.7 (Tab. 1). The content of organic C is very low, with 0.91 % in the uppermost (Ap-)horizon, which then decreases sharply to 0.22 % in the Brel1-horizon and reaches its minimum of 0.12 % in the lowermost (BrelCv)-horizon. In the Brel2-horizon (170–220 cm), the dithionite-extractable Fe-oxides reach their maximum, but still are in a very low range (Tab. 2). The share of amorphous (active) Fe is small, which is due to a low pedogenetical activity, which is similar to profile Lois 1. The particle size analysis reveals distinct relocation dynamics in the sediments. The gravel content is 25 % in the uppermost horizon (Ap), decreases to 4–11 % in the fossil horizons and increases again in the BrelCv-horizons to 14 and 24 %, respectively. The sand fraction shows a similar distribution pattern. Silt is slightly enriched in the Brel1-horizon with a content of 33 %, whereas it is between 19 and 25 % in the other horizons. The clay fraction shows the strongest dynamical behaviour with clear illuvation features in the lower horizons. In the Ap-horizon the clay content is 20 %, increasing to 43–48 % in the Brel1-, Brel2-, and the upper part of the BrelCv-horizon. In the lower part of the BrelCv-horizon the clay content decreases again to 16 % (Tab. 1). The soil texture of profile Lois 2 is loam in the uppermost horizon Ap, and in the lower horizons loamy clay to clay. Detailed investigations of profile Lois 2 can be taken from Haslinger & Heinrich (2008).

Profile Lois 2 shows no dynamic and active pedogenetical processes. However, the intense clay illuvation in the fossil horizons, particularly the Brel2-horizon, is noticeable.

Mineralogy

The rock sample G2/1 (BrelCv, 280 cm) corresponds to the 'Rehberg'-amphibolite with regard to mineralogy. However, the sample G2/1 sample shows a strong alternate layering, which is in contrast to the amphibolites of Lois 1. The layers which merely contain amphiboles are often very coarse, whereas the layers which contain amphibole, feldspar and clinozoisite are very fine-grained. The sample of G2/2 (Brel-

Cv, 380 cm), is very fine grained and predominated by carbonate in primarily dense layers or as framboidal components. Apart from carbonate, quartz, and feldspar; lithic fragments of amphibolite could be found. From the analysis of the thin section it can be concluded that this sample is a calc-sinter. As discussed in the chapter of Profile Lois 1, this calc-sinter could be a product of decalcification of loess or a weathering product of the marble on the western flank (profiles Lois 5 and 6) of the outcrop, or both. The mineral and lithic fragments of plagioclase and amphibole as well as the alternate layering of carbonate and silicate are a sign that detritus from the weathering of the amphibolite was deposited on top of the calc-sinter in colder periods (winter), subsequently followed by a mobilisation of carbonate-rich fluids from the marble in warmer periods (spring), which has lead to a precipitation of the calc-sinter in the profiles on the northern flank (profiles Lois 1 and 2), and to the intense carbonate illuviation in profiles Lois 1–4 and 7.

The thin section photographs of the rock samples of profile Lois 2 can be taken from Haslinger & Heinrich (2008).

The mineralogical composition of the soil horizons of profile Lois 2 shows a predominance of quartz, calcite and sheet silicates (Tab. 3). The quartz content is relatively stable (22–32 %) down to a depth of 270 cm below surface and decreases strongly in the lower part of the BrelCv-horizon (7 %). Calcite can be found primarily in the uppermost 170 cm and shows a strong decrease below the Brel2-horizon (220 cm) to 6–13 %. The sheet silicate content has an inverse distribution pattern. In the upper part of the profile (down to Brel1) the sheet silicates occur in moderate amounts (up to 21 %), whereas they increase significantly below the Brel2-horizon with contents of up to 56 %.

As in profile Lois 1 it could be observed that the influence of the host rock amphibolite is rather low. The calc-sinter apparently seals the contact between rock and solum. This fact is emphasized by the complete absence of chlorite in the lower horizons of Lois 2. If the weathering of the amphibolite played a role for the pedogenesis of the lowermost horizons, the chlorite content would be significantly higher or at least not lower than in the upper parts of the profile.

The clay mineralogical composition is dominated by smectite and illite. They show the same distribution pattern as in profile Lois 1 – from top to bottom the smectite increases and the illite decreases. Smectite occurs mainly in the classical low-charged form, which is demonstrated by the contraction of the 14 Å-peak to approximately 12 Å upon K-saturation (and not to 10 Å which would be typical for vermiculite). Kaolinite and chlorite occur only in minor amounts; vermiculite is missing almost entirely. The slightly increased content of (detrital) chlorite in the Ap-horizon points to an aeolian nature of the chlorite. Additionally, below the second horizon (Brel1, lower part) mixed-layer clay minerals occur at peaks between 30 and 34 Å, which emphasize the stronger weathering intensity in the fossil horizons. The calcite enrichment in the soil profiles down to the Brel1-horizon (170 cm) is due to the presence of the calc-sinter (rock sample G2/2), which is a product of the weathering of the marble on the western flank or from formerly superimposed carbonate-rich sediments (loess), respectively, as discussed above.

Geochemistry

The geochemical analyses of soil profile Lois 2 show similar contents and lack of soil dynamics, as in profile Lois 1. The influence of the agricultural use is only visible in the elevated Cu-values in the Ap-horizon; the K- and P-contents are not higher, unlike in profile Lois 1 (Tab. 4). The most important difference is the occurrence of the sinter-like rock (G 2/2). However, the Sr-contents in the amphibolite (G 2/1) are exceptionally high. Such high Sr-values are not reported in the doctoral thesis of Hödl (1985). An examination with SEM and microanalysis showed that the Sr does not come from the rock, but from the carbonate crust, which covers the amphibolite. Calcite (and especially its rhombic modification aragonite) is a known trap for Sr, where the Ca is substituted by the Sr.

Profile Lois 3

Soil physical and chemical parameters

As in the other two profiles, the pH-values are relatively constant. However, in the lower part of the B(t)-horizon (from 90 cm) the pH-value increases to over 8 (Tab. 1). The C_{org}-content is only slightly elevated in the uppermost (Ap-) horizon and decreases strongly in the Bh-horizon (0.6 %) and even more in the B(t)- and Brel-horizons (0.1 and 0.3 %). The pedogenic oxides are slightly higher than in the other two profiles, primarily in the fossil horizons (Tab. 2).

From the particle size distribution it can be seen that profile Lois 3 is high in clay content. Due to ploughing, the Ap-horizon shows a homogeneous mixture of sand, silt, and clay, with a gravel content of about 10 %. The lower horizons (Bh to Brel3) have a significantly higher clay content (between 41 and 57 %); the silt contents are between 32 and 39 %. Sand occurs only in minor amounts between 10 and 21 %. A sharp change of texture can be observed in the Brel3-horizon. This is due to the higher sand and gravel content (25 and 24 %) and a lower silt and clay content at 15 and 37 %, respectively. In the lowermost horizon (Brel 4), the texture changes again and the clay content reaches its maximum of 81 % (Tab. 1). The soil texture in the uppermost horizon (Ap) is sandy loam and loamy clay to clay in the lower horizons.

Detailed descriptions of profile Lois 3 can be taken from Haslinger & Heinrich (2008).

Mineralogy

The mineralogical composition of the soil samples in the horizons Ap to Brel3 of profile Lois 3 is dominated by quartz (34–51 %) and sheet silicates (21–50 %) (Tab. 3). In the Brel4-horizon the quartz content decreases sharply to 17 %, whereas the content of sheet silicates shows a sharp increase to 80 %, which is in good agreement with the results of the particle size analysis (clay content 81 %). The proportion of calcite is varying in the profile, with higher contents in the Brel1- and Brel3-horizon (17 and 32 %). The contents of feldspar and hornblende are very low.

The clay mineralogical analyses show a predominance of smectite, illite and kaolinite. Vermiculite and chlorite can only be observed in traces. In comparison to profile Lois 2, the kaolinite content is higher, which can be a result of the longer weathering processes the fossil horizons have undergone or from aeolian processes, where it is a product of the

weathering of feldspar from the amphibolite or the granites and gneisses of the Bohemian Massif. However, the longer weathering processes are also evident from the broader illite-peaks (10 Å).

Geochemistry

The distribution patterns of both the major and trace elements of the soil samples of profile Lois 3 are relatively constant over the whole profile and show no dynamical behaviour (Tab. 4). As in the other profiles, the Ap-horizon is enriched in P, S and Cu due to fertilization and phytosanitary measures. The only noticeable enrichment is that of Zr, which reflects the stro nger weathering processes the sediments in this profile have undergone.

Parallels between the profiles Lois 3 and Lois 7 will be discussed in the chapter of the soil micromorphological results of the neighbouring profile Lois 7.

Profile Lois 4

Soil physical and chemical parameters

The particle size distribution of profile Lois 4 shows a relatively homogeneous mixture, similar to profile Lois 3. The horizon Brel1 of Lois 4 corresponds to Brel2 of Lois 3; and Brel2 of Lois 4 corresponds to Brel3 of Lois 3, which is emphasized by the similar grain size distributions in these two profiles. However, the gravel content in the Brel2-horizon is lower than in the Brel3-horizon of Lois 3. The gravel enrichment however seems to be only a local phenomenon (Tab. 1). The soil texture of the Ap-horizon is loam and in the lower parts of the profile loamy clay to clay. The Brel1-horizon shows a strong enrichment in Fe-oxides, resulting in an intense red colouration (Tab. 2).

Mineralogy

Profile Lois 4 is dominated by quartz – especially in the Brel2-horizon – and sheet silicates (Tab. 3). The calcite content is surprisingly low given that the entire Brel2-horizon is covered by secondary carbonates. Apparently, the carbonate illuviation is not sufficient to significantly raise the proportion of calcite. In the Brel1-horizon illuviation of secondary carbonates occurs additionally on the surface of the aggregates and in the vertical and horizontal fissures and cracks. However, there is no significant increase in the calcite content. The quartz content is exceptionally high in the lowermost Brel2-horizon (62 %). Elevated quartz contents could also be observed in the profile Lois 3, whereas in this profile the quartz content does not exceed 51 %. The quartz cannot be a product of the underlying host rock alone, since the amphibolites contain only small amounts of quartz. Therefore, the quartz must also have a different source. Either it was blown in by wind from near loess deposits, or it was flushed in with sandy, Neogene material. In the area around Langenlois, deposits of quartz-rich Upper Miocene ('Pannonium') sediments, gravelly-sandy sediments of the so-called 'Hollabrunn-Mistelbach-Formation', and Middle Miocene ('Badenium') interbedded strata of conglomerate-marl-sand of the so-called 'Hollenburg-Karlstetten-Formation' are known (Roetzel 2002). These three sediment types possibly could have formed the basis of the profiles Lois 3 and 4, particularly in the Brel2-horizon.

Geochemistry
The geochemical analyses reflect the mineralogy of Lois 4. Furthermore, the contents of major and trace elements in the horizons Brel1 and Brel2 are in good accordance with their corresponding horizons in Lois 3 (Brel2 and Brel3) (Tab. 4). As in profile Lois 3, this profile shows no sign of dynamic pedogenesis. Comparable to Lois 3 are the elevated Cu-contents in the Ap-horizon and a Zr-enrichment in the entire profile, which is a sign of intense weathering processes.

Profile Lois 5

Soil physical and chemical parameters
The profile Lois 5 is a disturbed profile with backfill material (horizon designation Y) of 30 cm on top, which is a homogeneous mixture of gravel, sand, silt and clay, as in the Ap-horizon below (Tab. 1). The underlying fossil horizons BrelCv1 and BrelCv2 are mixed with the weathered host rock to a large extent, which leads to gravel contents of 43 and 31 % and sand contents of 30 and 29 %, respectively. The silt contents (12 and 18 %) and clay contents (15 and 24 %) are significantly lower. The soil texture of profile Lois 5 is sandy loam to loam. The pedogenic oxides in the Ap-horizon are lower than in the Ap-horizons of the other profiles, which lead to the conclusion that material from the lower horizons was used for the backfilling (Tab. 2).

Mineralogy
The mineralogical composition of profile Lois 5 is dominated by quartz, calcite and sheet silicates (Tab. 3). Plagioclase and hornblende exist in moderate amounts, and K-feldspar only in low amounts. The comparably high contents of hornblende in the backfill material and in the Ap-horizon cannot be a product of weathering processes, but must be derived from wind-blown detrital material.

The clay mineralogical composition of Lois 5 is different from the other profiles with respect to the very high smectite content. The amphibolite in this profile is more fragmented mechanically than the amphibolites in the other profiles and is therefore more chemically and mineralogically altered. As a consequence, more smectite could form in this profile, wheras in the other profiles, the illite still predominates. The mineralogy of the backfill material is comparable to the mineralogy of the lower horizons. Therefore, it can be concluded, that it is material from local sources. The low amounts of mixed-in construction debris seems to have no effect on the mineralogical and geochemical composition of this profile.

Geochemistry
The distribution of the chemical elements in profile Lois 5 is very stable and shows no dynamics (Tab. 4). Even the backfill material geochemically corresponds to the soil horizons below. Apparently, the backfill material has local sources and was only recently applied, since the Cu-content in the Ap-horizon is still high.

Profile Lois 6

Soil physical and chemical parameters
The profile Lois 6 is a partially disturbed profile with 250 cm

backfill material on top (horizons Y and YCv). This material is mixed with the weathered host rock as well as construction debris. Its gravel content is 18 and 26 %; and the sand content is 42 and 38 %, respectively (Tab. 1). Silt exists in proportions of 23 and 27 %, whereas clay occurs only in minor amounts (13 and 14 %). The horizons below show no signs of active pedogenesis and consist nearly entirely of weathered host rock (amphibolite and marble). In the Cv-horizons the particle size distribution was between 25 and 55 % for gravel; 33 and 53 % for sand; and minor amounts for silt (9–19 %) and clay (2–7 %). The soil texture of Lois 6 is sandy loam to loam in the upper part (backfill material), and in the lower (Cv-) parts loamy sand to sand. The chemical parameters are stable throughout the soil profile, however, a significant enrichment of Fe-oxides with contents of 6.10 g/kg could be found in the backfill material and the uppermost horizon below (Cv1, 40 cm), which is about twice as much than in the other horizons (Tab. 2).

Mineralogy
Profile Lois 6 developed on two different host rocks and is therefore mineralogically very different compared to the other five profiles. One host rock is the 'Rehberg'-amphibolite, as in profiles Lois 1 and 2; the other host rock is marble, which occurs as light pink-grey-auburn layers in the amphibolite. These marbles are described in Hödl (1985) as minor constituents in the 'Rehberg-Formation' as well as part of the significant amphibolite-marble-body of the 'Buschandlwandzug'. From this profile, only the marble was sampled (rock sample G 6/1). Apart from limestone as main constituent, diopside, biotite and graphite could be identified as accessories in the thin section. Mineralogically, profile Lois 6 is inhomogeneous, which reflects the two very different host rocks (Tab. 3). The thick backfill material layer is dominated by quartz, followed by plagioclase, sheet silicates and hornblende. In the lower part of the backfill layer, the calcite content increases to 17 %. Starting from horizon Cv1, the calcite predominates. The clay mineralogical composition is completely different to the other profiles. The smectite contents reach extreme values of up to 97 % in the Cv4-horizon. Illite can only be found in the backfill material in minor amount; in the lower horizons it is completely absent. The clay mineralogical composition of the lowermost horizon and the backfill material is very similar. Therefore, it can be concluded that material from the bottom of the vineyard was used for the construction of the neighbouring terrace.

Geochemistry
Geochemically, profile Lois 6 is characterized by the two host rocks amphibolite and marble with high SiO_2- and Ca-values (Tab. 4). Additionally, elevated contents of Sr could be found in the marble sample as well as in the horizons Cv1 to Cv3. The upper layer of the backfill material shows the highest contents of Cu, from which it can be concluded that near-surface material was used for the construction of the backfill layers. A plough layer is missing in profile Lois 6, since the host rock reaches up to the surface of the outcrop. Only the construction of the terrace with the backfill material (250 cm) makes an agricultural usage of this profile possible.

Profile Lois 7

Profile Lois 7 was sampled by Pavel Havlíček, Oldřich Holásek and Michal Vachek. The soil micromorphological descriptions were carried out by Libuše Smolíková according to KUBIENA (1956). The horizons of profile Lois 7 continue on the eastern flank in the horizons of profile Lois 3, whereas horizon 'a' of Lois 7 corresponds to horizon 'Ap' in Lois 3; horizon 'b' to horizon 'Bh', horizon 'c' to horizon 'Bt', horizon 'd' to horizon 'Brel1', horizon 'e' to horizon 'Brel2', horizon 'f' to horizon 'Brel3' and horizon 'g' to horizon 'Brel4' (Fig. 3).
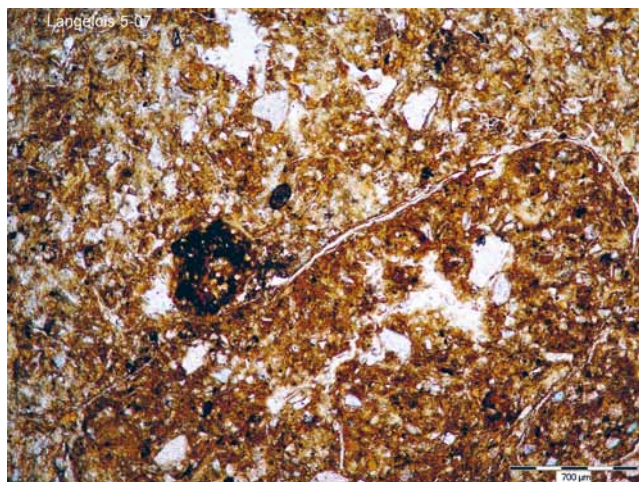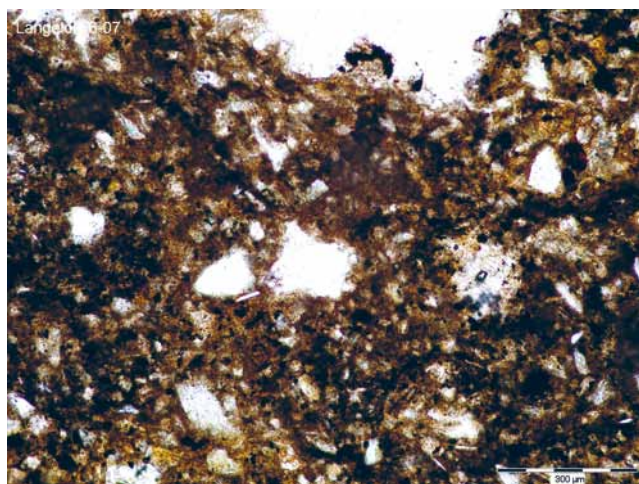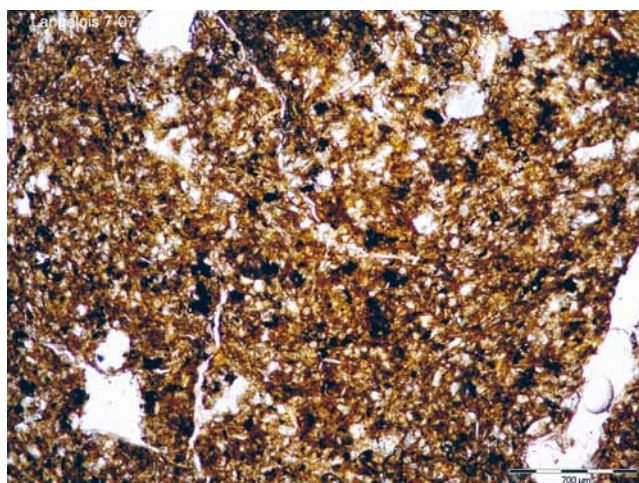
The increased clay content of the Luvisol can be observed in the soil thin sections of the upper two horizons of Lois 7 as well. It leads to the formation of numerous loamy concretions with sharp boundaries as well as an angular blocky structure and abrupt horizon boundaries in the Ap-horizon of Lois 3. Furthermore, stagnic properties could be observed in soil micromorphology which confirms the field observations for the two paleosols Lois 3 and 4. The mineralogical results of the micromorphology correspond very well with the mineralogy of Lois 3 which was measured with XRD. In the horizons 'b' and 'c' (Bh and Bt in Lois 3) garnet and

Fig. 3 a–g: Results of the soil micromorphological analyses of the horizons of profile Lois 7 from the uppermost (a) to the lowermost (g) horizon.

Abb. 3 a–g: Ergebnisse der bodenmikromorphologischen Analyse der Horizonte des Profils Lois 7 vom obersten (a) zum untersten (g) Horizont.

a) The deep yellowish brown to ochre yellow matrix (dry colour: 2,5 YR 5/6) is peptized. There are many spots, where the brown loam has fluidal structures and is highly birefringent. In the dense matrix only few quartz crystals can be found in the sand fraction. There are extraordinary big brown loam concretions, whereas some of them are broken. Weak stagnic properties in the form of Mn-concretions can be found. The entire matrix is distinctly layered. The horizontal fissures are empty; there are no calcite illuviations. The soil matrix is separated into angular aggregates by these fissures. The brown loam is in parautochthonous position.

b) The dark brown, but partially yolk-coloured matrix (dry colour: 5 YR 4/4) matrix consists of brown loam. The matrix is completely peptized, shows typical fluidal structures and a high optical activity. Furthermore, it is separated into distinct polyhedrons. Many cracks and fissures are present, which are broken very smoothly. The soil material is very fine-grained and corresponds to a silt with clayey components. The few sand grains are dominated by quartz, with rare occurrences of garnet, strongly weathered plagioclases and lithic fragments of quartzite. Many concretions of brown loam can be found, which show concentrical development. The pedogenetical signs in this horizon are very weak.

c) The reddish brown matrix (dry colour: 5 YR 6/4) is peptized with many plasmatic schlieren and fluidal structures. Many large brown loam concretions can be found, whereas Mn-concretions outbalance the Fe-concretions. Some of the concretions have a concentrical structure. The primary components are sandy, their mineralogical composition is diverse: quartz, plagioclase (fresh to weathered), orthoclase, mica, augite, amphibole, olivine, garnet, lithic fragments of quartzite etc. The structure is both primary (dense) and secondary (by pedogenesis) in the form of aggregates. The dense structure shows many cracks and fissures; in the aggregates many fine and medium pores could be found. There are signs of organism activities in the form of spherical aggregates, which have distinct boundaries and which are clearly darker than the surrounding matrix. These aggregates are coprolites of the fossil soil biota. The rare Mn-concretions sometimes have "explosive" boundaries. Few opal phytoliths can be found. The entire matrix is strongly recalcified (amorphous $CaCO_3$-modifications). The material of this horizon is brown loam derived from pedogenesis. After the formation of the brown loam during pedogenesis (climax stadium), this horizon was enriched with allochthonous components and carbonate and developed weak stagnic properties.
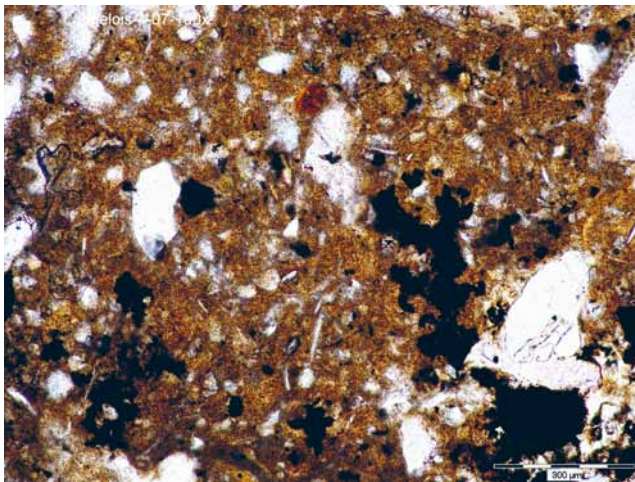
d) *The reddish brown and sometimes red matrix (dry colour: 5 YR 7/6) consists of peptized and sometimes flocculated plasma. However, the colouring of this horizon is not as uniform as in horizon c; additionally, orange and bifrefringent brown loam can be found. This orange loam seams the boundaries of the segregates and granules of the matrix as well as some pores. The structure of the horizon is very dense; most of the voids are cracks and fissures. The primary minerals are granulometrically larger than the minerals in horizon c. The sand fraction is dominated by quartz. Weak stagnis properties with abundant Mn-concretions can be found. Intense carbonate illuviations (amorphous $CaCO_3$-modifications) are present in the entire matrix, but also in the form of seams in the pores of the aggregates. This horizon is regarded as red loam, which is strongly polygenetic.*
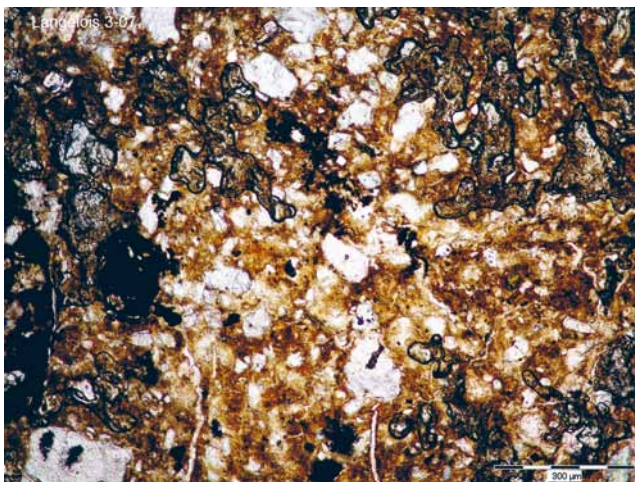
e) *This horizon shows irregular colouring from brownish red to reddish brown (dry colour: 5 YR 6/8). It consists of peptized and to a minor extent flocculated plasma. Both aggregate and granular structure can be found. Therefore, two different void structures are present. The sediment is silty, whereas sandy crystals of quartz, sometimes garnet, augite and fresh plagioclase occur. In this horizon, neither brown loam concretions nor carbonate illuviations can be observed. This horizon is red loam, which was enriched with allochthonous components at a later stage. This horizon corresponds to the Pedocomplex X (Günz/Mindel, Cromer) or older.*
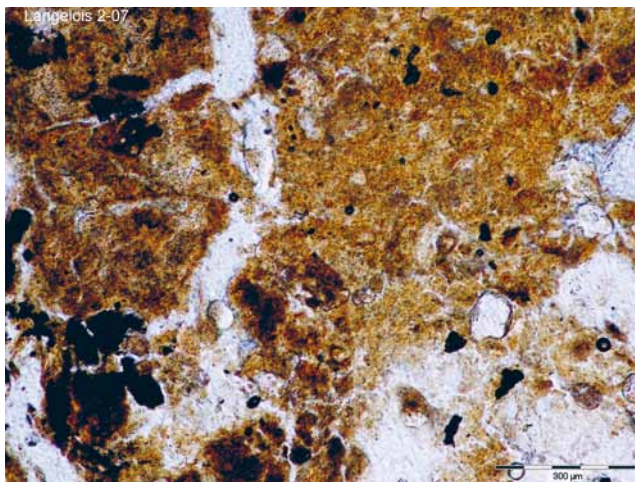
f) *The brown and primarily flocculated matrix (dry colour: 10 YR 7/4) is concentrated in granules. Furthermore, the matrix contains orange and peptized material as well as loess. Some of these components are seamed with orange brown loam, which is a sign of lessivation. Mn-seams are often developed on the outer boundaries of the orange seams.. The matrix is very dense and shows no typical structure. The substrate is poorly sorted and corresponds to a silt, whereas quartz crystals predominate. This mixed matrix, abundant brown loam concretions as well as Mn-concretions with "explosive" boundaries can be found. This horizon contains intense carbonate illuviations in the wide voids. The Mn-seams contain one generation of large calcite rhombohedrons, which fill all the remaining voids. Furthermore, abundant carbonate-"nests" can be found. In places, small, red coprogeneous elements of recent acarides (Acari) can be observed. The brown loam is friable, sandy and highly polygenetic. The deposition of the sediments was followed by a new sedimentation cycle of loess and lessivation. Weak stagnic properties and abundant carbonate illuvations can be found. Such extraordinarily complex polygenetical soils have only been reported from the Pedocomplex X (Günz/Mindel, Cromer) or older up to now.*
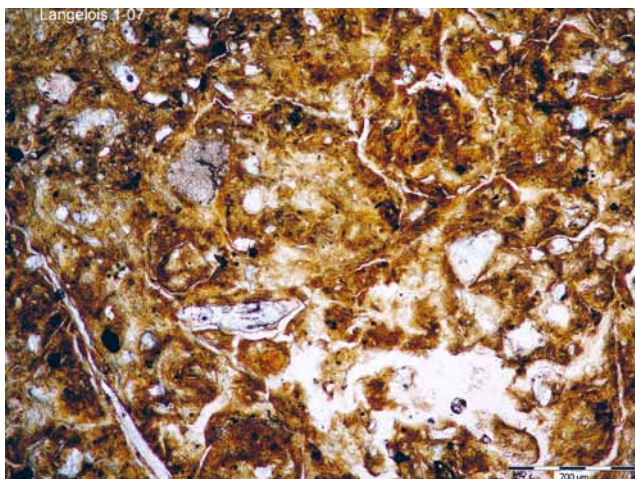
g) *The reddish brown matrix (dry colour: 7,5 YR 5/8) is peptized. The brown loam shows high optical activity and shows fluidal structures. The structure is segregated; the matrix is primarily separated in (sub)angular polyhedrons. Only in places, granules from the lower parts of the profile are incorporated. The primary components are silty and only rarely show larger particle sizes. Quartz is the only autochthonous mineral; sometimes, allochthonous plagioclase and biotite occur. Cracks and fissures are the only voids present; some of them have a horizontal orientation. Abundant brown loam concretions and rare Mn-concretions can be found, whereas the Mn-concretions are often broken. Weak and irregular recalcification features (amorphous $CaCO_3$-modifications) can be observed. This horizon is a red loam. Theses soils developed in Central Europe at the border of the Lower to Middle Pleistocene for the last time. In the Cromer-Interglacial (Günz/Mindel, Pedocomplex X), formerly called "red soils", such as Terra Rossa or Ferreto, developed.*

olivine could be identified in the soil thin section. The predominance of quartz in the entire profile and the occurrence of calcite in the form of calcite illuviation are in accordance with the results of Lois 3. In addition to the results of Lois 3, the results of the soil micromorphology showed that calcite does not only occur in the aggregates, but also as cutans in the pores (see Fig. 3, d). The colour descriptions in the soil thin sections of Lois 7 confirm the results of Lois 3 with respect to the increasing reddening from the upper to the lower part of the profile. However, the colour in the soil thin sections was described with a more yellowish hue than in the field analysis of the soil colour.

The red loams in the paleosols allow for an approximate age classification of these soils, since red loams were formed for the last time at the border between Lower and Middle Pleistocene. The investigations furthermore showed that the red loam horizons are strongly polygenetic, which emphasizes their classification into Pedocomplex X, Cromer Interglacial.

4 Summary and discussion

NW of Langenlois (Lower Austria) in an outcrop of loess-paleosol-sequences developed on ‚Rehberg'-amphibolite, six soil profiles (Lois 1 to 6) were investigated and sampled. Two soil profiles (Lois 1 and 2) developed on the 'Rehberg'-amphibolite; two on the amphibolites-marble-body of the 'Buschandlwandzug' (Lois 5 and 6); and two soil profiles are sequences of polycyclic paleosols with several fossil horizons without visible host rock (Lois 3 and 4). Profile Lois 7 was sampled separately and described thoroughly with regard to soil micromorphology. Parallels between Lois 7 and the other soil profiles, particularly with the neighbouring Lois 3, were observed.

The mineralogical composition of the profiles Lois 1 and 2, which developed on amphibolite, is dominated by quartz, calcite, hornblende and sheet silicates; the clay mineralogical composition by smectite and illite with minor amounts of chlorite and kaolinite. The two paleosols Lois 3 and 4 consist nearly entirely of quartz and sheet silicates. The dominance of sheet silicates results in extremely high clay contents in these two profiles. Calcite could only be found in minor amounts in Lois 3 and 4. Together with the high contents of kaolinite in the clay fraction, this emphasizes the long and intense weathering processes these sediments have undergone. The profiles 1–4 and 7 show decalcification in the upper parts of the profiles and illuviation of secondary carbonate in the lower parts. The carbonates precipitate mainly on the edges of the aggregates as well as within the aggregates (Lois 3, 4, and 7) or cover whole horizons and the host rock (Lois 1 and 2) with a thick, purely white crust. The profiles Lois 5 and 6 are characterized by the two very different host rocks amphibolite and marble; subsequently, the mineralogy of these two profiles is dominated by quartz, plagioclase, calcite, and sheet silicates. The clay fractions in both profiles contain partially extreme amounts of smectite (up to 97 %); illite occurs in minor amounts. The high smectite contents cannot be a product of amphibolite weathering alone, since the amphibolite is rather fresh. It is likely that the smectite is derived from pre-weathered material, e.g. Middle Pleistocene ('Badenium') sediments.

Noteworthy in the profiles 1–4 and 7 is the intense illuviation of secondary carbonate. The calcite covers the solum as well as the host rock amphibolite as a thick, purely white crust. The calcite crust is only present at the surface of the amphibolites and easy to remove by hand. In the profiles Lois 3, 4 and 7 the secondary carbonates can be found on the surface of the aggregates as well as in the pores of the aggregates. Such high amounts of carbonate cannot be a product of recent pedogenetical processes. Apparently, the carbonate was infiltrated from carbonate-rich sediments (loess) formerly on top of the profile which are now eroded. Furthermore, a calc-sinter layer was found in profile Lois 2. This calc-sinter could be derived from the marble layers which can be found on the western flank of the outcrop (Lois 5 and 6). The outcrop slightly declines from the western towards the northern and eastern flank. It is possible that calcite-rich solution mobilised during the weathering of the marble ran off laterally and precipitated in the profiles on the northern (Lois 1, 2 and 7) and eastern (Lois 3 and 4) flank. However, it is more likely that both processes – decalcification of formerly superimposed loess and precipitation from calcite-rich weathering solutions from marble – led to the intense calcite illuviation. The calc-sinter layer apparently seals the material flows between rock and solum. This hypothesis is supported by the results from the geochemical analyses.

The geochemical analyses showed that the amphibolites are enriched in Ba, Cr, Cu, Ni and Sr, which corresponds very well with the reported values of the 'Rehberg'-amphibolite (loc. typ.) (HÖDL 1985). However, as discussed above, the amphibolites have only limited influence on the soil parameters, mineralogy and geochemistry within profiles Lois 1 and 2. The geochemical distributions in profiles Lois 3 and 4 are very stable. All four soil profiles from Lois 1 to Lois 4 show similar geochemical compositions. Elevated Zr-contents could be found in the two paleosol profiles Lois 3 and 4 which is characteristic for intensively weathered sediments.

The soil profiles Lois 5 and 6 are also geochemically stable and influenced by the host rocks amphibolite and marble. The rocks of Lois 1, 2, 5, and 6 are only slightly weathered; therefore, there was no enrichment of chemical elements in the soil profiles. All soil profiles have elevated contents of Cu in the plough layer (Ap), which is due to phytosanitary measures in viniculture.

The soil profiles in the 'Red Outcrop' of Langenlois are relatively static profiles without significant recent pedogenetical processes. The agricultural use of the soils with accompanying tillage stimulates the pedogenesis to a small degree by mixing and aerating the upper soil layers which favours mainly lessivation, the only pedogenetical process active at present. In the paleosols, older signs of lessivation could be observed in the form of clay cutans on the edges of the aggregates and, additionally, weak stagnic properties. The profiles with no visible host rock (Lois 3, 4 and 7) are sequences of polycyclic sedimentation and subsequently several generations of fossil horizons. According to the soil micromorphological analyses, the soils of the 'Red Outcrop' can be classified into the Lower to Middle Pleistocene.

Acknowledgements

References

Döppes, D. & Rabeder, G. (eds.) (1997): Pliozäne und Pleistozäne Faunen Österreichs. – Mitteilungen der Kommission Quartärforschung der Österreichischen Akademie der Wissenschaften, 10: 411 S.

Fink, J., Fischer, H., Klaus, W., Kočí, A., Kohl, H., Kukla, J., Ložek, V., Piffl, L. & Rabeder, G. (1976): Exkursion durch den österreichischen Teil des nördlichen Alpenvorlandes und den Donauraum zwischen Krems und der Wiener Pforte. Mitteilungen der Kommission für Quartärforschung der Österreichischen Akademie der Wissenschaften, Band 1: 114 S.

Frank, Ch. & Rabeder, G. (1996a): Kleinsäuger und Landschnecken aus dem Mittel-Pliozän von Neudegg (Niederösterreich). – Beiträge zur Paläontologie, 21: 41–49.

Frank, Ch. & Rabeder, G. (1996b): *Helicodiscus* (*Hebetodiscus*) sp. (Pulmonata, Gastropoda) im Pliozän und Pleistozän von Österreich. – Beiträge zur Paläontologie, 21: 33–39.

Fuchs, W., Grill, R., Matura, A. & Vasicek, W. (1984): Geologische Karte der Republik Österreich 1:50.000, Blatt 38 Krems. – Geologische Bundesanstalt, 1 Blatt, Wien.

Haslinger, E. & Heinrich, M. (2008): Der „Rote Aufschluss" von Langenlois – Pedogenese und Mineralogie von Paläoboden-Sequenzen über Amphibolit. – Abhandlungen der Geologischen Bundesanstalt, 62: 71–79.

Havlíček, P. & Holásek, O. (1998): Bericht 1996 über quartärgeologische Untersuchungen auf den Blättern 21 Horn und 38 Krems. – Jahrbuch der Geologischen Bundesanstalt, 141/3: 327–328.

Havlíček, P., Holásek, O. & Smolíková, L. (2004): Bericht 2003 über geologische Aufnahmen in Quartäraufschlüssen auf Blatt 39 Tulln. – Jahrbuch der Geologischen Bundesanstalt, 144/3+4: 377–378.

Havlíček, P., Holásek, O., Smolíková, L. & Roetzel, R. (1998): Zur Entwicklung der Quartärsedimente am Südostrand der Böhmischen Masse in Niederösterreich. – Jahrbuch der Geologischen Bundesanstalt, 141/1: 51–71.

Havlíček, P., Holásek, O. & Smolíková, L. (2005): Bericht 2004 über geologische Aufnahmen im Quartär auf den Blättern 21 Horn, 37 Mautern, 38 Krems an der Donau, 40 Stockerau und 55 Obergrafendorf. – Jahrbuch der Geologischen Bundesanstalt, 145/3+4: 304–305.

Havlíček, P., Holásek, O. & Smolíková, L. (2006): Bericht 2005 über geologische Aufnahmen im Quartär auf den Blättern 21 Horn, 23 Hollabrunn und 23 Hadres. – Jahrbuch der Geologischen Bundesanstalt, 146/1–2: 69–70.

Hödl, M. (1985): Petrologie und Geochemie des Rehberger Amphibolites im niederösterreichischen Moldanubikum – Unveröffentlichte Dissertation der Universität Wien, Formal-Naturwissenschaftliche Fakultät. – 144 S.; Wien.

Holmgren, G. G. S. (1967): A rapid citrate-dithionite extractable iron procedure. – Soil Science Society of America Procedures, 31: 210–211.

IUSS Working Group WRB (2006): World reference base for soil resources 2006. 2nd edition. – World Soil Resources Reports, 103: 133 S; Rome (FAO).

Jaburová, I. (2009): Die quartären Landschaftsarchive in den Lössgebieten bei Langenlois und im östlichen Kremsfeld. – Diplomarbeit der Universität Wien. – 135 S.; Wien.

Kovanda, J., Smolíková, L. & Horáček, I. (1995): New data on four classic loess sequences in Lower Austria. – Sbornik geol. Věd. Antropozoikum, 22: 63–85.

Kubiena, W.L. (1956): Zur Methodik der Paläopedologie. – Actes du IV. Congrés Internationale du Quaternaire (Rome-Pise, Aout – Septembre 1953): 297–395.

Matura, A. (1989): Erläuterungen zu Blatt 37 Mautern (mit Beiträgen von Heinz, H.). – Geologische Bundesanstalt: 65 S.

Nestroy, O., Danneberg, O.H.; Englisch, M., Gessl, A., Hager, H., Herzberger, E.; Kilian, W.; Nelhiebel, P.; Pecina, E.; Pehamberger, A.; Schneider, W. & Wagner, J. (2000): Systematische Gliederung der Böden Österreichs. – Mitteilungen der Österreichischen Bodenkundlichen Gesellschaft, Heft 60: 124 S.

ON, Österreichisches Normungsinstitut (2006): Chemische Bodenuntersuchungen – Bestimmung der Acidität (pH-Wert). – ÖNORM L 1083: 2006 04 01: 7 S.

Rabeder, G. (1981): Die Arvicoliden (Rodentia, Mammalia) aus dem Pliozän und dem älteren Pleistozän von Niederösterreich. – Beiträge zur Paläontologie Österreichs, 8: 1–373.

Riedmüller, G. (1978): Neoformations and transformations of clay minerals in tectonic shear zones. – T MPM Tschermaks Mineralogische und Petrologische Mitteilungen, 25: 219–242.

Roetzel, R. (2002): 2.2. Molasse (T2–T5). – In: Schnabel, W. (ed.): Legende und kurze Erläuterung zur Geologischen Karte von Niederösterreich 1:200.000. – Geologische Bundesanstalt: 24–28.

Schultz, L.G. (1964): Quantitative interpretation of mineralogical composition from X-ray and chemical data for Pierre shale. – U.S. Geological Survey, Professional Paper, 391-C: 1–31.

Schwertmann, U. (1964): Differenzierung der Eisenoxide des Bodens durch Extraktion mit Ammoniumoxalat Lösung. – Zeitschrift für Pflanzenernährung und Bodenkunde, 105: 194–202.

Smolíková, L. (1997): Bericht 1996 über mikromorphologische und stratigraphische Bearbeitung quartärer Böden auf den Blättern 21 Horn, 22 Hollabrunn und 38 Krems. – Jahrbuch der Geologischen Bundesanstalt, 140/3: 353–354.

Smolíková, L. (1998): Bericht 1997 über Mikromorphologie und Stratigraphie der quartären Böden auf Blatt 38 Krems an der Donau. – Jahrbuch der Geologischen Bundesanstalt, 141/3: 329–330.

Smolíková, L. & Havlíček, P. (2007): Bericht 2005 und 2006 über mikromorphologische Untersuchungen von quartären Böden im Gebiet des unteren Kamptales auf den Blättern 21 Horn und 38 Krems. – Jahrbuch der Geologischen Bundesanstalt, 147/3–4: 682–683.

Steininger, F. (Hrsg.) (1999): Erdgeschichte des Waldviertels. 2. erweiterte Auflage. – Schriftenreihe des Waldviertler Heimatbundes, 38: 200 S.

Tamm, O. (1932): Über die Oxalatmethode in der chemischen Bodenanalyse. – Meddelingen Statens Skogsförsökanstalt, 27: 1–20.

Reconstructing Quaternary vegetation history in the Carpathian Basin, SE Europe, using n-alkane biomarkers as molecular fossils

Problems and possible solutions, potential and limitations

Michael Zech, Björn Buggle, Katharina Leiber, Slobodan Marković, Bruno Glaser, Ulrich Hambach, Bernd Huwe, Thomas Stevens, Pal Sümegi, Guido Wiesenberg, Ludwig Zöller

Abstract:

Over the recent years there has been increasing fossil charcoal and malacological evidence from loess-palaeosol sequences in the Carpathian (Pannonian) Basin that call into question the traditional paradigm of treeless full glacial palaeoenvironments. In order to contribute to this discussion we focus on plant-derived n-alkanes and evaluate their potential to serve as biomarkers for the reconstruction of vegetation history during the last glacial cycle. Recently published initial results show a strong degradation effect on the alkane pattern hindering the direct application of frequently used alkane ratios like nC31/nC27, which are in literature often used as vegetation proxies (grass vs. tree). In this paper we therefore introduce for the first time an end member model taking into account the different degree of organic matter (OM) degradation in soils/loess. The model is applied to the Crvenka loess-palaeosol sequence on the Bačka Loess Plateau (Vojvodina, Serbia) at the confluence of the Danube and Tisa Rivers. The results show grass dominance during the whole last glacial cycle. Some few trees likely contributed to the vegetation cover during glacial periods and during the Holocene, but not during the last interglacial and the Marine Isotope Stage (MIS) 3 interstadial. The reconstructed vegetation history is in agreement with previous malacological and charcoal findings as well as with climate and biome modelling results.

[Rekonstruktion der quartären Vegetationsgeschichte im Karpaten-Becken, Südost-Europa, mit Hilfe von n-Alkan Biomarkern als molekulare Fossilien: Probleme und mögliche Lösungen, Potenzial und Grenzen]

Zusammenfassung:

Seit einigen Jahren gibt es zunehmend Studien, die, basierend auf der Untersuchung von fossilen Holzkohlen und Schnecken-schalen aus Löss-Paläoboden Sequenzen, die traditionelle Vorstellung von weitestgehend baumlosen Steppen im Karpaten-Becken während der letzten Kaltzeit in Frage stellen. Mit unseren Arbeiten versuchen wir anhand von Biomarkern einen Beitrag zu dieser Diskussion zu leisten und herauszufinden, welches Potenzial in der Untersuchung von Alkan Biomarkern für die Rekonstruktion der Vegetationsgeschichte während der letzten glazialen Zyklen steckt. Kürzlich veröffentlichte erste Ergebnisse weisen darauf hin, dass der Degradationsgrad der pflanzenbürtigen organischen Substanz einen starken Einfluss auf das Alkanmuster in Böden hat und dass der in der Literatur häufig verwendete Alkanquotient nC31/nC27 kein reiner Vegetations-Proxy ist, sondern auch maß-geblich die unterschiedliche Degradation widerspiegelt. In der vorliegenden Arbeit führen wir daher erstmals einen End Member Modellierungsansatz ein, bei dem der Degradationsgrad der organischen Bodensubstanz mit berücksichtig wird. Das Modell wird auf die Loess-Paläoboden Sequenz Crvenka auf dem Bačka Loess Plateau (Serbien) zwischen Donau und Theiss angewendet. Die so für den letzten Interglazial-Glazial-Zyklus rekonstruierte Vegetationsgeschichte bestätigt die Holzkohle- und Mollusken-Befunde und deutet auf Gras-Steppen während des letzten Interglazials und –stadials hin (Marine Isotopenstadien (MIS) 5 bzw. 3). Die Ergebnisse machen deutlich, dass Steppen während des gesamten letzten glazialen Zyklus vorgeherrscht haben. Für das letzte Interglazial und das Interstadial der Marinen Isotopen Stufe (MIS) 3 deuten die Biomarker Befunde auf reine Grassteppen hin. Dagegen prägten in den Glazialen vermutlich auch vereinzelte Bäume das Landschaftsbild einer 'Taiga-Steppe'. Die so rekonstru-ierte Vegetationsgeschichte steht im Einklang mit den Holzkohle- und Schneckenfunden, wie auch mit Ergebnissen von Klima- und Biom-Modellierungen.

Keywords: *Quaternary, Carpathian Basin, Loess, Palaeosols, Biomarkers, Alkanes, Palaeovegetation*

Addresses of authors: **U. Hambach, L. Zöller,** Chair of Geomorphology, University of Bayreuth, Universitätsstr. 30, 95440 Bayreuth, Germany; **M**. **Zech B. Buggle, K. Leiber, B. Glaser, B. Huwe,** Soil Physics Department, University of Bayreuth, Universitätsstr. 30, 95440 Bay-reuth, Germany. E-Mail: michael_zech@gmx.de; **S. Marković,** Chair of Physical Geography, University of Novi Sad, Trg Dositeja Obradovića 3, 21000 Novi Sad, Serbia; **T. Stevens**, Centre for Earth and Environmental Science Research, Kingston University, Penrhyn Road, Kingston upon Thames, Surrey KT1 2EE, United Kingdom; **P. Sümegi**, Department of Geology and Palaeontology, University of Szeged, 6722, Szeged Egyetem u.2., Hungary; **G. Wiesenberg**, AgroEcoSystem Research Department, University of Bayreuth, Universitätsstr. 30, 95440 Bayreuth, Germany

1 Introduction

Over the last few years, more and more attention has been focused on the loess-palaeosol sequences of SE Europe by Quaternary scientists aiming at establishing pedo-, magne-to- and chronostratigraphies (Buggle et al. 2009; Fuchs et al. 2008; Markovic et al. 2008; Markovic et al. 2006) and at reconstructing palaeoenvironments and climate (Marko-vic et al. 2005; Markovic et al. 2007; Rudner & Sümegi 2001; Sümegi & Krolopp 2002; Willis et al. 2000; Zech et al. 2008a). Interestingly, there is increasing fossil charcoal and malacological evidence from loess-palaeosol sequences in the Carpathian Basin that call into question the tradi-tional paradigm of a treeless full glacial palaeoenvironment. Hence, Willis & Andel (2004) ask "trees or no trees?" in the title of their publication and thoroughly review all the
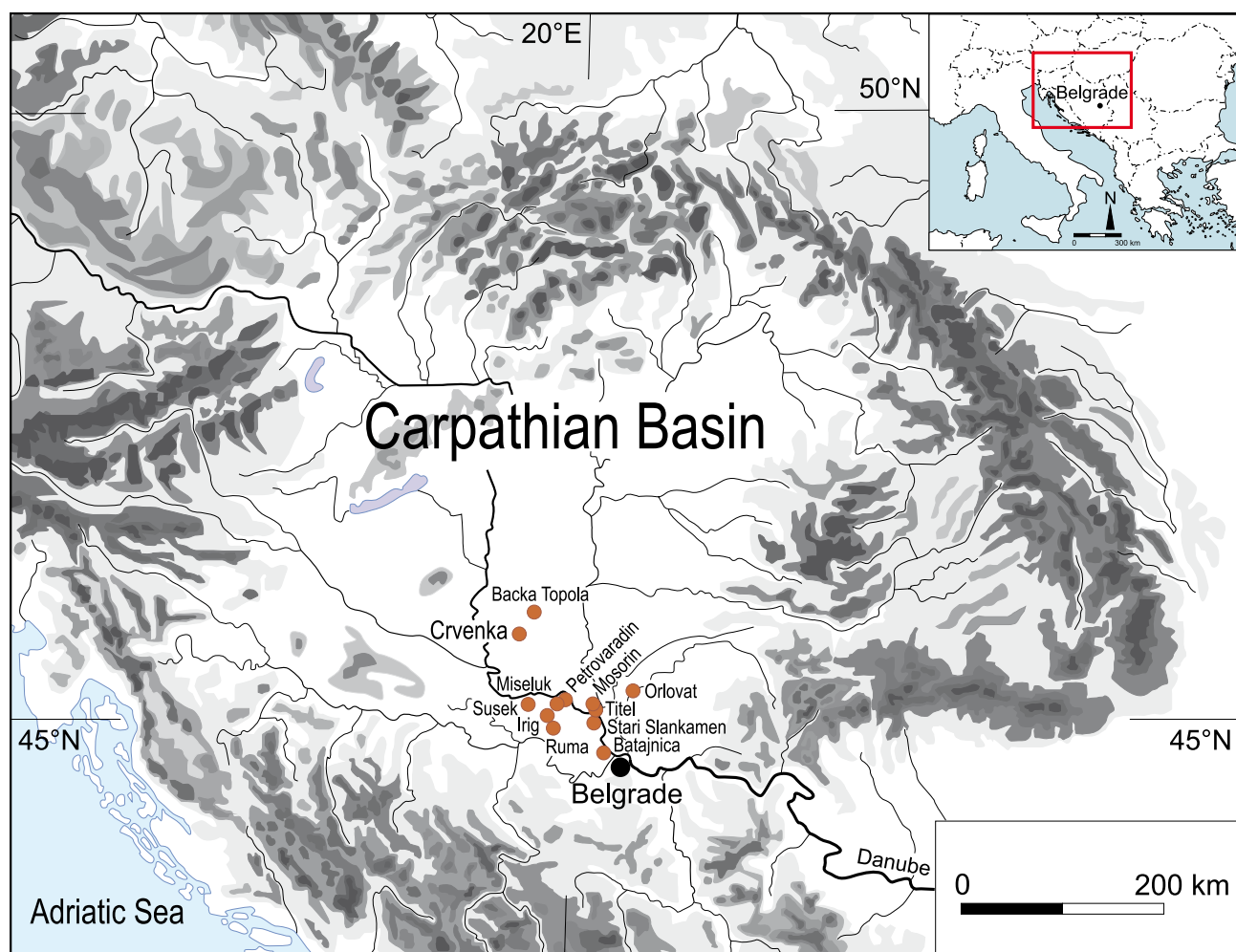
Fig. 1: Topographic map of the Carpathian Basin and the Vojvodina Province showing the geographic positions of the Crvenka and other loess exposures (Markovic et al. 2008).

Abb. 1: Topographische Karte des Karpaten-Beckens und der Vojvodina Provinz mit der geographischen Lage der Loess-Paläoboden Sequenz Crvenka und anderer Loessaufschlüsse (Markovic et al. 2008).

available fossil, genetic and palaeoclimatic evidence at that time. Although it was possible to find clear indicators for the presence of trees, the authors concluded that from the fossil evidence alone it is difficult to establish whether the proven trees grew in isolated pockets on an otherwise open tundra landscape, or in an open taiga forest. Potentially, biomarker studies, i.e. the searching for molecular fossil evidence in loess-palaeosol sequences using for example plant-derived n-alkanes, can contribute in the next years to a better understanding of the vegetation history in the Carpathian Basin.

n-Alkanes with 25 to 33 carbon atoms (nC25 – nC33) and a strong odd-over-even predominance (OEP) are important constituents of cuticular plant leaf waxes (Kolattukudy 1976). With the litter-fall they are deposited and stored in soils and sediments, for example in aeolian sediments, where they are assumed to be relatively resistant to biogeochemical degradation (Bourbonniere et al. 1997; Cranwell 1981). Furthermore, since different vegetation types reveal distinct alkane patterns and hence a so-called "chemical fingerprint", alkanes have the potential to serve as biomarkers. For instance, they are used to differentiate between autochthonous (lacustrine) and allochthonous (terrestrial) organic matter (OM) in lake sediments (Bourbonniere et al. 1997; Ficken et al. 2000; Mügler et al. 2008; Zech et al. 2008b), or to reconstruct vegetation changes, predominantly in terms of the

relative proportions of grasses and trees (Cranwell 1973; Schwark et al. 2002; Zech 2006). First n-alkane results for the Carpathian Basin presented by Zech et al. (2008a) indicate that the alkane pattern in soils and loess is not only strongly affected by the type of vegetation but also by OM degradation. In this paper we therefore propose a solution for this problem by establishing an end member model that (i) takes into account the degree of OM degradation and (ii) allows the differentiation of alkanes derived from grasses and herbs, versus alkanes derived from trees and shrubs. The model is applied to alkane results from the Crvenka loess-palaeosol sequence on the Bačka Loess Plateau, at the confluence of the Danube and Tisa Rivers. The potential and the limitations of the method are discussed.

2 Study Area and Pedostratigraphy

Large areas of the Carpathian Basin (Pannonian Basin) are covered with loess, often forming discontinuous plateau uplands between the alluvial plains of the Danube, Tisa, Sava and Tamiš Rivers. Close to the town Crvenka about 60 km northwest of Novi Sad in the Vojvodina Region (Serbia), a loess-palaeosol sequence of about 10 m thickness is exposed in a brickyard situated on the southwestern edge of the Bačka Loess Plateau (Fig. 1).
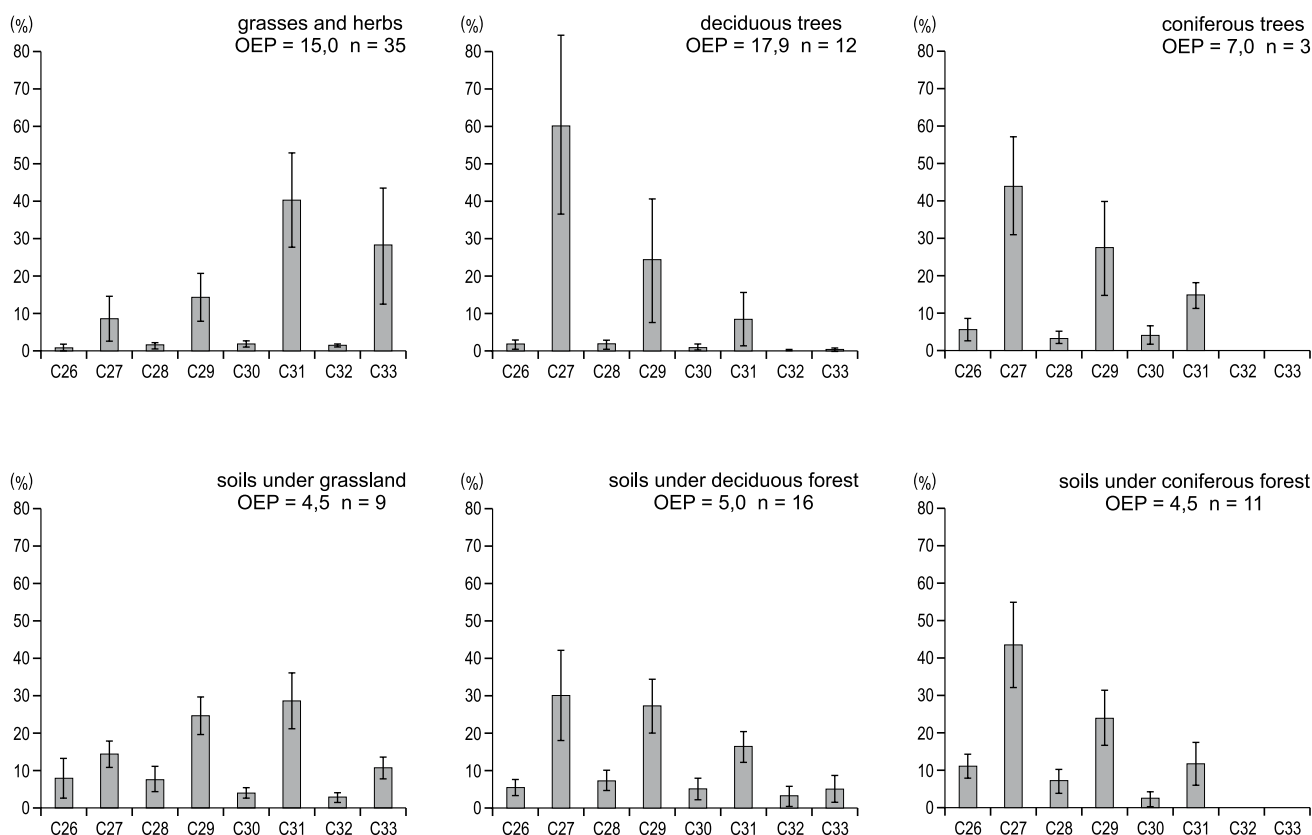
Fig. 2: Mean n-alkane distribution patterns from grasslands, deciduous and coniferous forests. OEP = odd over even predominance. Error bars indicate standard deviation. Based on data from ZECH et al. (2008a) MARSEILLE et al. (1999), PRÜGEL (1994), ROMMERSKIRCHEN (2006) and RUMPEL & WIESENBERG *(unpublished).*

Abb. 2: Durchschnittliches n-Alkan Verbreitungsmuster von Grasland, Laub- und Nadelwald. OEP = odd over even predominance. Die Fehlerbalken kenn-zeichnen die Standardabweichung. Nach Daten von ZECH et al. (2008a) MARSEILLE et al. (1999), PRÜGEL (1994), ROMMERSKIRCHEN (2006) und RUMPEL & WIESENBERG *(unveröffentlicht).*

Initial pedostratigraphical description and the first geochemical, grain-size and magnetic susceptibility results are provided by MARKOVIC et al. (2008) and ZECH et al. (2008a). According to these results, the Crvenka exposure contains a record of the last interglacial-glacial cycle with a ~2 m thick and clay-rich interglacial 'V S1' palaeosol (the prefix 'V' refers to the standard Pleistocene loess-palaeosol stratigraphy in the Vojvodina region (MARKOVIC et al. 2008) exposed at the bottom of the sequence. The overlaying ~8 m thick 'V L1' loess contains an interbedded weakly developed interstadial palaeosol complex ('V L1S1') and the top of the loess-palaeosol sequence is capped by the Holocene/modern topsoil ('V S0').

3 Material and Methods

During a field campaign in November 2007, the Crvenka exposure was cleaned by digging and logging trenches about 1 m wide and 0.5 m deep. Sampling for biomarker analysis was conducted by taking mixed samples every 25 cm, resulting in totally 43 samples from the sequence. Additionally, 12 samples for luminescence dating were taken from the exposure. Manuscripts dealing with a detailed description of the stratigraphical/pedological/geochemical/magnetic features, as well as the luminescence dating are in preparation. At the present state of research our chronostratigraphy for the Crvenka section is based on pedostratigraphic correlations to well dated sections of the region e.g. Surduk, Petrovaradin, Ruma (FUCHS et al. 2008; MARKOVIC et al. 2005; MARKOVIC et al. 2006), since the numerical dating results from Crvenka are not yet available.

In order to characterise the modern vegetation types with respect to their alkane pattern, mixed litter and topsoil samples were collected from several sites on the Fruska Gora Mountains about 10 km south of Novi Sad (mixed *Quercus sp. and Fagus sp.* forests) and from grasslands on the Titel Loess Plateau about 25 km east of Novi Sad (grass and herb vegetation) (Fig. 1).

Sample preparation of the n-alkanes was carried out at the University of Novi Sad, Serbia, and at the University of Bayreuth, Germany, using a modified method after ZECH & GLASER (2008). Free lipids were extracted with methanol/toluene (7/3) using Soxhlet apparatus and subsequently concentrated using rotary evaporation. The lipid extracts were purified on silica-alox columns (2g of each, 5% deactivated). n-Alkanes were eluted with 3*10 ml hexane/toluene (85/15). Quantification was performed on an HP 6890 gas chromatograph equipped with a flame ionisation detector (FID). 5α-Androstan and Hexatriacontane (nC36) were added as internal and recovery standards, respectively.
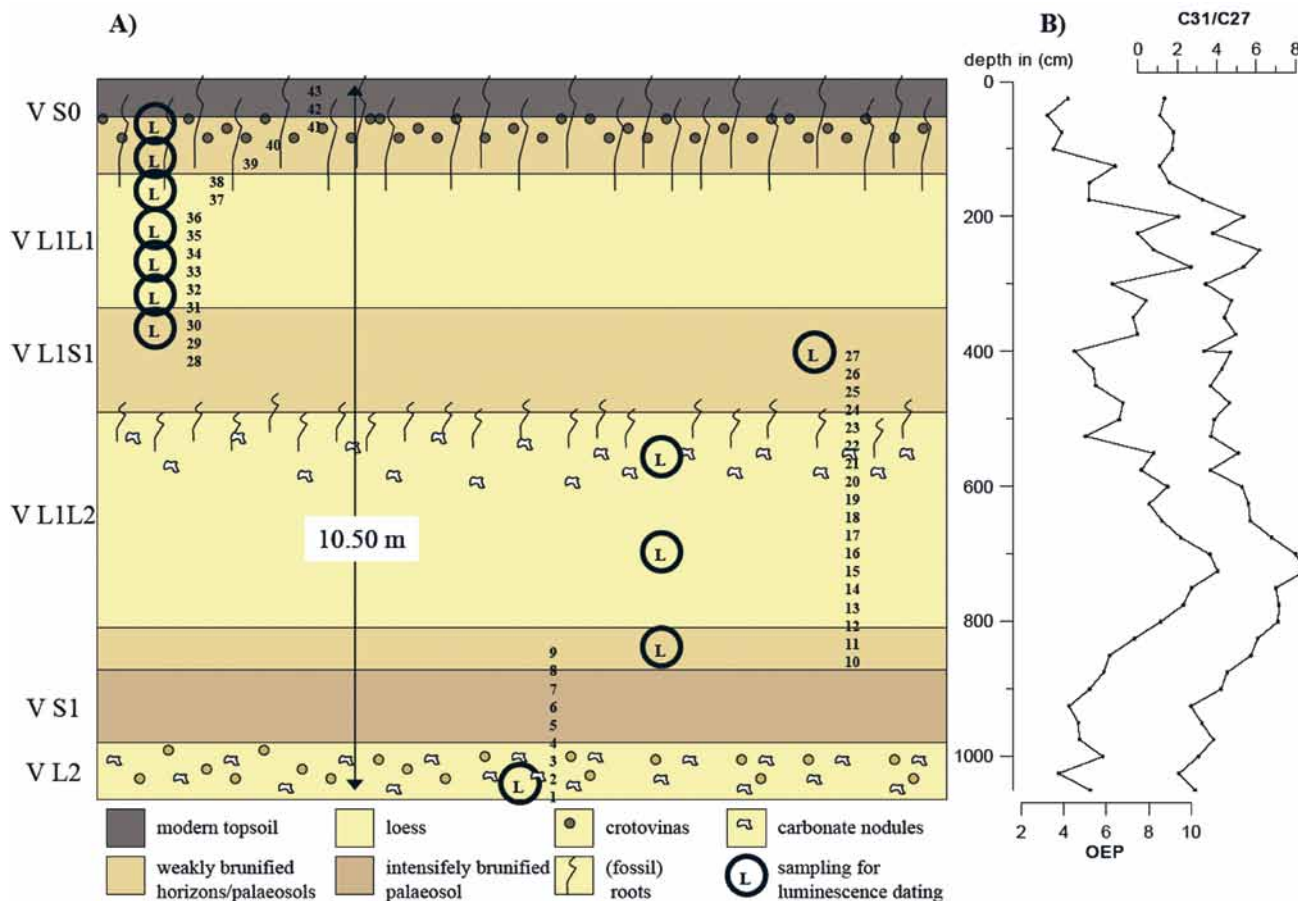
Fig. 3: A) Pedostratigraphy and sampling scheme for the Crvenka loess-palaeosol sequence (from ZECH et al. 2008a). B) Depth functions for the OEP and the alkane ratio C31/C27.

Abb. 3: A) Pedostratigraphie und Probenentnahmeschema für die Loess-Paläoboden Sequenz Crvenka (nach ZECH et al. 2008a). B) Tiefenfunktion für OEP und das Alkan-Verhältnis C31/C27.

4 Results and Discussion

4.1 n-Alkane distribution patterns of modern vegetation and soils

The n-alkane patterns obtained from the litter and topsoil samples collected from mixed *Quercus sp.* and *Fagus sp.* forests on the Fruska Gora Mountains and samples from grasslands on the Titel Loess Plateau are in agreement with findings in the literature. In order to increase our data set for the end member modelling, we additionally implemented data from MARSEILLE et al. (1999), PRÜGEL et al. (1994), ROMMERSKIRCHEN et al. (2006) and RUMPEL & WIESENBERG (unpublished).

Firstly, the fresh biomass reveals a strong odd-over-even predominance (OEP, Fig. 2) with mean values of 15.0, 17.9 and 7.0 for grasses and herbs, deciduous trees and conifers, respectively, where

$$OEP = (C27+C29+C31+C33)/(C26+C28+C30+C32).$$

Hence, high OEP values are typical for fresh undegraded cuticular plant leaf waxes. In comparison, lower OEP values (< 5) are characteristic for the topsoils (Fig. 2) and are often interpreted in terms of OM degradation. Secondly, it is striking that the alkane patterns of respective litter and topsoils are not identical, but become more balanced, i.e. for instance the ratios C31/C27 approach the values 1. This might be attributed to either an input of microbial or root biomass or to biodegradation (WIESENBERG et al. 2004).

In spite of these variations, it is valid that in forest litter and forest soils the n-alkanes C27 and C29 dominate, whereas in grasslands the alkanes C31 and C33 are more abundant (Fig. 2). These results explain why alkane ratios are used as tool to differentiate between forest and grassland vegetation in palaeoenvironmental studies (CRANWELL 1973; SCHWARK et al. 2002; ZECH 2006; ZHANG et al. 2006).

4.2 n-Alkane ratios from the Crvenka loess-palaeosol sequence

Recently, we tried a tentative palaeovegetational reconstruction for the Crvenka loess-palaeosol sequence based on alkane ratios (ZECH et al. 2008a). In fact, for instance the ratio C31/C27 varies widely between ~1 and 8.5 (Fig. 3B), with maxima characterising the loess units 'V L1L1' and 'V L1L2'. One may be tempted to interpret these variations in terms of grass-forest vegetation changes having occurred during the last glacial cycle. However, we rejected this idea, because (i) studying modern litter and respective topsoils indicates

that the ratio C31/C27 is prone to degradation effects (Fig. 2) and because (ii) C31/C27 correlates highly significantly with the OEP (R = 0.87, Fig. 3B), the latter having the potential to serve as degradation proxy. Hence it is likely, that most of the C31/C27 variations in the Crvenka dataset are caused by degradation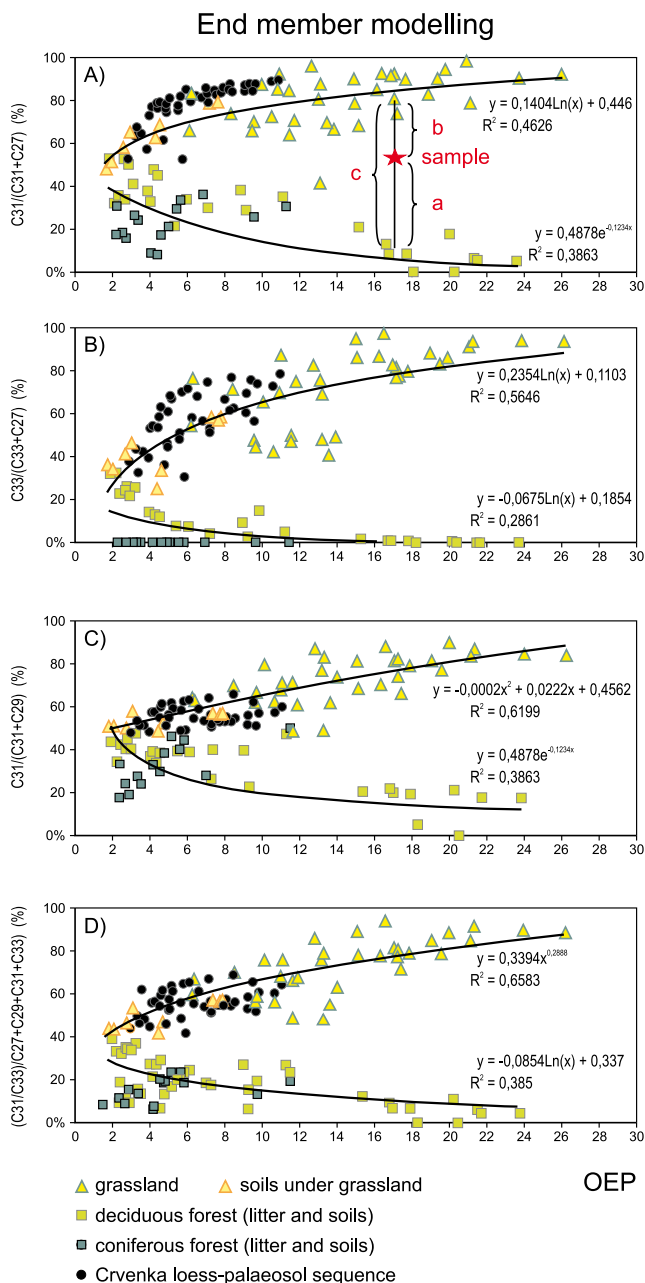 rather than by vegetation changes. Eventually, all biomarker-based reconstructions of vegetation changes have to be considered with caution unless it can be guaranteed that the organic matter is highly preserved throughout the whole archive (e.g. lake sediments) or a pronounced forest dominance (C31/C27 <1) alternated with a pronounced grass dominance (C31/C27 >1). In spite of this apparent impact of degradation on alkane ratios, we are aware of no published attempts to correct alkane biomarker results for this effect, neither qualitatively nor quantitatively, when using alkane ratios as vegetation proxies.

4.3 End member modelling – accounting for the degradation effect

As a result of OM degradation the originally high C31/C27 ratios in grasses and herbs decrease during decomposition and formation of soil OM (Fig. 2). This can be plotted as 'degradation line', using the OEP as proxy for degradation and plotting both fresh litter and topsoil samples from modern grasslands (Fig. 4A). Note that the ordinate is given as the proportion of C31 to the sum of C31 and C27 in percent and not as ratio of C31/C27. A degradation line can also be plotted for the litter and topsoils from forest sites, thus allowing a simplified description of the alkane ratio changes during degradation of OM derived from trees and shrubs.

Loess-palaeosol samples that were formed purely under one of these two vegetation types (end members) should plot on or close to the 'degradation lines'. Samples that were formed under a mixed vegetation should plot in-between the degradation lines (Fig. 4A). The percentage contribution of grasses and herbs versus trees and shrubs to the total content of fossil plant alkanes in a loess or palaeosol sample can be determined in two steps:

Firstly, using the OEP of the sample, the respective alkane ratio end members for grassland versus forest are calculated by means of the functions describing the 'degradation lines'.

Secondly, using the end members obtained for a certain sample, the % contribution of the two vegetation types is estimated by means of a two component mixing equation. Accordingly the quotient a/c gives the % alkane contribution of grasses and herbs, whereas the quotient b/c gives the % alkane contribution of trees and shrubs (Fig. 4A).

The most accurate results can be expected for samples with high OEP values, whereas accuracy should decrease with decreasing OEP values due to the converging degradation lines (Fig. 4A). Accuracy is furthermore limited by the scattering of the modern dataset. Furthermore, it should be mentioned that there is not only an interspecie variability of the alkane pattern producing the scattering around the degradation lines, but also an innerspecie variability. The latter can be caused by leaf and needle aging (Prügel et al. 1994) as well as by environmental stress (Shepherd & Griffiths 2006). Due to the scattering, modelling can result in negative percentage values for tree- or grass-derived alkanes (Fig. 5). However, this does not indicate that the idea of the model is wrong or invalid. It rather points to the limitation of the model to incorporate interspecie and innerspecie variability within grasslands and forests, respectively. In order to check the robustness of our end member model, we calculated the model not only with C31/C27, but additionally also for
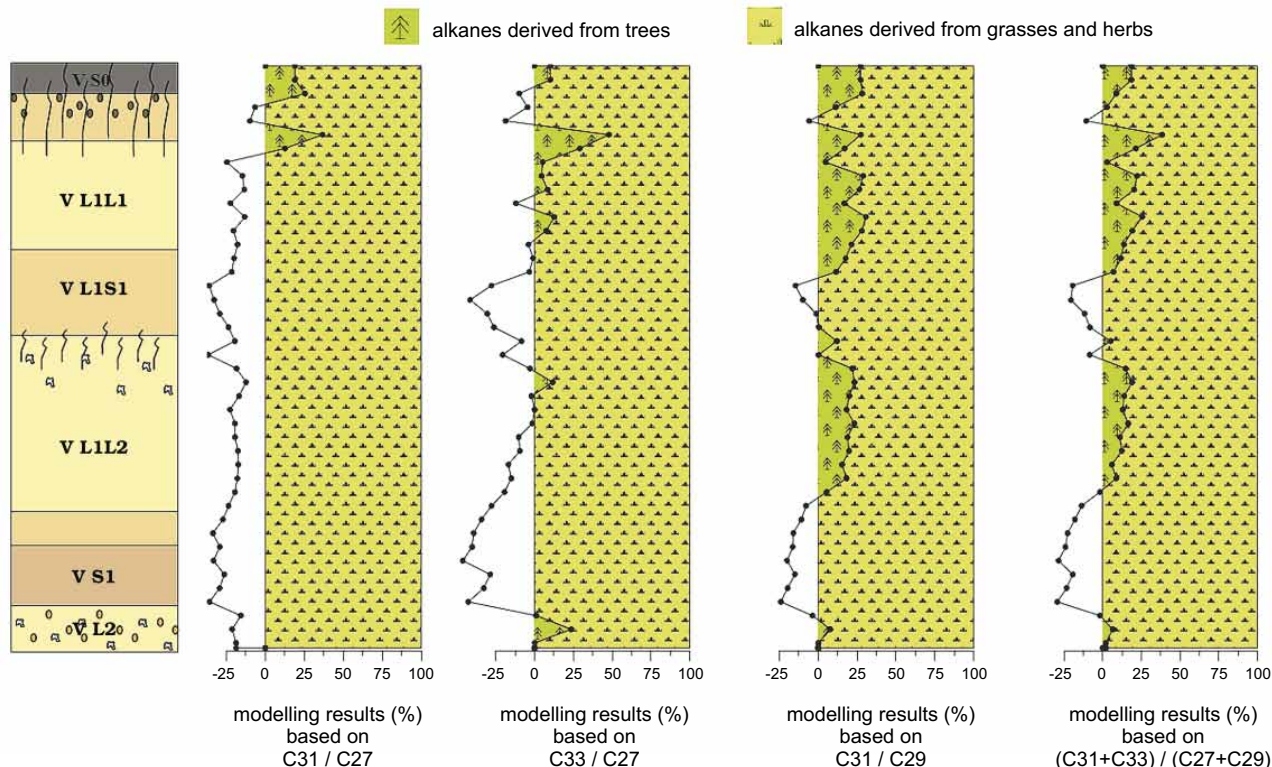

Fig. 4: End member modelling for the alkane ratios A) C31/C27, B) C33/C27, C) C31/C29 and D) (C31+C33)/(C27+C33). Trend lines were fitted to the data sets (own data and data from literature, see above) from modern grasslands and forests, respectively, describing 'degradation lines'. An estimated percentage contribution of tree-derived alkanes to a palaeosol sample can be calculated by the ratio a/c.

Abb. 4: End Member Modell für die Alkan-Verhältnisse A) C31/C7, B) C33/C27, C) C31/C29 und D) (C31+C33)/(C27+C33). Die Trendlinie wurde an die Datensätze von rezentem Grasland und Wäldern angepasst (eigene Daten und Literaturdaten, s. oben) und beschreibt eine Degradationslinie. Der Anteil von Alkanen in einer Paläobodenprobe, die von Bäumen stammen, kann aus dem Verhältnis A/C berechnet werden.

Fig. 5: Modelling results for the alkane ratios C31/C27, C33/C27, C31/C29 and (C31+C33)/(C27+C29). Although the observed variations could potentially be explained with inter- and innerspecie variability in grasslands, the contribution of some few trees to the alkane patterns during glacials and during the Holocene cannot be excluded. This latter scenario is supported by charcoal and malacological findings as well as by climate modelling results.

Abb. 5: Ergebnisse der Modellierung der Alkan-Verhältnisse C31/C27, C33/C27, C31/C29 und (C31+C33)/(C27+C29). Obwohl die gemessenen Variationen potenziell durch artspezifische Variabilitäten innerhalb der Graslandvegetation erklärt werden könnten, ist das Auftreten von Bäumen während der Glaziale und im Holozän durch das gezeigte Alkanmuster nicht auszuschließen. Letztere Annahme wird durch den Nachweis von Holzkohle und malakofaunistischen Funden ebenso bestätigt, wie durch die Resultate von Klimamodellen.

several other alkane ratios like C33/C27 (Fig. 4B), C31/C29 (Fig. 4C) and (C31+C33)/(C27/C29) (Fig. 4D).

4.4 Reconstruction of vegetation and climate history recorded in the Crvenka loess-palaeosol sequence

Fig. 4 depicts that most of the 43 loess-palaeosol samples from Crevenka plot close to the grass 'degradation lines' for all four illustrated alkane ratios. This finding proves that grassland dominated the study area throughout the last glacial cycle. On the one hand, within the methodological uncertainties of the end member model, the alkane biomarkers alone can not be cited as evidence for the occurrence of trees. On the other hand, it can not be concluded that trees did not contribute at least partly to the observed scattering of the Crvenka samples. Hence, given that the modelling results for all alkane ratios show similar shifts (Fig. 5) and aiming at contributing to the question "trees or no trees?", the alkane biomarker results may serve as one testimony amongst others.

According to the modelling results illustrated in Fig. 5, trees disappeared entirely at the beginning of the last interglacial and grassland prevailed during the formation of the 'V S1' palaeosol. Climatically, these findings can be interpreted in terms of warm steppic conditions with pronounced dry summer seasons. During MIS 4, when loess deposition started again ('V L1L2'), plant-derived OM is much better preserved (high OEP, Fig. 3) and alkane biomarkers indi-

cate that some few trees contributed to the vegetation cover (Fig. 5). This is in disagreement with the traditional suggestion of treeless cold steppic environments during cold and dry glacial conditions. For the 'V L1S1' interstadial palaeosol, correlated tentatively with the MIS 3, the modelling results suggest that trees retreated, presumably because the summer seasons were again too dry to support them. Trees only immigrated again during MIS 2, with the onset of further loess deposition ('V L1L1'). Both MIS 2 and the Holocene, the latter being represented by the 'V S0' soil, have experienced several major fluctuations in the proportion of trees to the vegetation cover at the study site. The brunified subsoil horizon of 'V S0' reveals a marked re-expansion of pure grassland (Fig. 5). Probably, this reflects warmer climatic conditions with lower net precipitation in the Early-to Mid-Holocene. This interpretation is supported by the climate modelling results of KUTZBACH & GUETTER (1986) for the continental interiors of Eurasia between 30 and 60 ° N.

The alkane biomarker results presented above suggest that full glacial conditions in the Carpathian Basin were not generally characterised by treeless cold steppic environments Instead, rather open taiga forest prevailed even on the loess plateaus. This scenario is not only supported by other palaeoecoligical proxies like fossil charcoal and molluscs (SÜMEGI & KROLOPP 2002; WILLIS & ANDEL 2004; WILLIS et al. 2000), but also by modelling results (STAGE_3-PROJECT). Accordingly, the majority of the Carpathian Basin was not covered by steppes during the last glacial maximum (LGM),

but rather by evergreen taiga. Palaeoenvironmentally and –climatologically, one can conclude that in spite of lower precipitation levels than experienced today, reduced evapotranspiration due to lower temperature, and thus a higher net moisture budget, is responsible for sufficient water being available for trees to grow during glacial periods. Also the palaeoclimatic modelling results of Kutzbach & Guetter (1986) support this conclusion, suggesting that for the LGM, reduction of evaporation was a stronger influence on water availability than the associated decrease in precipitation, especially at 45–55°N. In contrast to the glacial conditions, during interglacial/-stadial periods seasonal summer dryness (higher temperature and evaporation combined with less summer precipitation) may have impeded the expansion of forests, at least on the loess plateaus.

Some preliminary conclusions concerning loess sedimentation during the last glacial cycle can be drawn from these findings. The loess plateaus in the Carpathian Basin were covered by vegetation capable to filter aeolian dust during the whole last glacial cycle. However, it seems that loess sedimentation did not depend crucially on the vegetation type, but rather on the dust supply originating from the glacial braided river systems during the glacial periods (Buggle et al. 2008; Smalley & Leach 1978). This supports the appellation 'Danube Loess' (name of the special session during the DEUQUA meeting 2008 in Vienna) for many of the aeolian sediments of the Carpathian Basin.

5 Conclusions and Outlook

In order to contribute to the discussion over "trees or no tress" (Willis & Andel 2004) in the Carpathian Basin during full glacial conditions, we investigated the alkane patterns of modern forests and grasslands, as well as those recovered from the Crvenka loess-palaeosol sequence on the southwestern edge of the Bačka Loess Plateau. Results from the modern study sites suggest (i) that the plant-derived alkane biomarkers have the potential to differentiate between OM derived from forests versus OM derived form grasslands; (ii) that the alkane ratios do not only depend on the type of vegetation but also on the degree of OM degradation. We therefore propose an end member model based on the alkane patterns of litter and topsoils from modern study sites that takes into account the degradation dependency (using the OEP as degradation proxy) of different alkane ratios.

The results for the Crvenka loess-palaeosol sequence firstly demonstrate the potential of the alkane biomarker method for terrestrial archives, where pollen are often intensively degraded. Secondly, they clearly show that grasses dominated the vegetation cover during the whole last glacial cycle. The accuracy of the model is limited by the scattering of the modern datasets for grasslands and forests. Nevertheless, the modelling results for different alkane ratios reveal similar and systematic shifts, which may have been caused by small and varying proportions of trees. Accordingly, pure grassland prevailed during the last interglacial and interstadial, whereas some few trees contributed to the soil OM during glacial periods and hence during loess deposition. This questions the traditional and palynologically derived paradigm of treeless full-glacial palaeoenvironments, but is in apparent agreement with charcoal and malacological findings

from the Carpathian Basin as well as with modelling results.

Ongoing work focuses on δD and δ18O analyses in plant-derived biomarkers from loess-palaeosol sequences. Recently, we have established the respective method for δ18O and demonstrated its potential to serve as climate proxy in modern litter and soils (Zech & Glaser 2009). Hence, water stress of plants, which we make responsible for Quaternary vegetation changes in our study area rather than cold temperatures, could be addressed more quantitatively in the future.

References

Bourbonniere, R.A., Telford. S.L., Ziolkowski, L.A., Lee, J., Evans, M.S. & Meyers, P. (1997): Biogeochemical marker profiles in cores of dated sediments from large North American lakes. – In: R.P. Eganhouse (ed.): Molecular Markers in Environmental Geochemistry, ACS Symposium Series: 133–150; Washington DC (American Chemical Society).

Buggle, B., Glaser, B. Zöllerm L., Hambach, U., Markovic, S. Glaser, I. & Gerasimenko, N. (2008): Geochemical characterization and origin of Southeastern and Eastern European loesses (Serbia, Romania, Ukraine). – Quaternary Science Reviews, 27: 1058–1075.

Buggle, B., Hambach, U., Glaser, B., Gerasimenko, N., Markovic S., Glaser, I. & Zöller, L. (2009): Stratigraphy, and spatial and temporal paleoclimatic trends in Southeastern/Eastern European loess–paleosol sequences. – Quaternary International, 196/1–2: 86–106.

Cranwell, P.A. (1973): Chain-length distribution of n-alkanes from lake sediments in relation to post-glacial environmental change. – Freshwater Biology, 3: 259–265.

Cranwell, P.A. (1981): Diagenesis of free and bound lipids in terrestrial detritus deposits in a lacustrine sediment. – Organic Geochemistry, 3: 79–89.

Ficken, K.J., Li, B., Swain, D.L. & Eglinton, G. (2000): An n-alkane proxy for the sedimentary input of submerged/floating freshwater aquatic macrophytes. – Organic Geochemistry, 31: 745–749.

Fuchs, M., Rosseau, D.-D., Antoine, P., Hatté, C., Gauthier, C., Markovic, S. & Zöller, L. (2008): Chronology of the Last Climatic Cycle (Upper Pleistocene) of the Surduk loess sequence, Vojvodina, Serbia. – Boreas, 37: 66–73.

Kolattukudy, P.E. (1976): Biochemistry of plant waxes. – In: P.E. Kolattukudy (ed.): Chemistry and Biochemistry of Natural Waxes: 290–349; Amsterdam (Elsevier).

Kutzbach, J. & Guetter, P. (1986): The influence of changing orbital parameters and surface boundary conditions on climate simulations for the past 18000 years. – Journal of the Atmospheric Sciences, 43: 1726–1759.

Markovic, S., Bokhorst, M.P., Vandenberghe, J., McCoy, W.D., Oches, E.A., Hambach, U., Gaudenyi, T., Jovanovic, M., Zöller, L., Stevens, T. & Machalett, B. (2008): Late Pleistocene loess-palaeosol sequences in the Vojvodina region, north Serbia. – Journal of Quaternary Science, 23: 73–84.

Markovic, S., McCoy, W.D., Oches, E.A., Savic, S. Gaudenyi, T. Jovanovic, M., Stevens, T., Walther, R., Ivanisevic, P. & Galovic, Z. (2005): Paleoclimate record in the Late Pleistocene loess-paleosol sequence at Petrovaradin Brickyard (Vojvodina, Serbia). – Geologica Carpathica, 56: 545–552.

Markovic, S., Oches, E., McCoy, W., Frechen, M. & Gaudenyi, T. (2007): Malacological and sedimentological evidence for "warm'' glacial climate from the Irig loess sequence, Vojvodina, Serbia. – Geochemistry Geophysics Geosystems, 8, Q09008. DOI:10.1029/2006GC001565.

Markovic, S., Oches, E., Sümegi, P., Jovanovic, M. & Gaudenyi, T. (2006): An introduction to the Middle and Upper Pleistocene loess-paleosol sequence at Ruma brickyard, Vojvodina, Serbia. – Quaternary International, 149: 80–86.

Marseille, F., Disnar, J.R., Guilet, B. & Noack, Y. (1999): n-Alkanes and free fatty acids in humus and A1 horizons of soils under beech, spruce and grass in the Massif-Central (Mont-Lozère), France. – European Journal of Soil Science, 50: 433–441.

Mügler, I., Sachse, D., Werner, M., Baiqing, X., Guangjian, W. Tandong, Y. & Gleixner, G. (2008): Effect of lake evaporation on dD values of lacustrine n-alkanes: A comparison of Nam Co (Tibetian Plateau) and Holzmaar (Germany). – Organic Geochemistry, 39: 711–729.

Prügel, B., Loosveldt, P. & Garrec, J.P. (1994): Changes in the content and constituents of the cuticular wax of *Picea abies* (L.) Karst. in relation to needle ageing and tree decline in five European forest ageas. – Trees, 9: 80–87.

Rommerskirchen, F., Plader, A., Eglinton, G., Chikaraishi, Y. & Rullkötter, J. (2006): Chemotaxonomic significance of distribution and stable carbon isotopic composition of long-chain alkanes and alkan-1-ols in C4 grass waxes. – Organic Geochemistry, 37: 1303–1332.

Rudner, Z. & Sümegi, P. (2001): Recurring Taiga forest-steppe habitats in the Carpathian Basin in the Upper Weichselian. – Quaternary International, 76/77: 177–189.

Schwark, L., Zink, K. & Lechtenbeck, J. (2002): Reconstruction of postglacial to early Holocene vegetation history in terrestrial Central Europe via cuticular lipid biomarkers and pollen records from lake sediments. – Geology, 30/5: 463–466.

Shepherd, T. & Griffiths, D.W. (2006): The effects of stress on plant cuticular waxes. – New Phytologist, 171: 469–499.

Smalley, I. & Leach, J.A. (1978): The origin and distribution of the loess in the Danube Basin and associated regions of East-Central Europe – a review. – Sedimentary Geology, 21: 1–26.

Stage_3-Project: – ftp://ftp.essc.psu.edu/pub/emsei/pollard/Stage3/PLOT_NEW.

Sümegi, P. & Krolopp, E. (2002): Quatermalacological analyses for modeling of the Upper Weichselian palaeoenvironmental changes in the Carpathian Basin. – Quaternary International, 91: 53–63.

Wiesenberg, G.L.B., Schwarzbauer, J., Schmidt, M.W.I. & Schwark, L. (2004): Source and turnover of organic matter in agricultural soils derived from n-alkane/n-carboxylic acid compositions and C-isotope signatures. – Organic Geochemistry, 35: 1371–1393.

Willis, K. & Andel, T. (2004): Trees or no trees? The environments of central and eastern Europe during the Last Glaciation. – Quaternary Science Reviews, 23: 2369–2387.

Willis, K., Rudner, E. & Sümegi, P. (2000): The Full-Glacial Forests of Central and Southeastern Europe. – Quaternary Research, 53: 203–213.

Zech, M. (2006): Evidence for Late Pleistocene climate changes from buried soils on the southern slopes of Mt. Kilimanjaro, Tanzania. – Palaeogeography, Palaeoclimatology, Palaeoecology, 242: 303–312.

Zech, M. & Glaser, B. (2008): Improved compound-specific $\delta^{13}C$ analysis of n-alkanes for application in palaeoenvironmental studies. – Rapid Communications in Mass Spectrometry, 22: 135–142.

Zech, M. & Glaser, B. (2009): Compound-specific $\delta^{18}O$ analyses of neutral sugars in soils using GC-Py-IRMS: problems, possible solutions and a first application. – Rapid Communications in Mass Spectrometry, accepted.

Zech, M., Buggle, M., Markovic, S., Lucic, T., Stevens, T., Gaudenyo, T., Jovanovic, M., Huwe, B. & Zöller, L. (2008a): First Alkane Biomarker Results for the Reconstruction of the Vegetation History of the Carpathian Basin (SE Europe). – In: Reitner, J, Fiebig, M., Neugebauer-Maresch, C., Pacher, M. & Winiwarter, V. (eds.): Veränderter Lebensraum – Gestern, Heute und Morgen, DEUQUA Symposium 2008. – Abhandlungen der Geologischen Bundesanstalt, 62: 123-127.

Zech, M., Zech, R., Morras, H., Moretti, L., Glaser, B. & Zech, W. (2008b): Late Quaternary environmental changes in Misiones, subtropical NE Argentina, deduced from multi-proxy geochemical analyses in a palaeosol-sediment sequence. – Quaternary International, 196: 121–136.

Zhang, Z., Zhao, M., Eglington, G., Lu, H. & Huang, C. (2006): Leaf wax lipids as paleovegetational and paleoenvironmental proxies for the Chinese Loess Plateau over the last 170 kyr. – Quaternary Science Reviews, 20: 575–594.

Late Glacial and Holocene aeolian sands and soil formation from the Pomeranian outwash plain (Mecklenburg, NE-Germany)

Dedicated to the 75th birthday of Wolfgang Janke

Mathias Küster, Frank Preusser

Abstract: The nature, duration and intensity of Late Glacial and Holocene aeolian sand and soil formation is established for two dune profiles from the Pomeranian outwash plain using a multidisciplinary approach (sedimentology, pedology, palynology, geochronology). During the Late Glacial period, coversands accumulated as thin sheets on plateau areas of the outwash plain, interrupted by the formation of the Finow soil. The spreading of dense vegetation cover during the Early Holocene resulted in stabilisation of the landscape surface and subsequent soil formation. After intensive medieval deforestation, surface destabilisation caused partial reworking of the coversands, resulting in the formation of dunes and a hummocky topography. One of the dunes investigated formed entirely within the Late Subatlantic. This study highlights the spatial and temporal variability of aeolian activity in areas where suitable grain sizes were made available during different periods after deglaciation.

[Spätglaziale und holozäne Flugsande und Bodenbildungen aus dem Pommerschen Sandergebiet (Mecklenburg, NE-Deutschland)]

Kurzfassung: Anhand von zwei Dünenprofilen wird die Art, Dauer und Intensität von spätglazialen und holozänen Flugsand- und Bodenbildungen innerhalb des Pommerschen Sandergebietes dargestellt. Hierfür wurde ein interdisziplinärer Ansatz aus Sedimentologie, Pedologie, Palynologie und Geochronologie verwendet. Während des Spätglazials kommen auf den Sanderhochflächen flache Flugsanddecken zur Ablagerung, unterbrochen durch die Bildung des Finowbodens. Durch die Ausbreitung einer geschlossenen Vegetationsdecke im Frühholozän, erfolgt eine Stabilisierung der Reliefoberfläche mit anschließender Bodenbildung. Nach intensiven mittelalterlichen Rodungen werden die Oberflächen erneut destabilisiert. Es kommt zur partiellen Aufarbeitung der Flugsande resultierend in Dünenbildungen und einem kuppigen Relief. Eine der untersuchten Dünen wurde dabei komplett im späten Subatlantikum gebildet. Diese Studie unterstreicht die zeitlich-räumliche Variabilität äolischer Aktivität, wobei Umlagerungen entsprechender Korngrößen während verschiedener Phasen nach der Deglaziation ermöglicht wurden.

Key words: *aeolian sands, Finow Soil, fossil soils, Late Glacial, Holocene dune formation, Geschiebedecksand (GDS)*

Addresses of authors: **M. Küster,** University of Greifswald, Institute of Geography and Geology, Friedrich-Ludwig-Jahn-Straße 16, D-17487 Greifswald. E-Mail: mathias.kuester@uni-greifswald.de; **F. Preusser,** University of Bern, Institute of Geological Sciences, Baltzerstrasse 1+3, CH-3012 Bern

1 Introduction

Throughout the European sand belt fossil soils of different age provide evidence of surface stability, while aeolian deposits mirror phases of morphodynamic activity (Schirmer 1999a). Comprehensive stratigraphic investigations in the adjacent areas of northern Brandenburg, Schleswig-Holstein and Poland resulted in a conceptional model for the timing of aeolian phases in northern Central Europe (Manikowska 1991; Teschner-Steinhardt & Müller 1994; Bussemer et al. 1998; Müller 1999, 2000; Mauz et al. 2005, Hilgers 2007). Previous studies in Mecklenburg-Vorpommern have largely focussed on the coastal region (Janke 1971; Kliewe & Janke 1978; Kaiser et al. 2006), and investigations from the inland are rare (e.g., Dieckmann & Kaiser 1998). This paper contributes to filling this gap by presenting new results on the chronology of aeolian processes and soil formation within the Pomeranian outwash plain.

2 Study area

The study area is situated on the Pomeranian outwash plain, between the ice-marginal zones of the Frankfurt Phase (18.4 ka BP) and the Pomeranian Phase (15.2 ka BP, Marks 2002). Despite its overall southern slope, the outwash plain offers a differentiated geomorphology, comprising older till areas, numerous kettle holes and meltwater channels. The latter depressions, which reflect glaciofluvial sedimentation between and over melting dead ice during Weichselian deglaciation (Nitz 1984), were subsequently filled with lakes and fens. Areas of dunes and aeolian coversands supplement the geomorphic inventory. The profiles investigated here (BF-1 and ZW-1) are part of dune complexes which are situated south of the village Blankenförde (Fig. 1), and are built up of widespread coversands and dune bodies with a hummocky morphology (Küster et al. 2008).

3 Methods

Fieldwork consisted of digging the pits manually, cleaning the faces and describing soil and sediment properties following the guidelines of the Ad-hoc-AG Boden (KA 5, 2005). Colours were determined according to MUNSELL-COLOR-CHART. The content of organic material was measured by loss on ignition (LOI) at 550 ℃ for 2 hours. The soil pH was determined in 0.01 M CaCl$_2$. The grain size distribution of
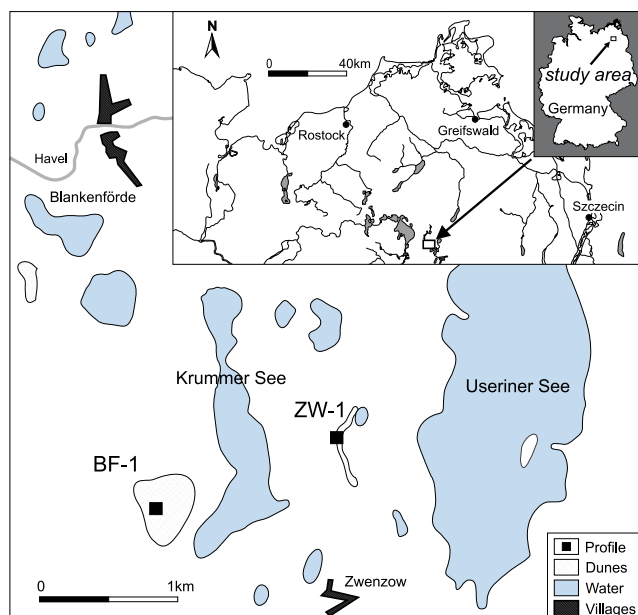
Fig. 1: Location of the study area in northeast Germany.

Abb. 1: Lage des Untersuchungsgebietes in Nordostdeutschland.

the fraction ≤ 2 mm was determined by a combined sieve and sedimentation procedure (Köhn 1928). Element concentrations (sample + LiBo$_2$ (2 g) + Li$_2$Bo$_4$O$_7$ (1,9320 g)) were measured using a Phillipps PW 2404 RFA-spectrometer. Weathering indices were calculated based on the element molar-ratios (Ruxton 1968; Kronberg & Nesbitt 1981; Harnois 1988). Pollen samples were separated by acetolyses (Beug 2004) and non-aboreal pollen (NAP) were related to the amount of 100 tree pollen. A radiocarbon sample (Erl-12081) was determined by the AMS-laboratory Erlangen using charcoal and calibrated using CALIB 5.0 (Stuiver et al. 2005). Ages are given as years before present (1000 a = 1 ka) and are correlated with the chronology recently summarised by Litt et al. (2007).

Optically stimulated luminescence (OSL) dating of quartz (150–200 μm) was carried out using a modified Single Aliquot Regenerative Dose (SAR) protocol (Murray & Wintle, 2000). A preheat temperature of 230℃ for 10 s prior to all OSL measurements was identified as appropriate from the results of SAR performance testes. Equivalent dose and standard error were calculated from the mean of replicate measurements (no indication for partial bleaching or postdepositional mixing). The concentration of dose rate relevant elements was determined by high-resolution low-level gamma spectrometry (Tab. 1). Sampling depth (for cosmic dose

rate) and present sediment moisture have been used for dose rate calculation.

4 Results

Profile BF-1

This profile has been divided into three units that will be described in stratigraphical order (Fig. 2).

Unit I

The basal part of the section consists of non-stratified sands. The grain size distribution reveals a homogenous sediment unit of fine and medium sand with very sporadic fine gravel. The top of Unit I is made up of a brownish, root penetrated soil horizon (2Bwb) of fine and medium sand, with a higher amount of gravel, silt and clay than the underlying sediments. Prominent pebbles at its base show traces of aeolian polishing. Because of the stratigraphical position and the lithology this sediment is classified as "Geschiebedecksand" (GDS) following German terminology (Berendt 1863). Together with the non-stratified sands below, this unit is interpreted as a periglacial cover bed (Lembke 1972). As typically for most other parts of NE-Germany, the GDS coincides with a brownish soil horizon (Kopp et al. 1969, Kopp 1970; Bussemer 2005). Because of missing stratified basal sediments a periglacial cover bed with perstruction zones is not documented (Kopp et al. 1969; Kopp & Jäger 1972). The weathering indices highlight the brownish soil horizont as the main weathering zone (Tab. 2). OSL-dating (MN 584) of this horizon yields an age of 15.5 ± 1.0 ka.

Unit II

The middle unit of the dune profile is made up of homogenous sands, dominated by medium and fine sands. With decreasing depth a decrease of the fine sand fraction is observed, while the fractions of medium sand, silt and clay increase. A fossil Cambisol (IUSS Working Group WRB 2006) separates Unit I from Unit II. The organic content (LOI) is prominent in the buried humic horizon (Apb), but less dominant than for the modern humic horizon (Unit III), due to the advanced mineralisation. The Bwb-horizon, comprising diffusely distributed charcoal fragments, shows a lower LOI value. The weathering indices characterise the brownish horizon as the second main weathering zone within the profile. Because of its facies character Unit II is classified as aeolian

Table 1: Summary data of OSL dating with concentration of dose rate relevant elements (K, Th, U), sediment water content, resulting dose rate, equivalent dose (D$_E$) and OSL age.

Tab 1: Zusammenfassung der OSL-Datierungen mit Konzentration der für die Dosisleistung relevanten Elemente (K, Th, U), Sediment-Wassergehalt, resultierende Dosisleistung (D$_E$) und OSL-Alter.

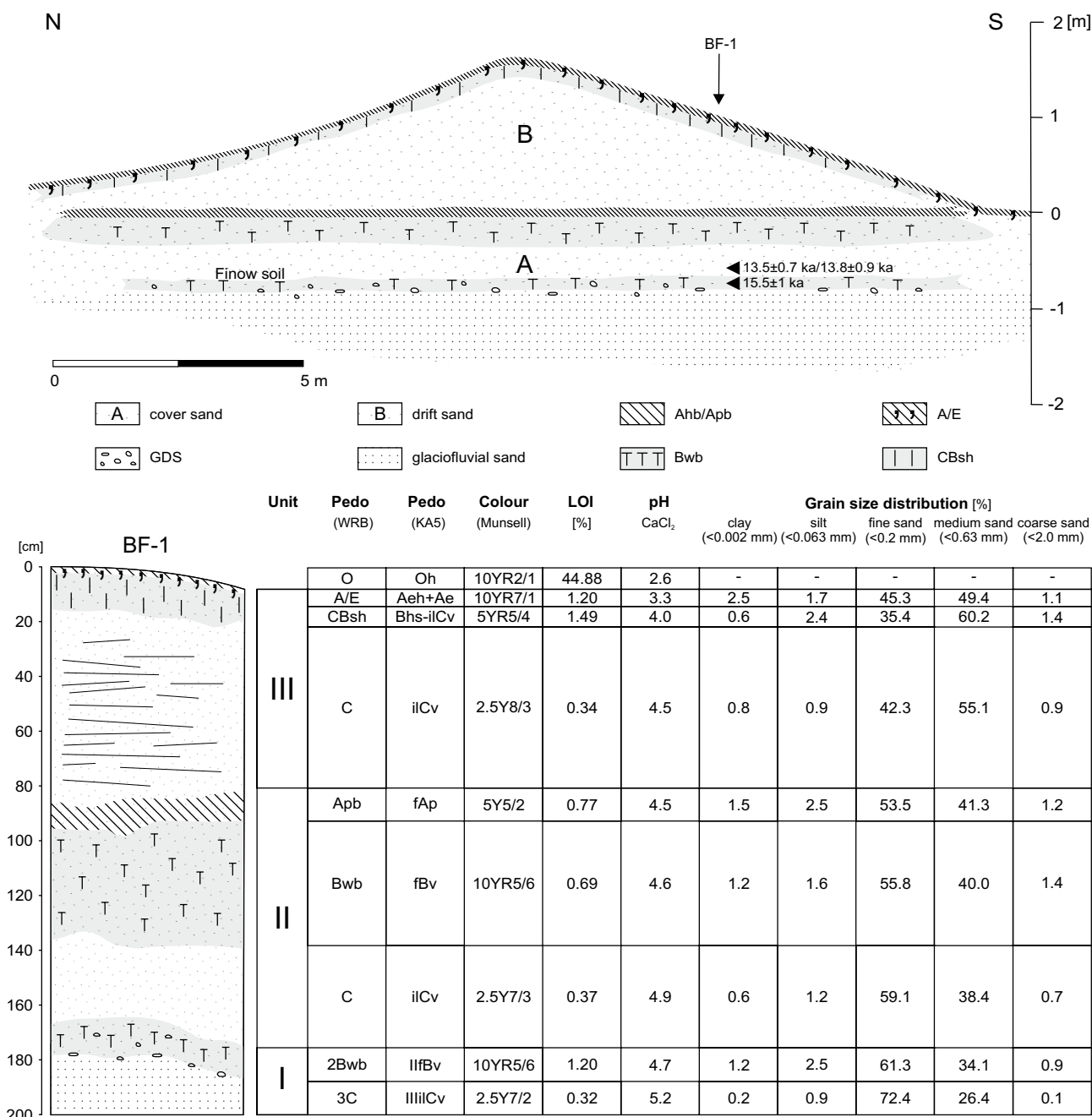| Sample	K [%]	Th [ppm]	U [ppm]	W [%]	Depth [m]	D [Gy ka-1]	DE [Gy]	OSL age [ka]
MN582	0.88 ± 0.02	2.13 ± 0.13	0.59 ± 0.02	4 ± 1	1.70	1.25 ± 0.05	17.3 ± 0.9	13.8 ± 0.9
MN583	0.88 ± 0.02	2.32 ± 0.06	0.65 ± 0.01	4 ± 1	1.75	1.28 ± 0.05	17.3 ± 0.6	13.5 ± 0.7
MN584	0.93 ± 0.02	7.56 ± 0.17	1.30 ± 0.03	8 ± 1	1.80	1.76 ± 0.07	27.3 ± 1.4	15.5 ± 1.0

Fig. 2: Cross-section through a sequence of aeolian sands of the plateau areas and pedological parameters of profile BF-1 (modified from Küster et al. 2008).

Abb. 2: Profilschnitt durch eine Flugsandsequenz der Hochflächen und pedologische Parameter des Profils BF-1 (verändert nach Küster et al. 2008).

| Unit | Pedo (WRB) | Pedo (KA5) | Colour (Munsell) | LOI [%] | pH CaCl₂ | Grain size distribution [%] | | | | |
						clay (<0.002 mm)	silt (<0.063 mm)	fine sand (<0.2 mm)	medium sand (<0.63 mm)	coarse sand (<2.0 mm)
	O	Oh	10YR2/1	44.88	2.6	-	-	-	-	-
	A/E	Aeh+Ae	10YR7/1	1.20	3.3	2.5	1.7	45.3	49.4	1.1
	CBsh	Bhs-ilCv	5YR5/4	1.49	4.0	0.6	2.4	35.4	60.2	1.4
III	C	ilCv	2.5Y8/3	0.34	4.5	0.8	0.9	42.3	55.1	0.9
	Apb	fAp	5Y5/2	0.77	4.5	1.5	2.5	53.5	41.3	1.2
II	Bwb	fBv	10YR5/6	0.69	4.6	1.2	1.6	55.8	40.0	1.4
	C	ilCv	2.5Y7/3	0.37	4.9	0.6	1.2	59.1	38.4	0.7
I	2Bwb	IIfBv	10YR5/6	1.20	4.7	1.2	2.5	61.3	34.1	0.9
	3C	IIIilCv	2.5Y7/2	0.32	5.2	0.2	0.9	72.4	26.4	0.1

coversand (Schirmer 1999b). Two samples obtained from the base of this unit yield OSL ages of 13.8 ± 0.9 ka (MN 582) and 13.5 ± 0.7 ka (MN 583), respectively. Pollen samples from the fossil humic horizon (Apb) indicate an open, deforestated landscape, reflected by a high proportion of non-tree-pollen, such as *Artemisia*, *Calluna vulgaris* and *Plantago lanceolata* (Fig. 3). The abundence of species such as *Secale* and *Scleranthus* implies intensive agricultural use in the surroundings, palynologically dating the horizon to the Late Subatlantic (Xb, Firbas 1949).

Unit III

The grain size distribution of Unit III is dominated by medium sand and subordinate fine sand. With decreasing depth an increase in silt and clay is recognised, like in the un-

derlying complex. The partly observed horizontal, slightly inclined bedding indicates sediment accumulation as low-angle aeolian deposits (Fryberger et al. 1979). Despite the relatively low maximum thickness of 1.8 m, the sand unit creates an intensive hummocky topography, a feature regionally known as "Kuppendüne" (Pyritz 1972).

The upper part of Unit III is characterized by a podzolized Arenosol (IUSS Working Group WRB 2006) or a Podsol-Regosol (Ad-hoc-AG Boden 2005). Despite the weak development of the soil, the advanced differentiation into an eluvial and an illuvial horizon, reflected in both colour and loss on ignition values, indicate a final state of a transformation to a podzol (Lundström et al. 2000; Behrendt et al. 2002). Pollen analyses of the O-horizon suggests a closed forest vegetation during the time of soil formation. Based on the rapid decrease of non-tree-pollen compared to the Apb horizon and
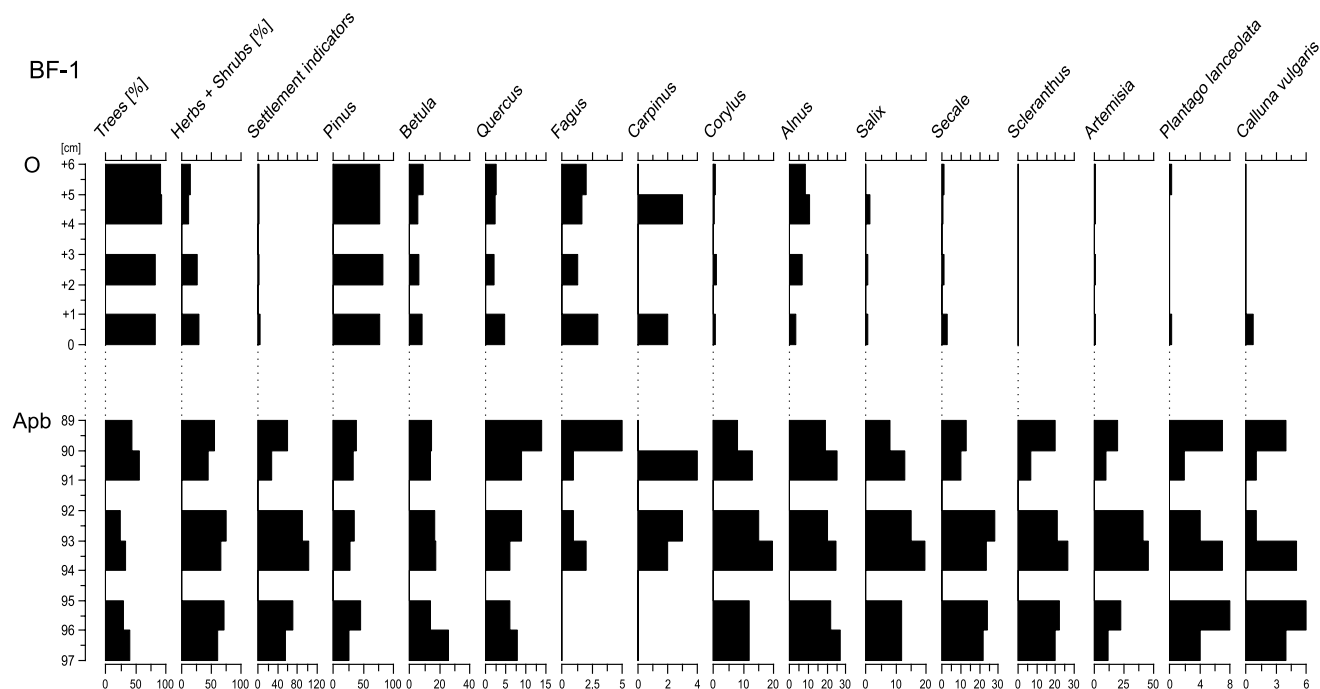
Fig. 3: Selected pollen data from humic horizons of profile BF-1. / Abb. 3: Ausgewählte Pollendaten aus Humushorizonten des Profils BF-1.

the dominance of *Pinus sylvestris*, it can reasonably be assumed that a vegetation cover established during the Youngest Subatlantic (Xc, FIRBAS 1949).

Profile ZW-1

Alongside the western margin of a peat filled depression a linear dune was investigated, comprising profile ZW-1 (Fig. 4). The basal part shows a fossil Cambisol (IUSS WORK-ING GROUP WRB 2006). High LOI values and a widespread occurrence of charcoal indicate an intensive anthropogenic impact. The exceptionally thick fossil humic horizon can be separated into three parts (Apb). Each part reflects a separate phase of aeolian sedimentation and, due to agricultural use (ploughing), ends on a sharp upper limit to aeolian sand which are free of humus. A charcoal sample at the bottom of the humic horizon reveals a radiocarbon age of 815±44 ^{14}C yr BP (1154–1280 AD, 97,4 %-2σ calibrated, STUIVER et al. 2005) and provides a maximum age for the onset of aeolian activity. It can thus be concluded that the entire dune was formed during the Late Subatlantic, representing a "Holocene dune"

(DULIAS 1999). At the top a weakly podzolized Arenosol (IUSS WORKING GROUP WRB 2006) represents the result of modern soil formation.

5 Discussion

Deposition of glaciofluvial sands in the area terminated during the Late Pleniglacial, prior 15 ka ago, as indicated by the OSL date for the basal part of the sections. The following Late Glacial period is set between the Mecklenburg Phase and the middle Preboreal (KLIEWE 2004). The periglacial cover bed of profile BF-1 (Unit I) provides evidence of intensive cryogenic, postsedimentary modification of the plateau-sites. The genesis of the "Geschiebedecksand" (GDS) as the central element of periglacial cover beds has been discussed in detail, and the relevant key elements are discussed below. On sandy slopes within the Weichselian periglacial belt solifluction, nival runoff, concurrent winnowing of fines (abluation sensu LIEDTKE (1990)) and aeolian processes are the main processes involved in its formation (BUSSEMER et al. 1993). For the plateau sites KOPP et al. (1969), KOPP (1970), KOPP & JÄGER

Table 2: Major element analysis and chemical weathering indices of profile BF-1 (soil horizons according to IUSS WORKING GROUP WRB 2006).

Tab. 2: Hauptelementanalyse und chemische Verwitterungsindizes des Profils BF-1 (Bodenhorizonte nach IUSS WORKING GROUP WRB 2006).

| Horizon	SiO_2 [%]	Al_2O_3 [%]	Fe_2O_3 [%]	MnO [%]	MgO [%]	CaO [%]	Na_2O [%]	K_2O [%]	P_2O_5 [%]	TiO_2 [%]	Ruxton (1968) SiO_2/Al_2O_3	Kronberg & Nesbitt (1981) Ordinate	Abscissa	Harnois (1988) CIW
A/E	91.89	2.34	0.47	0.01	0.06	0.21	0.43	0.93	0.02	0.23	66.61	0.47	0.99	68.12
CBsh	89.60	2.43	0.64	0.01	0.08	0.21	0.43	0.94	0.05	0.23	62.55	0.47	0.98	68.83
C	92.66	2.70	0.70	0.02	0.10	0.25	0.50	0.98	0.05	0.31	58.34	0.46	0.98	67.92
Apb	92.56	2.74	0.56	0.02	0.09	0.22	0.57	0.99	0.06	0.19	57.37	0.47	0.98	67.30
Bwb	92.24	3.07	0.58	0.01	0.09	0.22	0.49	1.02	0.06	0.19	51.01	0.43	0.98	72.03
C	91.79	2.89	0.65	0.02	0.11	0.27	0.55	1.07	0.05	0.21	53.81	0.47	0.98	67.49
2Bwb	89.43	4.31	0.85	0.02	0.14	0.26	0.51	1.16	0.06	0.28	35.21	0.37	0.97	76.70
3C	92.85	2.86	0.65	0.02	0.11	0.25	0.48	1.09	0.02	0.20	55.14	0.46	0.98	69.55
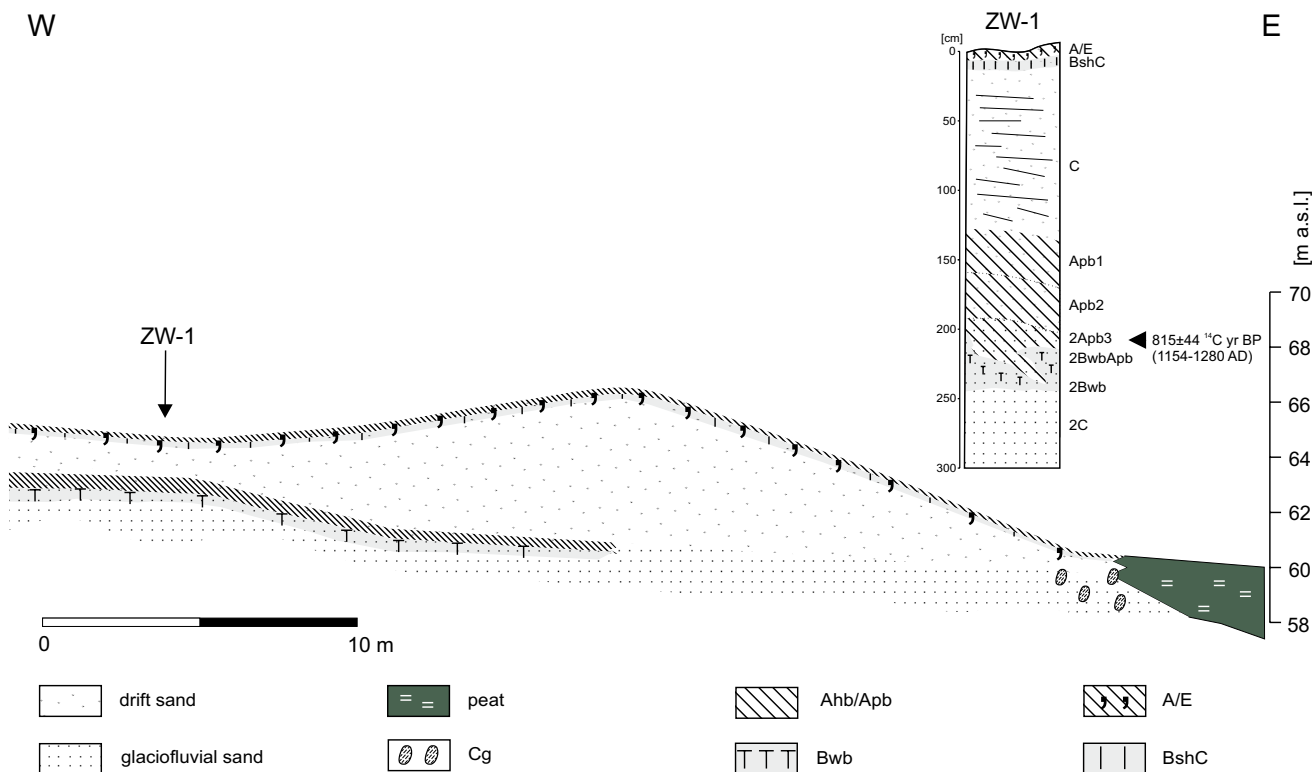
Fig. 4: Cross-section through a Holocene dune and pedology of profile ZW-1 (soil horizons according to IUSS Working Group WRB 2006).

Abb. 4: Profilschnitt durch eine holozäne Düne und Pedologie des Profils ZW-1 (Bodenhorizonte nach IUSS Working Group WRB 2006).

(1972) and Kopp & Kowalkowski (1990) favour cryogenic destratification as the main formation process for the GDS. These authors describe this process as a post- or synsedimentary – in situ – modification of the sediment matrix under periglacial conditions. The gravel-bed at its base with ventifacts represents a desert pavement indicating deflation and is a prevalent phenomenon in glacial landscapes of NE-Germany (Lembke 1972). In terms of genetic processes, the "Beuningen Gravel Bed" (BGB), which is widespread in western Europe and forms an important marker horizon in the Late Weichselian coversand stratigraphy (Vandenberghe 1985, Kasse 2002), might be a close correlative to the clast pavements observed here. While Kolstrup (1980) suggests a two-phase development for the BGB with a fluvial phase causing deposition of coarse sand and gravel followed by a deflation phase, Kasse et al. (2007) consider a synsedimentary fluvio-aeolian regime. The formation of the BGB has been dated to the Late Pleniglacial (c.14–18 ka, Kasse et al. 2007).

The non-stratified glaciofluvial sands at Blankenförde suggest a relative enrichment of gravel on the surface due to frost heave under permafrost conditions after glaciofluvial sedimentation, thereby destroying former glaciofluvial sediment structures (French 2007). This phase was most likely followed by an aeolian phase causing deflation of fine materials and modification of gravel to ventifacts (Fig. 5).

For the final formation of the GDS Bussemer (2002) assumes processes including sedimentation and cryogenic destratification of sediments. At this juncture the (coarse) silt content of the GDS gives evidence of aeolian sedimentation, typical within regions of sandy plains (Altermann 1970). Therefore the charakter of the GDS as a parautochthonous facies can be stressed (Bussemer 2002). OSL dating (MN 584)

of the GDS sediments indicates a Late Pleniglacial to Late Glacial age.

Within the GDS a weakly developed Cambisol was identified, which is parallelised with the Finow soil, which has widespread occurrence in Brandenburg (Germany) (Schlaak 1993, 1998, 1999, Bussemer et al. 1998). Occurences of this palaeosol were reported from Poland and Mecklenburg-Vorpommern (Kowalkowski et al. 1999; Lorenz et al. 2002; Kaiser 2003, Kaiser et al. 2009). For the Netherlands, NW-Germany, the Altdarss area of Mecklenburg-Vorpommern (southern Baltic coast) and central Poland a stratigraphically identical but pedologically different soil was found, the Usselo soil (Hijszeler 1957; Dücker & Maarleveld 1957; Kasse 1999; Kaiser & Clausen 2005; Kaiser et al. 2006). It is classified as a weakly podzolized Arenosol (IUSS Working Group WRB 2006) or a weakly podzolized Regosol (Ad-hoc-AG Boden 2005). There is no sufficient explanation for the apparent provenances of both palaeosols so far. A compilation of 63 ages from Usselo and Finow soils in northern Central Europe reveals a substantial time range for soil formation between the Older Dryas and the Younger Dryas, with single outliers in the Preboreal (Kaiser et al. 2009). Hence, formation of these palaeosols can based on geochronological data not securely be correlated to the Allerød, as often assumed, and it is more appropriate to interpret these soils as being of Late Glacial age (Kaiser et al. 2009). The two consistent OSL ages (MN 582 and MN 583) of the overlying Unit II of Profil BF-1 indicate that the Finow soil at Blankenförde was fossilized at least ~13.5 ka ago by Late Glacial aeolian activity.

Palynological records from Lake Müritz provide evidence of an increasing vegetation cover within the Mecklenburg

Lake District during the Preboreal (Lampe et al. 2009), implying successive stabilisation of the surface at Blankenförde after Late Glacial sediment translocation, i.e. since the Early Holocene. Therefore the increasing silt content within Unit II (and Unit III, profile BF-1) is interpreted as reflecting a decrease in wind strength due to a closing vegetation cover (Dücker & Maarleveld 1957). The fossil Cambisol at the top of Unit II reflects a subsequent surface stability (Rohdenburg 1970) enabling soil formation within Late Glacial aeolian substrate. Because of its minor thickness compared to undisturbed Cambisols, a phase of soil erosion of unknown age, prior to the formation of the buried humic horizon (Apb), is assmued. The absolute values of weathering indices document a lower weathering intensity compared to the time of Late Glacial palaeosol formation, possibly due to higher Late Glacial climate variability or/and a higher initial degree of weathering of the blown-out parent material. Biogenic mixing during soil formation is well documented by the absence of sedimentary structures, diffusely distributed charcoal fragments and a slightly lower content of organic matter of the Bwb-horizon compared to the humic horizon (Apb) above (Andersen 1979; Helbig et al. 2002). However, a syndepositional character of the charcoal could also be assumed. Pollen analysis of the fossil humic horizon reveals a partly open landscape, indicating intensive deforestation during Medieval Times, reflecting the maximum age of the aeolian sands on top (Lüders 1961). Most likely, Late Holocene human landscape disturbance led to an interruption of soil formation, causing sediment translocations in the sense of soil erosion (Bork 1988). Late Glacial coversands were reworked resulting in the formation of new dunes.The facies of these Young Holocene aeolian sands can be classified as drift sands (Castel et al. 1989; Castel 1991; Koster et al. 1993), and the onset of this youngest aeolian phase can be placed into the 13th century (profile ZW-1). Within profile

BF-1 the increasing content of medium sand, with a concurrent decrease in the content of fine sand, provides evidence of the selective effect of successive deflation processes: coarse grain sizes are relatively enriched, whereas fine grains are depleted (Goossens & Gross 2002). This was followed by Late Holocene soil formation, which can be classified in the study area as a weakly podzolized Arenosol (IUSS Working Group WRB 2006). For the maritime influenced Denmark Stützer (1998) concludes a rate of podzolization within aeolian sands of 1 cm per decade. Taking the thickness of the podzolic horizons of soil formation into account, a remarkably lower rate is recorded in the study area, probably due to its more subcontinental character.

6 Conclusions

The "Geschiebedecksand" (GDS) on sandy plateau sites as a stratigraphic marker in NE-Germany is of periglacial origin due to frost heave, deflation, aeolian sedimentation and finally destratification. The timing oft its formation seems comparable with the Beuningen Gravel Bed in western Europe. The Late Glacial Finow soil developed in GDS and was buried by Late Glacial coversands about 13.5 ka ago. Afterwards, a long phase of surface stablility lasted until the Late Holocene. Pollen analyses of humic horizons give evidence of intensive human impact (mainly deforestation) during the Medieval, causing soil erosion and reshaping of the morphology at the plain sites. A phase of dune sand accumulation post dating the 13th century provides evidence of strong human impact at around this time.
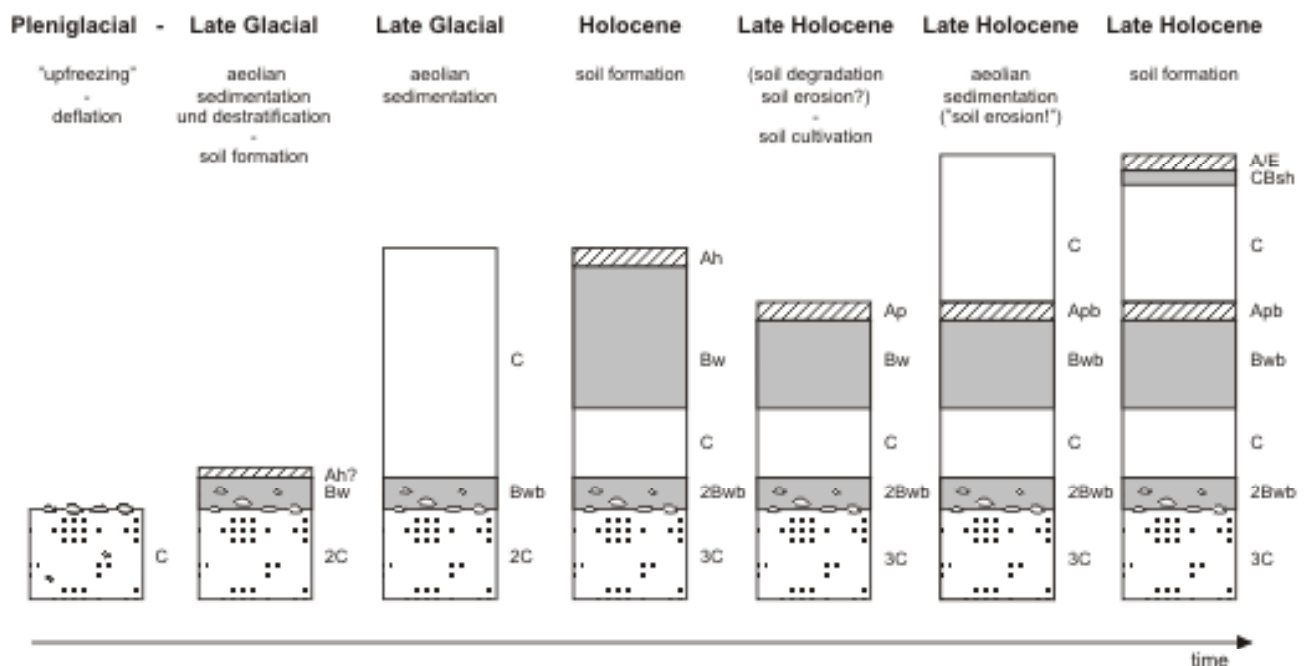
Acknowledgements

Fig. 5: Genesis of profile BF-1 including sedimentary processes and soil formation (soil horizons according to IUSS Working Group WRB 2006).

Abb. 5: Genese des Profils BF-1 einschließlich sedimentologischer Prozesse und Bodenbildung (Bodenhorizonte nach IUSS Working Group WRB 2006).

References

AD-HOC-AG BODEN (2005): Bodenkundliche Kartieranleitung. 5. Auflage. – 438 S.; Hannover (BGR).

ALTERMANN, M. (1970): Periglaziale Decksedimente. In: RICHTER, H., HAASE, G., LIEBEROTH, I. & RUSKE, R. (eds.): Periglazial-Löß-Paläolithikum im Jungpleistozän der DDR. – Petermanns Geographische Mitteilungen, Ergänzungsheft, 274: 232–250.

ANDERSEN, S.T. (1979): Brown earth and podzol: soil genesis illuminated by microfossil analysis. – Boreas, 8: 59–73.

BEHRENDT, A., KAFFKE, A. & MUNDEL, G. (2002): Ein fossiler Podsol in Brandenburg – Ursachen seiner Entstehung und ein Vergleich zu seinem Folgeboden. – Archiv für Acker- und Pflanzenbau und Bodenkunde, 48: 213–226.

BERENDT, G. (1863): Die Diluvialablagerungen in der Mark Brandenburg. – Zeitschrift der deutschen geologischen Gesellschaft, 15: 640–642.

BEUG, H.-J. (2004): Leitfaden der Pollenbestimmung für Mitteleuropa und angrenzende Gebiete. – 542 S.; München (Pfeil Verlag).

BORK, H.-R. (1988): Bodenerosion und Umwelt - Verlauf, Ursachen und Folgen der mittelalterlichen und neuzeitlichen Bodenerosion. Bodenerosionsprozesse. Modelle und Simulation. – Landschaftsgenese und Landschaftsökologie, 13: 249 S.

BUSSEMER, S. (2002): Periglacial cover-beds in the young moraine landscapes in northern Eurasia. – Zeitschrift für Geomorphologie, N. F. Suppl.-Bd., 127: 81–105.

BUSSEMER, S. (2005): Die Braunerde in ihrer nordbrandenburgischen Typusregion. Brandenburgische geowissenschaftliche Beiträge, 12/1–2: 3–12.

BUSSEMER, S., GÄRTNER, P. & SCHLAAK, N. (1993): Neue Erkenntnisse zur Beziehung von Relief und geologischem Bau der südlichen baltischen Endmoräne nach Untersuchungen auf der Neuenhagener Oderinsel. – Petermanns Geographische Mitteilungen, 137: 227–239.

BUSSEMER, S., GÄRTNER, P. & SCHLAAK, N. (1998): Stratigraphie, Stoffbestand und Reliefwirksamkeit der Flugsande im brandenburgischen Jungmoränenland. – Petermanns Geographische Mitteilungen, 142: 115–125.

CASTEL, I.I.Y. (1991): Micromorphology of the transition peat – Holocene drift sand deposits in the northern Netherlands. – Zeitschrift für Geomorphologie, N. F. Suppl.-Bd., 90: 29–43.

CASTEL, I., KOSTER, E. & SLOTBOOM, R. (1989): Morphogenetic aspects and age of Late Holocene eolian drift sands in Northwest Europe. – Zeitschrift für Geomorphologie, N. F., 33: 1–26.

DIECKMANN, O. & KAISER, K. (1998): Pedologische und geomorphologische Befunde zur historischen Bodenerosion im Müritz-Nationalpark (Mecklenburg-Vorpommern). – In: ASMUS, I, PORADA, H.T., SCHLEINERT, D. (eds.): Geographische und historische Beiträge zur Landeskunde Pommerns. – Sonderband der Greifswalder Geographischen Arbeiten: 59–67.

DÜCKER, A. & MAARLEVELD, G.C. (1957): Hoch- und spätglaziale äolische Sande in Nordwestdeutschland und in den Niederlanden. – Geologisches Jahrbuch, 73: 215–234.

DULIAS, R. (1999): Holocene dunes in southern Poland. In: SCHIRMER, W. (ed.): Dunes and fossil soils. – GeoArchaeoRhein, 3: 137–146 ; Münster (LIT).

FIRBAS, F. (1949): Die spät- und nacheiszeitliche Waldgeschichte Mitteleuropas nördlich der Alpen. Bd. 1: Allgemeine Waldgeschichte. – 480 S.; Jena (Fischer Verlag).

FRENCH, H.M. (2007): The Periglacial Environment. 3rd Edition. – 478 S.; Chichester (Wiley).

FRYBERGER, S.G., AHLBRANDT, T. S. & ANDREWS, S. (1979): Origin, sedimentary features, and significance of low-angle eolian "sand sheet" deposits, Great Dunes National Monument and Vicinity, Colorado. – Journal of Sedimentary Petrology, 49/3: 733–746.

GOOSSENS, D. & GROSS, J. (2002): Similarities and dissimilarities between the dynamics of sand and dust during wind erosion of loamy sandy soil. – Catena, 47: 269–289.

HARNOIS, L. (1988): The CIW Index: A new chemical index of weathering. – Sedimentary Geology, 55: 319–322.

HELBIG, H., DE KLERK, P. KÜHN, P. & KWASNIOWSKI, J. (2002): Colluvial sequences on till plains in Vorpommern (NE Germany). – Zeitschrift für Geomorphologie, N. F. Suppl.-Bd., 128: 81–100.

HIJSZELER, G.C.W.J. (1957): Late-glacial human cultures in the Netherlands. – Geologie en Mijnbouw, 19: 288–302.

Hilgers, A. (2007): The chronology of Late Glacial and Holocene dune development in the northern Central European lowland reconstructed by optically stimulated luminescence (OSL) dating. Phd-Thesis. University of Cologne.

IUSS WORKING GROUP WRB (2006): World reference base for soil resources 2006. 2nd edition. World Soil Resources Reports No. 103.: 145 S.; Rome (FAO).

JANKE, W. (1971): Beitrag zu Entstehung und Alter der Dünen der Lubminer Heide sowie der Peenemünde-Zinnowitzer Seesandebene. – Wissenschaftliche Zeitschrift der Universität Greifswald, Mathematisch-Naturwissenschaftliche Reihe, 20, 1/2: 39–54.

KAISER, K. (2003): Geoarchäologie und landschaftsgeschichtliche Aussage spätpaläolithischer und frühmesolithischer Fundplätze in Mecklenburg-Vorpommern. – Meyniana, 55: 49–72.

KAISER, K. & CLAUSEN, I. (2005): Palaeopedology and stratigraphy of the Late Palaeolithic Alt Duvenstedt site, Schleswig-Holstein (Northwest-Germany). – Archäologisches Korrespondenzblatt, 35: 447–466.

KAISER, K., BARTHELMES, A., CZAKÓ PAP, S., HILGERS, A., JANKE, W., KÜHN, P. & THEUERKAUF, M. (2006): A Lateglacial palaeosol cover in the Altdarss area, southern Baltic Sea coast (northeast Germany): investigations on pedology, geochronology and botany. – Netherlands Journal of Geosciences 85/3: 197–220.

KAISER, K., HILGERS, A., SCHLAAK, N., JANKOWSKI, M., KÜHN, P., BUSSEMER, S. & PRZEGIETKA, K. (2009): Palaeopedological marker horizons in northern central Europe: characteristics of Lateglacial Usselo and Finow soils. – Boreas, 38: 591–609.

KASSE, C. (1999): Late Pleniglacial and Late Glacial aeolian phases in The Netherlands. – In: SCHIRMER, W. (ed.): Dunes and fossil soils. – GeoArchaeoRhein, 3: 61–82; Münster (LIT).

KASSE, C. (2002): Sandy aeolian deposits and environments and their relation to climate during the Last Glacial Maximum and Lateglacial in northwest and central Europe. – Progress in Physical Geography, 26: 507–532.

KASSE, C., VANDENBERGHE, J., DE CORTE, F. & VAN DEN HAUTE, P. (2007): Late Weichselian fluvio-aeolian sands and coversands of the type locality Grubbenvorst (southern Netherlands): sedimentary environments, climate record and age. – Journal of Quaternary Science, 22/7: 695–708.

KLIEWE, H. (2004): Weichsel-Spätglazial. – In: KATZUNG, G. (ed.): Geologie von Mecklenburg-Vorpommern. – S. 242–251; Stuttgart (Schweizerbart).

KLIEWE, H. & JANKE, W (1978): Zur Stratigraphie und Entwicklung des nordöstlichen Küstenraumes der DDR. – Petermanns Geographische Mitteilungen, 122/ 2: 81–91.

KÖHN, M. (1928): Bemerkungen zur mechanischen Bodenanalyse: III. Ein neuer Pipettapparat. – Zeitschrift für Pflanzenernährung, Düngung, Bodenkunde, 11: 50–54.

KOLSTRUP, E. (1980): Climate and stratigraphy in northwestern Europe between 30.000 BP and 13.000 BP, with special reference to the Netherlands. – Mededelingen Rijks Geologische Dienst, 32/15: 181–253.

KOPP, D. (1970): Kryogene Perstruktion und ihre Beziehung zur Bodenbildung im Moränengebiet. – In: RICHTER, H., HAASE, G., LIEBEROTH, I & RUSKE, R. (eds.): Periglazial-Löß-Paläolithikum im Jungpleistozän der DDR. – Petermanns Geographische Mitteilungen, Ergänzungsheft, 274: 269–279.

KOPP, D. et al. (1969): Ergebnisse der forstlichen Standortkartierung in der Deutschen Demokratischen Republik. Potsdam.

KOPP, D. & JÄGER, K.-D. (1972): Das Perstruktions- und Horizontprofil als Trennmerkmal periglaziärer und extraperiglaziärer Oberflächen im nordmitteleuropäischen Tiefland. – Wissenschaftliche Zeitschrift der Universität Greifswald, Mathematisch-Naturwissenschaftliche Reihe, 21/1: 77–84.

KOPP, D. & KOWALKOWSKI, A. (1990): Cryogenic and pedogenic perstruction in tertiary and quaternary deposits, as exemplified in the outcrop of Sternebeck. – Quaternary studies in Poland, 9: 51–71.

Koster, E. A., Castel, I. I. Y. & Nap, R. L. (1993): Genesis and sedimentary structures of late Holocene aeolian drift sands in northwest Europe. – In: Pye, K. (ed.): The dynamics and environmental context of aeolian sedimentary systems. – Geological Society Special Publication, 72: 247–267; London (Geological Society).

Kowalkowski, A., Nowaczyk, B. & Okuniewska-Nowaczyk, I. (1999): Chronosequence of biogenic deposits and fossil soils in the dune near Jasień, Western Poland. – In: Schirmer, W. (ed.): Dunes and fossil soils. – GeoArchaeoRhein, 3: 107–127; Münster (LIT).

Kronberg, B.I. & Nesbitt, H.W. (1981): Quantification of weathering, soil geochemistry and soil fertility. – Journal of Soil Science, 32: 453–459.

Küster, M., Janke W., Lampe, R., Lorenz, S., Meyer, H. & Naumann, M. (2008): Rekonstruktion holozäner Bodenerosion anhand von Kolluvien, Flugsanddecken und Seesedimenten im Sander des Pommerschen Stadiums (NO-Deutschland). – Abhandlungen der Geologischen Bundesanstalt, 62: 173–177.

Lampe, R., Lorenz, S., Janke, W., Meyer, H., Küster, M. Hübener, T. & Schwarz, A. (2009): Zur Landschafts- und Gewässergeschichte der Müritz. Umweltgeschichtlich orientierte Bohrungen 2004–2006 zur Rekonstruktion der nacheiszeitlichen Entwicklung. – In: Nationalparkamt Müritz (ed.): Forschung und Monitoring, Band 2, 94 S.; Greifswald (Geozon).

Lembke, H. (1972): Die Periglazialerscheinungen im Jungmoränengebiet der DDR. – Wissenschaftliche Zeitschrift der Universität Greifswald, Mathematisch-Naturwissenschaftliche Reihe, 21/1: 71–76.

Liedtke, H. (1990): Abluale Abspülung und Sedimentation in Nordwestdeutschland während der Weichsel-(Würm)-Eiszeit. – In: Liedtke, H. (ed.): Eiszeitforschung: 261–269; Darmstadt (Wissenschaftliche Buchgesellschaft).

Litt, T., Behre, K.-E., Meyer, K.-D., Stephan, H.-J. & Wansa, S. (2007): Stratigraphische Begriffe für das Quartär des norddeutschen Vereisungsgebietes. – Quaternary Science Journal, 56/1–2: 7–65.

Lorenz, S., Rother, H. & Kaiser, K. (2002): Die jungquartäre Gewässernetzentwicklung der Krakower Seen und der Nebel (Mecklenburg) – erste Ergebnisse. – Greifswalder Geographische Arbeiten, 26: 79–82.

Lüders, R. (1961): Altersbestimmung an einem doppelten Podsolprofil aus dem Emsland. – Zeitschrift für Pflanzenernährung, Düngung, Bodenkunde, 94: 47–53.

Lundström, U.S., van Breeman, N. & Bain, D. (2000): The podzolization process. A review. – Geoderma, 94: 91–107.

Manikowska, B. (1991): Vistulian and Holocene aeolian activity, pedostratigraphy and relief evolution in Central Poland. – Zeitschrift für Geomorphologie, N.F. Suppl.-Bd., 90: 131–141.

Marks, L. (2002): Last Glacial Maximum in Poland. – Quaternary Science Reviews, 21: 103–110.

Mauz, B., Hilger, W., Müller, M.J., Zöller, L. & Dikau, R. (2005): Aeolian activity in Schleswig-Holstein (Germany): Landscape response to Late Glacial climate change and Holocene human impact. – Zeitschrift für Geomorphologie, N.F. 49: 417–431.

Müller, M.J. (1999): Genese und Entwicklung schleswig-holsteinischer Binnendünen. – Berichte zur deutschen Landeskunde, 73: 129–150.

Müller, M.J. (2000): Altersbestimmung an schleswig-holsteinischen Binnendünen mit Hilfe von Paläoböden. – Trierer Bodenkundliche Schriften,1: 23–31.

Murray, A.S. & Wintle, A.G. (2000): Luminescence dating of quartz using an improved single-aliquot regenerative-dose protocol. – Radiation Measurements, 32: 57–73.

Nitz, B. (1984): Grundzüge der Beckenentwicklung im mitteleuropäischen Tiefland – Modell einer Sediment- und Reliefgenese. – Petermanns Geographische Mitteilungen, 128: 133–142.

Pyritz, E. (1972): Binnendünen und Flugsandebenen im Niedersächsischen Tiefland. – Göttinger Geographische Abhandlungen, 61: 1–153.

Rohdenburg, H. (1970): Morphodynamische Aktivitäts- und Stabilitätszeiten statt Pluvial- und Interpluvialzeiten. – Eiszeitalter u. Gegenwart, 21: 81–96.

Ruxton, B.P. (1968): Measures of the degree of chemical weathering of rocks. – Journal of Geology, 76: 518–527.

Schirmer, W. (1999a): Dune phases and fossil soils in the European sand belt. – In: Schirmer, W. (ed.): Dunes and fossil soils. – GeoArchaeoRhein, 3: 11–42; Münster (LIT).

Schirmer, W. (1999b): Definitions concerning coversand, fossil soil and paleosol. – In: Schirmer, W. (ed.): Dunes and fossil soils. – GeoArchaeoRhein, 3: 187–190; Münster (LIT).

Schlaak, N. (1993): Studie zur Landschaftsgenese im Raum Nordbarnim und Eberswalder Urstromtal. – Berliner Geographische Arbeiten, 76: 1–145.

Schlaak, N. (1998): Der Finowboden – Zeugnis einer begrabenen weichselspätglazialen Oberfläche in den Dünengebieten Nordostbrandenburgs. – Münchener Geographische Abhandlungen, Reihe A, Band A49: 143–148.

Schlaak, N. (1999): Typical aeolian sand profiles and palaeosols of the Glien till plain in the northwest of Berlin. – In: Schirmer, W. (ed.): Dunes and fossil soils. – GeoArchaeoRhein, 3: 97–105; Münster (LIT).

Stuiver, M., Reimer, P.J. & Reimer, R.W. (2005). CALIB 5.0 [www program and documentation].

Stützer, A. (1998): Early stages of podzolisation in young aeolian sediments, western Jutland. – Catena, 32: 115–129.

Teschner-Steinhardt, R. & Müller, M. (1994): Zur Genese und dem Alter der Dünen im Bereich der Havel-Niederung, Berlin-Tegeler Forst. – Die Erde, 125: 123–138.

Vandenberghe, J. (1985): Paleoenvironment and stratigraphy during the Last Glacial in the Belgian-Dutch Border Region. – Quaternary Research, 24: 23–38.

Coastal evolution of a Holocene barrier spit (Bug peninsula/NW-Rügen) deduced from geological structure and relative sea-level

Michael Naumann , Reinhard Lampe, Gösta Hoffmann

Abstract:

The Bug peninsula/NW Rügen located at the south-western Baltic coast has been investigated to study coastal barrier evolution depending on Holocene sea-level rise. In this so far minor explored coastal section 25 sediment cores, seven ground-penetrating radar tracks and six sediment-echosounder tracks were collected from which six depositional facies types were derived. The data show that the recent peninsula consists of an about 10 m thick Holocene sediment sequence, underlain by Pleistocene till or (glaci-) fluviolimnic fine sand. Although no absolute age data could be gathered to estimate the chronostratigraphy of the sedimentary sequence the relation of the depositional facies to the local relative sea-level curve allow the reconstruction of the palaeogeographic evolution of the Bug barrier spit.

The marine inundation of the area occurred around 7,000 BC during the Littorina transgression. In this stage the sea level rose rapidly and generated a fast increasing subaquatic accommodation space, where fine clastic material was deposited nearly or below the wave base and levelled the former relief. Accumulative coastal landforms grew to only minor extent because the accommodation space increased faster than it was filled with material from neighbouring eroding cliffs. Since the time the sea-level rise decreased accumulation became more dominant and the main barrier was built up in only some two thousand years. According to the beach ridge formations visible on the barrier´s surface the shoreline development of the Bug peninsula can be divided into two evolutionary stages depending on wave impact, erosion and overwash.

Today, the barrier displays a volume of 66.4 million m³ according to a feeder cliff retreat of at about 2000 m. Although the barrier seems to be in maturity stage some features points to instability. Coastal protection measures in the north prevent breakthrough and detachment. Waterway dredging in the south inhibited further elongation and accretion with spits growing from Hiddensee. Without these measures the barrier would disintegrate and be reshaped by inlet generation and increasing erosion in the north and inlet closure and beach progradation in the south.

[Küstenentwicklung einer holozänen Nehrung (Halbinsel Bug/NW-Rügen) abgeleitet aus der geologischen Struktur und dem relativen Meeresspiegel]

Kurzfassung:

Die an der südwestlichen Ostseeküste gelegene Halbinsel Bug/NW Rügen wurde untersucht, um die Entwicklung von Haken und Nehrungen unter dem Einfluss des holozänen Meeresspiegelanstiegs zu studieren. Als Datengrundlage dienten 25 Sedimentkerne, sowie sieben Georadar- und sechs Sedimentecholotprofile, aus denen sechs Lithofaziestypen abgeleitet wurden. Danach besteht die Nehrung aus einer durchschnittlich 10 m mächtigen holozänen Sedimentfolge, die auf pleistozäner Basis aus Geschiebemergel und (glazi-)fluviolimnischen Feinsanden lagert. Obwohl keine absoluten Altersdaten gewonnen wurden, kann die Sedimentabfolge mit der lokalen relativen Meeresspiegelkurve problemlos korreliert und eine Modellvorstellung für die Nehrungsentwicklung geschlussfolgert werden.

Die marine Inundation des Untersuchungsgebietes erfolgte um 7.000 BC während der Littorina-Transgression. In diesem Stadium stieg der Meeresspiegel rapide an und generierte einen schnell wachsenden Akkumulationsraum, in dem feinklastisches Material an oder unter der Wellenbasis akkumulierte und zu einem Reliefausgleich beitrug. Akkumulative Küstenformen bildeten sich nur in geringem Maße, da der Akkumulationsraum schneller wuchs als er durch das aus der Küstenerosion stammende Material aufgefüllt werden konnte. In dem Maße, indem der Meeresspiegelanstieg sich verlangsamte, gewann die Akkumulation an Bedeutung und der Hauptteil der Nehrung wurde innerhalb von rund zweitausend Jahren landfest. Entsprechend dem Verlauf von Strandwällen auf seiner heutigen Oberfläche lassen sich zwei Entwicklungsphasen aushalten, die von unterschiedlichen wellenenergetischen, erosiven und overwash-Prozessen bestimmt werden.

Gegenwärtig besitzt die Nehrung ein Volumen von 66,4 Mio m³, woraus sich auf einen Rückgang des benachbarten Kliffs von rund 2000 m schließen lässt. Obwohl die Nehrung entwicklungsmäßig in ihrem Reifestadium angelangt zu sein scheint, deuten einige Merkmale auf zunehmende Instabilität hin. Im nördlichen Bereich verhindern Küstenschutzmaßnahmen einen Nehrungsdurchbruch und beginnende Auflösung. Im Süden haben Fahrwasserbaggerungen eine weitere Längenzunahme und das Zusammenwachsen mit Haken von Hiddensee verhindert. Ohne diese Maßnahmen würde die Nehrung durch Seegattbildung und zunehmende Erosion im Norden und Seegattschließung und zunehmende Uferprogradation im Süden eine neue Gestalt annehmen.

Adresses of authors: **M. Naumann,** Baltic Sea Research Institute Warnemünde, Seestraße 15, 18119 Rostock-Warnemünde, Germany. E-Mail: michael-naumann@io-warnemünde.de; **R. Lampe,** Institute of Geography and Geology, University of Greifswald, Jahnstraße 16, 17487 Greifswald, Germany; **G. Hoffmann,** Applied Geosciences Dept., German University of Oman, PO BOX 1816, Athaibah, PC 130, Sultanate of Oman
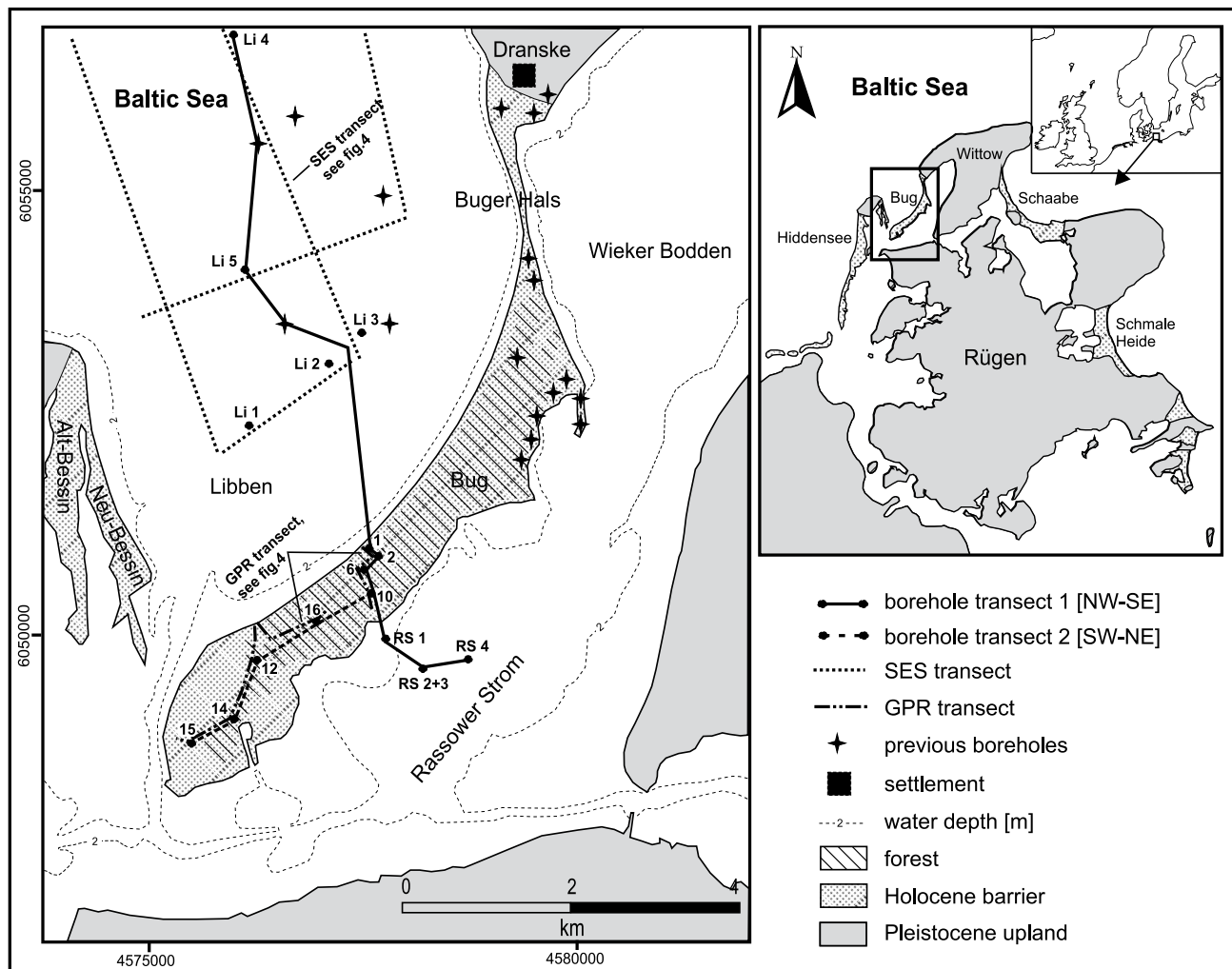
Fig. 1: Map of the study area and sites of boreholes and transects. / Abb. 1: Karte des Untersuchungsgebietes und Lage der Bohrungen und Transekte.

1 Introduction and aims

The succeeding presentation is thematically integrated in the "Sinking Coasts"-project (SINCOS) in which the interactions between the geo-, eco-, climate and socio-economic system of the southern Baltic Sea region during the past 9,000 years have been investigated in an interdisciplinary manner (Harff et al. 2005). In this context the coastal evolution of various barrier spits along the northeast German Baltic Sea coast has to be elaborated depending on the interplay of a glacially shaped relief and the postglacial relative sea-level (rsl) development. Both inherited relief and rsl determine the accumulation space available to build up accumulative coastal landforms. The relation between the accumulation space and the sediment supply provided by cliff and near-shore erosion and longshore sediment transport ascertain the time needed to fill the accumulation space and to generate subaerial landforms. It is the main target of the project to describe the initiation and development of these landforms in relation to sea-level variations, to determine their evolutionary stage and stability and to deduce information about their future behaviour. Here, we present results of on- and offshore investigations performed in a typical section of NE coastal Germany to determine the character of the sedimentary deposits, their geological layering and to derive a standard profile. The sediment distribution data is used to calculate roughly the sediment volume of the barrier and to estimate the retreat of adjacent cliff sections. From the spatial distribution of the depositional facies, their relations to the local rsl curve and from the courses of different generations of beach ridges on the peninsula's surface a simple reconstruction of the barrier development is derived. Finally, conclusions about its stability and future development will be drawn.

2 Study area

Rügen is the largest German island at the southern Baltic Sea coast. Its coastal relief is characterized by bluff sections composed of Cretaceous chalk and/or Pleistocene outwash and till, interspersed with low barriers, spits and accreting forelands composed of Holocene sand and, to a minor extent, gravel. The barriers and spits provide shelter to some lagoons (locally called 'bodden'). The Holocene coastal segments owe their existence to sediment supplied alongshore from eroding sandy or loamy bluffs along the Pleistocene headlands. The cliff sections where the barrier necks are connected to the headlands act as hinge points and the proximal barriers display a similar retreat as the neighbouring cliffs. The dynamics of the more distal parts of the barriers depend more on wave climate, sediment supply and the depth of the receiving basin.
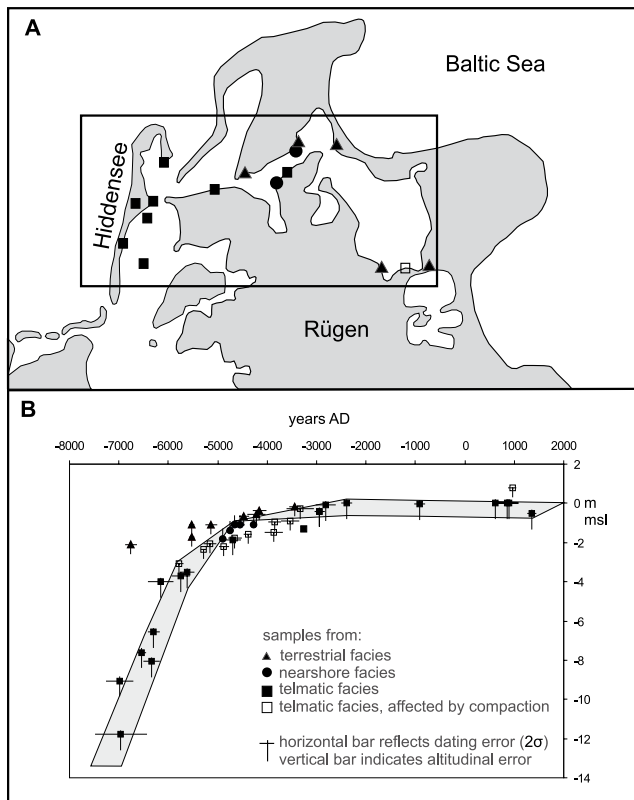
Fig. 2: Sampling sites (A) and relative sea-level curve of N- Rügen /Hiddensee (B). Triangles point to data from terrestrial deposits, circles to archaeological finds from marine nearshore deposits and black squares represent data from telmatic environments. White squares indicate data which are influenced by sediment compaction. Horizontal bars represent twofold standard deviation (2σ), vertical bars indicate estimated altitude error of sea level position. The error envelope indicates the interval where the sea level was most probably located.

Abb. 2: Probenahmepunkte (A) und relative Meeresspiegelkurve für das Gebiet N-Rügen /Hiddensee (B). Dreiecke entsprechen Daten aus terrestrischen Ablagerungen, Kreise markieren archäologische Funde aus marinen Seichtwasserablagerungen und schwarze Quadrate repräsentieren Daten aus telmatischem Milieu. Weiße Quadrate markieren Daten, die durch Sedimentkompaktion beeinflusst sind. Die horizontalen Balken zeigen die doppelte Standardabweichung (2σ) der Datierung, vertikale Balken den geschätzten Höhenfehler der Meeresspiegelposition an. Die Fehlerhüllkurve gibt den Bereich an, in dem der Meeresspiegel mit größter Wahrscheinlichkeit gelegen hat.

The Bug peninsula builds the north western part of Rügen island (Fig. 1). It is a 9 km long Holocene barrier spit with an area of 6.5 km² and a 24 km long coastline. The width varies from a minimum of only 65 m at the neck in the north (Buger Hals) to a maximum of 1.5 km in the south-western part. The relief is generally flat with mean heights between +0.8 m and +1.5 m mean sea level (msl) and a maximum of +3.7 m msl at dunes exposed to the open sea.

Since the first third of the twentieth century the study area was used as a military base. Due to the adherent access restrictions it was poorly investigated. Since 1991 the area is part of the National Park "Vorpommersche Boddenlandschaft" and again access is strongly limited. Therefore, previous surveys were done to only minor extent by mapping surface structures (Schütze 1931) and by drilling one borehole in the northern part from which a detailed sediment description is available (Kliewe & Janke 1991). Some building-ground surveys around the former military harbour were

performed related to renaturation tasks from which rather vague information exist. Central, southern and offshore areas remained so far unexplored.

According to Schütze (1931) the land surface structures can be divided into two categories: the flat areas consist of levelled previous beach ridge and dune systems, the remaining areas are characterized by wide spaced curvilinear beach ridges. The course of the -2 m isobath shows that the nearshore area surrounding the peninsula is wide and particularly shallow along the eastern and southern lagoonal side (Wieker Bodden, Rassower Strom) and narrow and steep with inclinations of 6 to 8 degrees along the coast exposed to the Libben bight in the west (Fig. 1). In the north the peninsula is connected via the Buger Hals to Wittow, the most northern Pleistocene morainic upland of Rügen with cliffs up to +27 m msl high. The western shore of the Libben bight is build by the Hiddensee island with its distinctive, up to 72 m high cliffs and two adjoining barrier spits (Alt- and Neu-Bessin). Today, the Hiddensee sediment transport system is not or not significantly connected to the sediment transport system of the Bug peninsula due to a dividing inlet in between (Fig. 1).

The water-level history in the Baltic basin is characterized by an alternation of freshwater and brackish/marine phases with water tables of different heights varying between -15 to -40 m msl (Björk 1995; Lampe 2005). Due to the altitudinal position of the Pleistocene subground of the Bug peninsula none of them has influenced the investigation area. After the postglacial ocean water table had risen to the land surface altitude in the Danish Belts the Baltic basin became permanently connected to the North Sea at around 7,200 BC (Bennike et al. 2004, Rössler 2006). The subsequent sea level rise is called the Littorina transgression (named after the marine gastropod *Littorina littorea)* which completely reshaped the area of the today southern Baltic coast. During the early transgression phase the rise occurred rapidly with an ascent of about 10 mm/yr but slowed later on. Earlier investigations have shown that on Rügen the sea level reached a position of -5 m msl at c. 6,000 BC and a level between -1 to -0.5 m msl at c. 4,500 BC (Kliewe & Janke 1982). For the subsequent some thousand years the sea level showed no significant variations but started to rise again at about 1000 AD (Late Subatlantic Transgression, Lampe & Janke 2004; Lampe 2005).

In this study no absolute age data could be gathered. The chronostratigraphical framework, therefore, bases on results from adjacent areas, such as the barriers Hiddensee, Schmale Heide and Schaabe, the north Rügen lagoons (Fig. 1) and their coastal sediment wedge as well as the numerous well dated archaeological on- and offshore sites known from this region (Möbus 2000; Barthel 2002; Lübke 2005; Lampe 2005a,b). From these studies a set of 42 reliable AMS ¹⁴C-data was derived and arranged to a rsl curve (Fig. 2) which specify the data previously published by Kliewe & Janke (1982). The curve represents the sea-level development in a spatially limited area of only about 30 km in diameter. Thus, the error due to differential earth crustal motions is avoided which is inherently included when using a larger sampling area in which isostatic movements occur (Kiden et al. 2002).

According to a long-term gauge record the recent sea-level rise rate in the north Rügen area amounts to c. 0.6 mm/yr (Dietrich & Liebsch 2000). This is the lowest value ob-

served along the northeast German Baltic coast and points to the influence of ongoing glacio-isostatic movements. Although not yet exactly quantifiable the recent regional eustatic rise is estimated to about 1 mm/yr which in turn leads to a glacio-isostatic uplift of c. 0.4 mm/yr. The zero-uplift isobase runs around 75 km further south. Tidal variations are below 0.1 m and negligible for the southern Baltic Sea (MINISTERIUM FÜR BAU, LANDESENTWICKLUNG UND UMWELT MECKLENBURG-VORPOMMERN 1994). Therefore, coastal dynamic processes in this area are generally steered by inherited relief, sea-level variation and sediment supply.

3 Methods

To collect geophysical and sediment data from terrestrial as well from offshore sites of the peninsula, three field campaigns were performed in 2002, 2005 and 2008. In cooperation with the Leibniz Institute for Applied Geophysics, Hannover, ground-penetrating radar (GPR) surveys were conducted at the central and southern peninsula (Fig.1; dash-dotted lines). A SIR-10 respectively SIR-20 set from GSSI with a 100 MHz antenna were used to determine the bedding structures within the upper sediment layers. Reflectors are recorded for two-way-travel times of up to 200 ns and were related to depth using a constant v = 0.07 m/ns derived from repeated common midpoint measurements. These parameters allowed a subsurface imaging of the upper 8 m below

land surface. To optimise the resolution in various depths additional GPR profiles were recorded along two previous tracks. One connects the cores Bug 1–10 and a second runs from the coast into south-western direction along the cores Bug 11–15. At these sites different antenna frequencies were tested (200, 100 and 50 MHz) using a RAMAC-GPR set. As a result the 50 MHz antenna was used to detect the base of the Holocene sediments which was expected in depths at about 10 m below surface.

According to the GPR measurements 16 core sites were identified at both track positions where reflectors were clearly visible or were minor / no resolution of the subsoil did not allow the identification of any subsoil layering. To derive geological cross sections across the barrier the sites were arranged to one profile crossing the peninsula from northwest to south-east perpendicular to the coastline (Fig.1, cores Bug 1–10) and to a second profile running lengthwise (cores Bug 10–16). The objective was to detect both the bases of the Holocene and the marine sediments, and to identify the composition of the marine deposits. For the drilling process a hydraulic powered drill and extraction tool was applied. Depending on the penetration resistance of the sediments three different diameters of half-open testing probes (80, 50, 36 mm) were used. A maximum depth of -13.85 m msl was reached at core Bug 15.

In 2008 a third campaign was performed to collect offshore data on board the research vessel "Prof. Albrecht

Tab.1: Facies types differentiation of the Bug peninsula and features of classification.

Tab.1: Faziesdifferenzierung der Halbinsel Bug und Merkmale der Klassifikation.

| Facies type	Grain size Md - median So - sorting	Organic content	Carbonate content	Fauna **species / abundance / type of shell destruction / salinity range** (abundance: 1-very low, 2-low, 3-modest, 4-high, 5-very high)	Environment
glacial	clayey-sandy matrix, gravel, stones, chalk Md: 0.32 mm So: 1.27	none	very high	no sample analysed	glacial
fluviolimnic	fine sand Md: 0.19 mm So: 1.32	none	medium to high	*Bryozoa* / 1 / small fragments / ?	freshwater / (aeolian?)
shoreface	fine to medium sand Md: 0.09 mm So: 1.59	none, sometimes thin organic layers of ~ 10%	none	*Mytilus edulis* / 1 / fragments / 15–40 PSU *Cerastoderma edule* / 1 / fragments / >5 PSU *Littorina littorea* / 1 / unbroken / >9 PSU	brackish - marine
slack water	silt, upper parts fine sandy Md: 0.05 mm So: 1.89	7–15 %	none	*Mytilus edulis* / 4 / fragments / 15–40 PSU *Cerastoderma sp.* / 3 / fragments – bivalve / >5 PSU *Hydrobia ulvae* / 2 / fragments - unbroken / >4 PSU *Cyprideis torosa* / 2 / single shells - bivalve / 8–9 PSU	brackish - marine
nearshore	fine to medium sand Md: 0.18 mm So: 1.27	none, sometimes thin organic layers of ~ 10%	none	*Mytilus edulis* / 4 / fragments / 15–40 PSU *Cerastoderma sp.* / 3 / fragments & single shells / >5 PSU *Hydrobia ulvae* / 2 / / >4 PSU	brackish - marine
beach	medium to coarse sand, gravel, small stones Md: 0.45 mm So: 1.39	none, sometimes botanical macro remains of the drift line	none	*Mytilus edulis* / 3 / fragments / 15–40 PSU *Cerastoderma sp.* / 2 / fragments / >5 PSU *Hydrobia ulvae* / 1 / fragments / >4 PSU	brackish – marine/ (aeolian?)
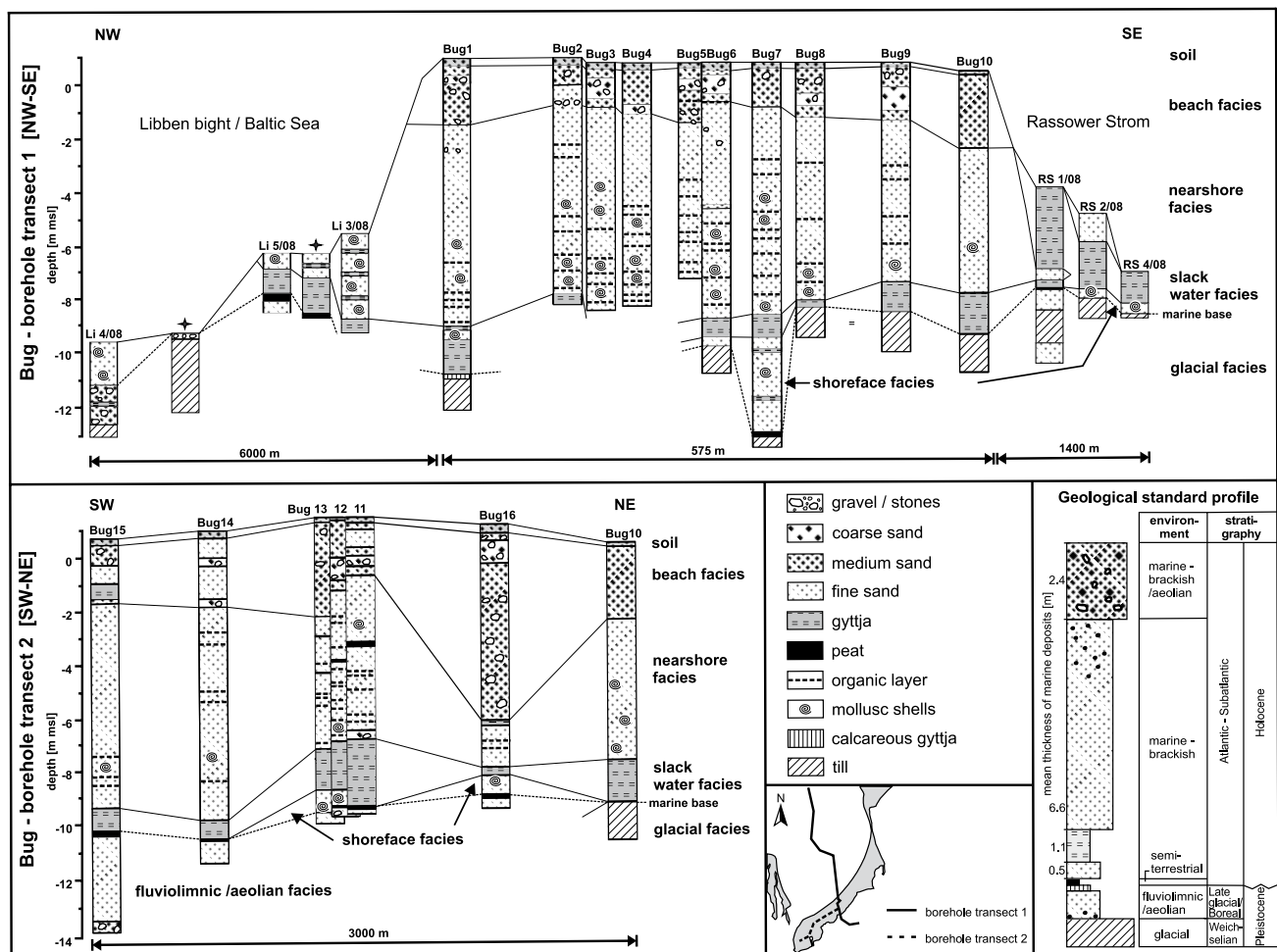
Fig. 3: Core profiles and facies distribution along two transects (for location see Fig. 1) and geological standard profile of the sediment sequence in the study area.

Abb. 3: Bohrkernprofile und Faziesverteilung entlang zweier Transekte (zur Lage s. Abb. 1) sowie geologisches Normalprofil der Schichtenabfolge des Bugs.

Penck". Six sediment-echosounding (SES) transects were recorded in the Libben bight with an Innomar SES-96 set by using a frequency of 6 kHz and 1500 m/s sound velocity (Fig. 1; dotted lines). This setting delivered useful information about reflectors up to 8 m below sediment surface. Signals from larger depths were mainly multiples. Five vibrocores were taken of 3.80 m maximal length (Li 3/08) to allow interpretation of detected SES reflectors. From board the research barge "Bornhöft" additional 4 sediment cores were taken in the shallow lagoon Rassower Strom to expand the shorenormal barrier cross section to south-eastern direction. Thereby, a maximum penetration of 6.60 m below sediment surface was reached at core RS 1/08.

All cores were classified into lithological units characterized by grain size, calcium carbonate and organic content as well as the occurrence and species assemblage of macrofossils. In five exemplary cores (Bug 1, 9, 11, 15, 16) the units identified were sampled for lab analysis and closer characterization. The granulometric composition of 48 samples was measured by dry sieving, 13 fine clastic samples were analysed using an optical laser sizer device (Fritsch Analysette 22). To characterize the grain size distribution the Trask-parameters median and sorting were calculated (Füchtbauer & Müller 1970). Organic content was determined as loss on ignition at 550 ℃, carbonate content was determined qualitatively according to AG Boden (1994). From 16 samples (11

samples from Bug 13 and additional samples from the basal marine layers from Bug 11; 15; 16) the palaeo-environments in which the different sediments were deposited were analysed by determination of faunal remnants, mainly from molluscs.

4 Results

Lithofacial units

The analysis of the geophysical and lithological data along with previously achieved field data from the northern Bug lead to the identification of six different sedimentary facies units. As distinctive features were used: i) the grain size distribution and deduced parameters such as median and sorting as surrogates for the transport and deposition dynamics, ii) the organic content of the sediment which indicates deposition under temperate and faintly dynamic conditions, iii) a low or missing calcium-carbonate content as an indicator that the primary Pleistocene material underwent weathering during relocation and redeposition, iv) species assemblage, mainly from molluscs, which points to a certain salinity of the palaeo-environment (Peacock 1993), while the degree of shell destruction reflects the water dynamics. An overview about the lithological units, the related facies types and the classification features is given in table 1. The geological
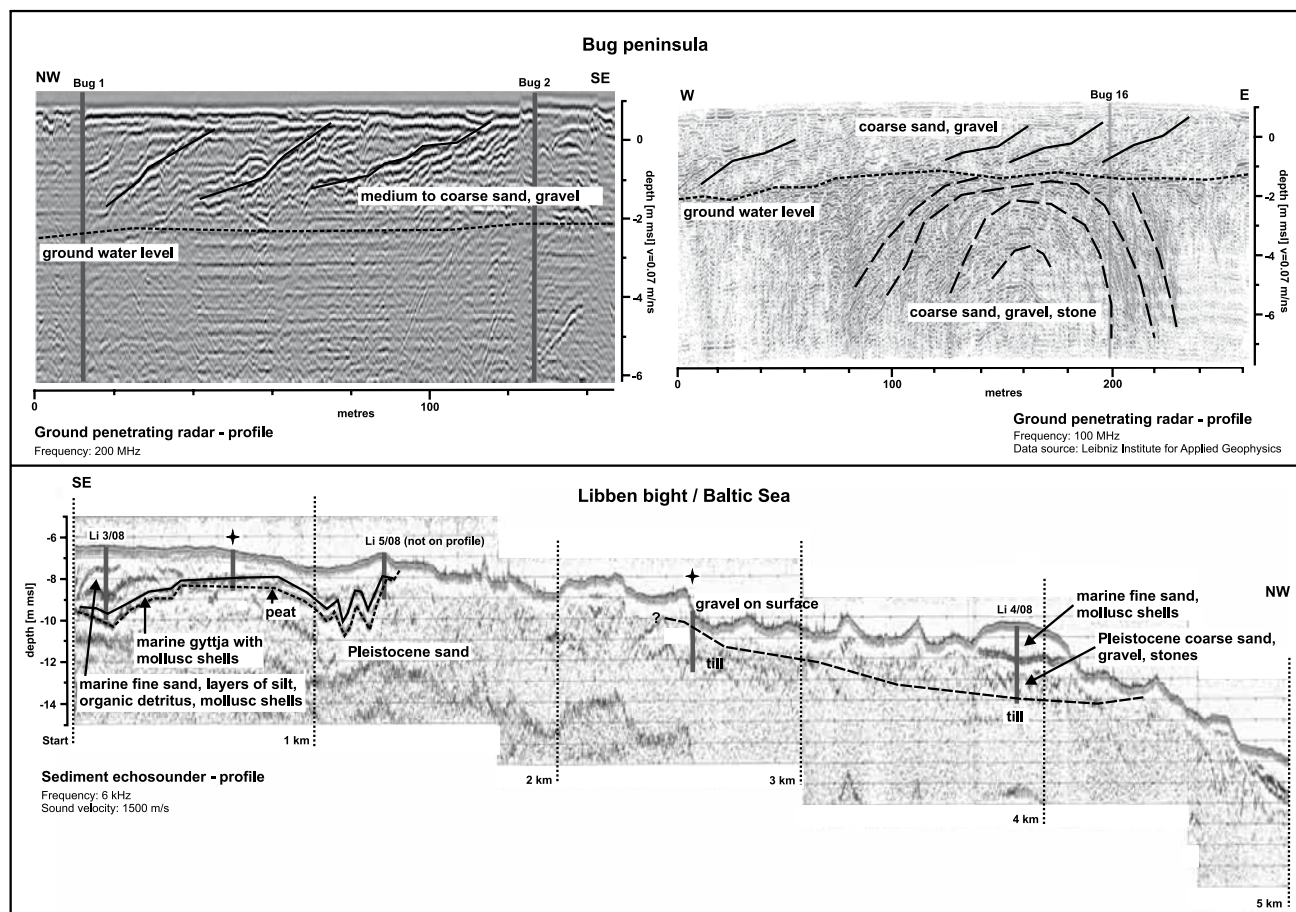
Fig. 4: Two ground penetrating radar profiles from the central and southern peninsula (for location see Fig. 1) showing bedding structures of progradational beach ridges (upper section). Sediment-echosounding profile from the Libben bight (for location see Fig. 1) showing distribution of different sediments in the subground (lower section).

Abb. 4: Zwei Bodenradar-Profile aus dem zentralen bzw. südlichen Bereich der Halbinsel (zur Lage s. Abb. 1), die Lagerungsstrukturen progradierender Strandwälle zeigen (oben). Sedimentecholot-Profil aus der Libben-Bucht (zur Lage s. Abb. 1), welches die Verteilung unterschiedlicher Sedimente am Meeresboden verdeutlicht (unten).

standard profile of the Bug (Fig. 3) was deduced considering the mean thickness and the vertical succession of the observed units. In the following paragraphs the observed facies units are described more detailed.

At nearly all borehole positions the sediment sequence started (except in Li 3/08; Bug 2–5) with a diamicton, a calcareous clayey to sandy matrix with admixtures of coarser grains like gravel and stones. Although it may be of slightly different origin we subsume all of them under the glacial facies type till. The upper boundary of the till is located in depths between -9 to -14 m msl in the central part of the peninsula (Fig. 3; borehole transect 1), whereas in the southern part the till surface was not reached and must be located lower than -14 m msl (Fig. 3; borehole transect 2). In the Libben bight the boundary was found in the same depth range as in the central Bug area. Farther offshore the covering sediment wedges and till forms the sea bottom (Fig. 4; SES-profile).

Above the till calcareous fine sand follows containing *Bryozoa* relicts, which originate from Cretaceous sediments. This sandy unit was detected below -9.50 m msl and is spatially limited to the south western part of the peninsula (Fig. 3; borehole transect 2, cores Bug 11–16) and to some nearshore areas of the Libben bight (Fig. 4; SES-profile). The sand is of (glaci-)fluvial or -lacustrine origin as many other sandy

sediment bodies of the same character and altitudinal position known from the vicinity. In places lake marl or calcareous gyttja were found in flat depressions on the sand surface and point to deposition in shallow lakes under warmer climate conditions. All these freshwater sediments were combined in the fluviolimnic facies unit.

The subsequent transition from freshwater to marine environmental conditions was often marked by the occurrence of semi-terrestrial peat (semi-terrestrial facies), which developed close to the water level in sheltered zones. Layers of 3 to 15 cm thickness were found in various depths between -8 and -13 m msl and on top of diverse deposits (till, fine sand, calcareous gyttja).

The sediment in the hanging wall was always clearly deposited in a marine environment. Non calcareous fine sand with minor contents of well preserved marine molluscs (*Cerastoderma sp., Mytilus edulis, Littorina littorea*) are related to the shoreface facies. Found in small depressions between -8.20 and -12.80 m msl it occurs only sub-dominant in the study area (cores Bug 6, 7, 12, 13, 16 and RS 1, 2, 4).

It is overlain by a consolidated dark grey to black coloured gyttja containing 7 to 15 weight per cent of organic matter. At the base reworked peat and botanical macro remains like wood were sometimes visible. In the lower part a massive occurrence of shells of marine molluscs (*Cerastoderma sp.,*

Mytilus edulis, Hydrobia ulvae) and ostracods (*Cyprideis torosa*) is symptomatic. Predominantly, the shells are arranged in tiers which consist of shell fragments but bivalve shells with intact ligaments are often found in between. Both grain size and shell distribution point to deposition under calm water conditions near the storm wave base, where dislocation and redeposition occur occasionally (slack water facies). The sediment type is widespread in the subground of the peninsula and fills the back-sided lagoon, ranging in depths between -3.70 m and -10.50 m msl. To the upper boundary the content of organic matter as well as the amount of mollusc shells decreases and the mean grain sizes gets a bit coarser due to a larger fine sand fraction.

The nearshore facies is characterized by non calcareous fine to medium sands with numerous 1 to 5 cm thick interbedded layers of organic detritus and/or mollusc shells. Fragments of *Cerastoderma sp.* and *Mytilus edulis* are readily identifiable and indicate a marine-brackish depositional environment. Fine sand is the dominant grain size pointing to shallow water conditions where sediment is transported mainly in suspension. Within the unit a slight coarsening upward and a decreasing amount of organic layers and mollusc shells indicate growing water dynamics and redeposition intensity. Owing a calculated mean thickness of 6.6 m this sediment unit builds the main part of the barrier comprising approximately two third of the Holocene sediment volume.

The uppermost sediment unit shows a mixed and less well sorted grain size spectrum. It consists of medium to coarse sand containing gravel and some small stones, too. The lack of fine clastic material and the occurrence of heavy fragmented mollusc shells indicate rough water and sediment dynamics characteristic for beach facies. The spatial occurrence is different across the peninsula but dominant where beach ridge formation takes place. The depth interval in which the sediment unit appears reaches from the land surface down to -2 m msl.

A schematic overview about the distribution of the lithofacial units is depicted in two geological cross sections (Fig. 3). The glacial, fluviolimnic and semi-terrestrial deposits are separated from the brackish-marine deposits by a more or less erosive surface, the marine base. It is built by the lower boundary of the shoreface or the slack water facies.

The vertical succession and the mean thickness of the marine layers are shown in the geological standard profile. Hence follows that the thickness of the Holocene sediment sequence of the Bug pensinsula amounts to around 10 m. A similar thickness was found for other barriers along the southwestern Baltic coast (Hoffmann 2004, Hoffmann et al. 2005).

Internal bedding structures

GPR/SES investigations along on- and offshore transects facilitate the correlation of the lithofacial units identified from the sediment cores and the determination of their spatial distribution. Internal bedding structures might be attributed to specific depositional processes allowing a more precise reconstruction of the palaeogeographic evolution.

The SES profile running perpendicular to the coastline of the Bug (Fig.1 and Fig. 4; lower section) shows the transition from the Arkona Basin in the NW to the inner Libben bight. From the edge of the Arkona Basin at profile km 4.5 to km 1.4 the sea bottom is rough and covered with numerous boulders, which are evident from the many spikes on the sediment surface. The sediment cores taken show that till appears near to the surface and is covered by lag sediment. A flat, 400 m wide sand bar was observed at the border to the Arkona basin (core Li 4/08) deposited on the till. The subaquatic boundary of the barrier is located close to core Li 5/08 at profile km 1.3 and around 3 km offshore the Bug peninsula. Here, under marine sand the most seaward occurrence of the slack water facies was observed which can be traced into the subground of the today barrier.

GPR records from the barrier show bedding structures in the upper subsurface down to -2 m msl (Fig. 4; left upper section). Unfortunately, the occurrence of salty groundwater prevents a reception of information from greater depths. The bedding structures are characterised by a constant inclination towards the sea and are clearly related to accretionary beach ridges evident at the surface. The structures were also found in some flat areas where no beach ridges occur on the surface. This is most probably caused by subsequent erosion and levelling of the former relief due to overwash processes during storm floods.

Information from bedding structures at greater depths is limited to some central parts of the peninsula having less salty groundwater in the subsoil (Fig. 4, right upper section). Here, a massive coarse grained marine sediment body was identified, proven by core Bug 16. The GPR record shows strata down to -6 m msl with complementary inclinations. In a depth of about -1.5 to -2 m msl the sediment body is discordantly overlain by accretionary beach ridges as described above.

5 Interpretation

From the spatial distribution of the lithofacial units and the information about sediment bedding structures a model of the coastal development in the study area is deduced. Thereby, the rsl curve of N-Rügen/Hiddensee (Fig. 2) is used for information about sea-level rise rates, changes in accommodation space and the relation of the sediment deposition to time scale. Fig. 5, left side, illustrates in seven characteristic stages the vertical sediment accumulation on a 10 km long geological cross section, running lengthwise the peninsula from the south-western barrier tip to Dranske village in the north-east (cf. Fig. 1). The stages are related to periods known from previous investigations as characteristic for the regional landscape evolution (Lemke 1998, Lemke et al. 2001; Kaiser 2001). On the right side of Fig. 5 the coastline evolution is depicted in four plan-view sketches A-D within which the recent coastline is drawn by a dotted line.

The first sketch (Fig. 5, left side) displays the till surface at the end of the last pleniglacial around 12,000 BC. The stratigraphic classification within the Weichselian glacial period cannot be specified, but a relation to the North Rügen ice-marginal zone is obvious (Kliewe 1975). The till surface at the Wittow headland near Dranske is found at about +5 m msl. From there it drops gradually around 20 m to southwestern direction. During the Late glacial period this depression was partly filled with (glaci-)fluviolimnic sand accumu-
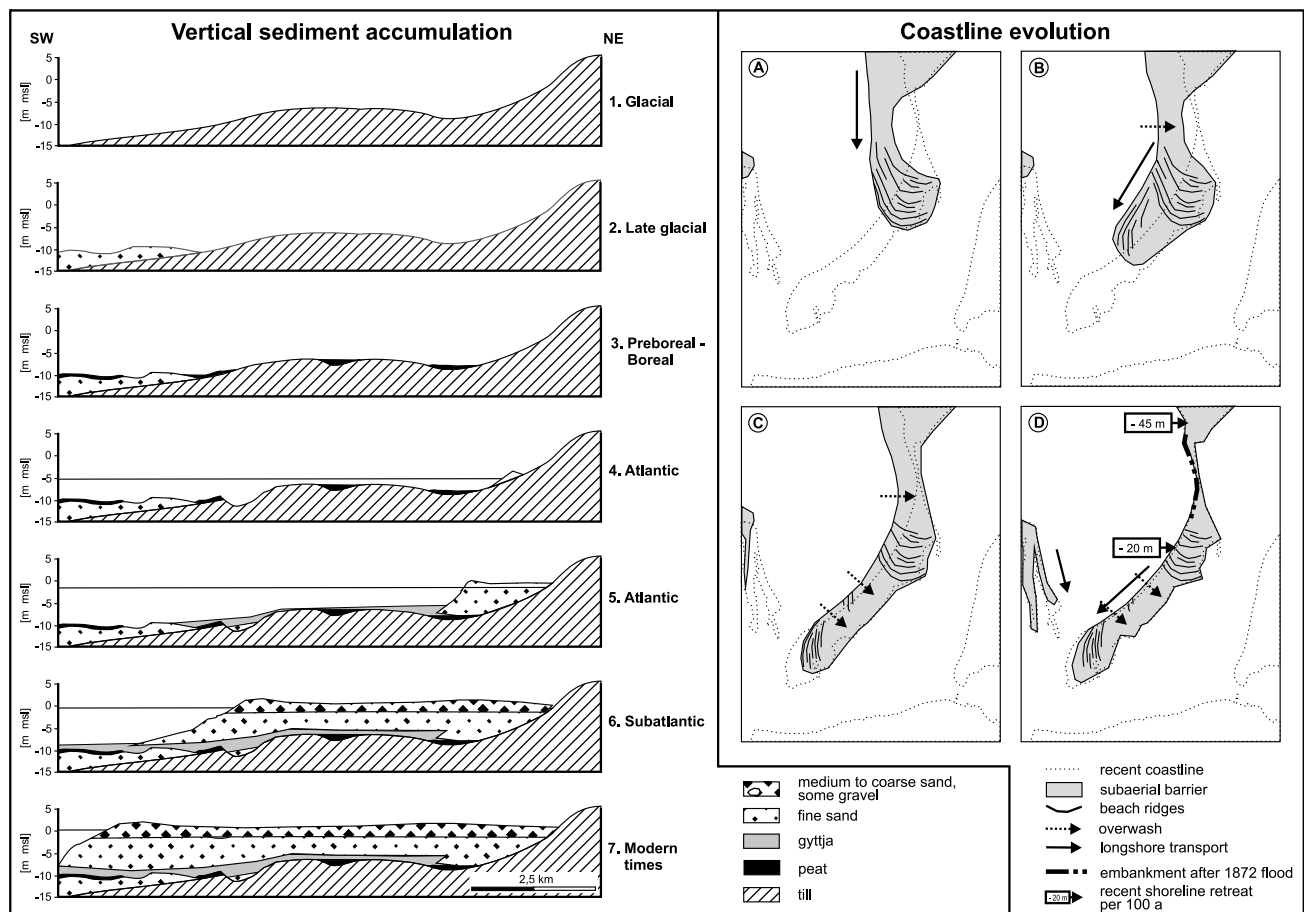
Fig. 5: Coastal evolution of the Bug peninsula, illustrated in seven evolutionary stages showing the vertical sediment accumulation (left part), and by four plan view sketches showing the shoreline development (right part).

Abb. 5: Küstenentwicklung der Halbinsel Bug. In sieben Entwicklungsstadien ist die vertikale Sedimentakkumulation wiedergegeben (linker Teil), vier Kartenskizzen verdeutlichen die Uferlinienentwicklung (rechter Teil).

lated in channels and basins where meltwater drained in western directions (MÖBUS 2000) towards the Arkona Basin (stage 2).

After final ice melting the area felt dry and terrestrial evolution started due to the water-level fall in the Baltic basin to -40 m during the Younger Dryas/Early Preboreal. Interstadial deposits (e.g. Allerød) are well known from the wider vicinity but were not found in the study area. Likewise, from the Younger Dryas significant wind-driven sediment redeposition is known from the region. Although not proven in the study area it has to be considered that the fluviolimnic sand was relocated to some extent. After the onset of the Holocene and a rise of the ground-water table mires or shallow lakes came into being on the gently undulating land surface. In the waters lake marl or calcareous gyttja were deposited (for instance in core Bug 1 at -10.50 m msl) but most waters turned soon into mires and desiccated (stage 3).

In a fourth stage the groundwater table started to rise again caused by the Littorina transgression. Basal peat developed in a narrow belt in front of the transgressing shoreline. The local rsl curve (Fig. 2) shows that the sea-level reached the study area c. 7,000 BC, which was subsequently rapidly inundated. The shoreface facies unit which covers the basal peat deposits is interpreted as a trailing edge sand sheet (Roy et al. 1994), which was left behind a transgressing beach ridge. It filled small depressions and channels eroded during the inundation thereby levelling the surface. Perhaps, the flat

sand body found on the SES transsect at km 3.8 to 4.1 between -10 to -12 m msl (Fig. 4) is a relic barrier overstepped by the rapid rising sea level. Today it seems to be shaped and nourished by contour bounded currents and sand transport between the headlands of Hiddensee and Wittow.

The fifth sketch shows the status at the end of the main transgression phase about 4,500 BC. In the period between the fourth and the fifth stage the sea level rose rapidly and generated fast increasing subaquatic accumulation space, where fine clastic material (slack water facies) was deposited near at or below the wave base. Wave impact from NW to NE and related cliff abrasion provided material for longshore transport. However, accumulative coastal landforms grew still to only minor extent because the accommodation space increased faster than it was filled. Since the time the sea-level rise decreased accumulation became more dominant and the main barrier was built up in only some two thousand years. In this time span the lagoon became separated from the open sea. The coastline was located more westerly and the barrier spit grew into southern direction. Beach ridges were north-south oriented with their ends turned to east (Fig. 5; plan view A).

The final development is depicted in the last two sketches, where sediments of nearshore and beach facies shaped the peninsula. While erosion and shoreline transgression continued in the northern part sediment aggradation and spit elongation dominated at the tip of the peninsula. With increasing

length the peninsula's tip became more and more sheltered by Hiddensee island. While ongoing abrasion took place in the less sheltered northern section decreasing wave impact and altered wave refraction changed the elongation at the tip to south-westerly direction (Fig. 5; plan view B). Probably, the latter process proceeded discontinuously. It must be assumed that the accumulation of the gravelly beach ridge found in borehole Bug 16 (Fig. 3 and Fig. 4) coincided with a retardation in the elongation process, caused by the large volume of coarse material to be deposited. As the remaining barrier is composed of sandy sediments a coarse glacifluvial deposit of rather limited extent is hypothesized as the source of the gravel. Due to complete abrasion and redeposition and/or incomplete survey data the primary location of the source is unknown but is estimated NW of the today beach ridge. Similar deposits are known from the wider vicinity of the study area (Jacob 1987, Schwarzer et al. 2000) and corroborate this interpretation.

Since the sea level started to rise faster again at about 1000 AD the barrier was particularly shifted landwards by erosion and overwash. Therefore, only the very ends of the former beach ridges remained in the north and central barrier sections (Fig. 5; plan view C) now interspersed with overwash plains. After the destructive storm flood in 1872, during which the narrow neck of the barrier (Buger Hals) was inundated and scoured, an embankment was built for protection (Fig. 5; plan view D). Since then erosion decreased but artificial nourishment is still required to prevent breakthrough. More recently, the southern barrier section was strongly affected, too. For a few decades dredging operations in the now abandoned waterway between Hiddensee and Bug caused decreasing spit elongation while the dredged material was spoiled at the lagoon-sided tip of the peninsula (Fig. 5; plan view D). Future development unaffected by human intervention would probably lead to a permanent closure of the inlet between the Neu-Bessin spit and the Bug and a detachment of the peninsula's neck from the Wittow headland. While the remaining peninsula would shrink in the north the material eroded would cause beach ridge progradation in the south.

To get an impression how much material was accumulated in the barrier and how extensive the abrasion at the neighbouring cliffs must have been, the volume of the marine sediments was calculated. Due to missing information about the relief and the sediment distribution at both seeward and lagoonward shorefaces fringing the barrier the calculation was restricted to the volume enclosed by the marine base below the peninsula's land area and whose surface (Hoffmann & Lampe 2007). This volume amounts to 66.4 million cubic metres (Naumann 2006). As the only feeding section the adjacent 8 km long and on average 8 m height cliff at Wittow is assumed which implies a cliff retreat of 1,040 m. However, the factual abraded volume must have been much larger. Firstly, as the shoreface volume was ignored in the calculation and secondly, because the fine fraction of the abraded Pleistocene material, which amounts to c. 40 %, became not completely involved in the coastal sedimentary system. A portion was deposited in the slack water facies, but the remaining part accumulated as mud in deeper offshore basins. Hence, the real cliff retreat might amount to twice the calculated value. The recent retreat rates account

to 45 m/100 yr at the Wittow cliff section and 20 m/100 yr at beaches along the sheltered inner Libben bight (Ministerium für Bau, Landesentwicklung und Umwelt Mecklenburg-Vorpommern 1994). Considering that the oldest beach ridges still visible on the only 500 m wide barrier have an age of about 5,000 to 6,000 years (Schütze 1931, Kliewe & Janke 1978) this means that the abrasion rates must have been significantly lower in the period after 4,500 BC. This finding is interpreted as a consequence of the some thousand years displaying no rsl rise (Fig. 2) and were related to decreasing shoreline erosion. Only the onset of the Young Subatlantic Transgression was associated again with higher shoreline dynamics. Although the anew rise which started at about 1000 AD was interrupted during the Little Ice Age it continued since 1850 AD as documented in gauge records (Dietrich & Liebsch 2000).

The conclusion that over some thousand years the lateral translation was rather low when compared with recent displacement rates seems to be in conflict with the occurrence of marine gyttja (slack water facies) in boreholes Li 3/08 and Li 5/08 (Fig. 3 and 4) about 3 km offshore. One is tempted to conclude an initial barrier in the west from the boreholes which subsequently migrated to the recent position. However, the gyttja was found where the pre-transgressional relief displays a depression with an inclination of the surface towards the south and/or east (Fig. 4). Even the rising ground water would cause a lagoonary water in a position such as this. Although not proven by borings we speculate that this depression is part of a larger depression the centre of which is located in the area SW of the Bug spit. Here, the deepest position of the marine base is reached in boreholes Bug 14 and Bug 15 at about -10 m. From the southern tip of the Alt-Bessin (Fig. 1) a position of the marine base of -12 m was reported by Hurtig (1954) and of -20m at central Hiddensee by Barthel (2002). The connecting channel between the depression and the rising sea was obviously not located in the Libben bight and must be assumed farther west in the Hiddensee area (Fig. 1). For this reason the occurrence of the marine gyttja 3 km offshore the today peninsula is not in contradiction to the evolutionary stages of the peninsula depicted in Fig. 5.

6 Conclusions

The investigated barrier represents a paraglacial, drift aligned coastal system (Forbes et al. 1995). It became established on a slightly undulating surface of glacigenic and glacifluvial origin with low inclination towards the Baltic Sea basin. The barrier evolution started with the arrival of the Littorina transgression about 7,000 years BC as a beach ridge migrated over the land surface and finally stranded at the Wittow headland. Its trailing edge sand sheet levelled the inundated and scoured surface. During the next some two thousand years the sea-level rise rate was still high and the accommodation space grew faster than it was filled by the sandy material provided by cliff erosion. The sea-level rise slowed down at 4,500 BC and came virtually to a halt at 4,000 BC due to compensating glacio-isostatic uplift. Since then the accommodation space shrunk and fast spit elongation took place. Erosion at the headland hinge point and along the barrier shoreline drove the barrier landwards thereby migrat-

ing over gyttja accumulated in the backbarrier lagoon. The propagation direction was changed after the extending barrier grew into the shelter of the windward located island Hiddensee. Ongoing erosion along the shoreline caused overwash processes which enhanced barrier transgression.

Today the barrier displays a volume of 66.4 million m³ according to a feeder cliff retreat of at least 1,040 m, but probably about 2,000 m, which is in the range of the general coastal retreat along the NE German and neighbouring Polish coast (Uścinowicz 2006). Although the barrier seems to be in maturity stage some features points to instability. Coastal protection measures at the barrier neck in the north prevent imminent breakthrough and detachment. Waterway dredging in the south inhibited further elongation and accretion with spits growing from Hiddensee. Without these measures the barrier would disintegrate and be reshaped by inlet generation and increasing erosion in the north and inlet closure and beach progradation in the south.

Acknowledgment

References

AG Boden (1994): Bodenkundliche Kartieranleitung (4. Auflage). – 392 S.; Hannover (BGR).

Barthel, A. (2002): Aufbau und Entwicklung der holozänen Sedimente der Insel Hiddensee und deren Modellierung mit geostatistischen Methoden. – Thesis, Geographisches Institut, Universität Greifswald, 109 S.

Bennike, O., Jensen, J. B., Lemke, W., Kuijpers, A. & Lomholt, S. (2004): Late- and postglacial history of the Great Belt, Denmark. – Boreas 33: 18–33.

Björk, S. (1995): A review of the history of the Baltic Sea, 13.0-8.0 ka BP. – Quaternary International, 27: 19–40.

Dietrich, R. & Liebsch, G. (2000): Zur Variabilität des Meeresspiegels an der Küste von Mecklenburg-Vorpommern. – Journal of Coastal Research, 28/6: 615–623.

Forbes, D.L., Orford, J.D., Carter, R.W. G., Shaw, J. & Jennings, S.C. (1995): Morphodynamic evolution, self-organisation, and instability of coarse-clastic barriers on paraglacial coasts. – Marine Geology, 126: 63–85.

Füchtbauer, H. & Müller, G. (1970): Sediment-Petrologie. Teil II Sedimente und Sedimentgesteine. – 726 S.; Stuttgart (Schweizerbart'sche Verlagsbuchhandlung).

Harff, J., Lampe, R., Lemke, W., Lübke, H., Lüth, F., Meyer, M. & Tauber, F. (2005): The Baltic Sea - A Model Ocean to Study Interrelations of Geosphere, Ecosphere, and Anthroposphere in the Coastal Zone. – Journal of Coastal Research, 21/3: 441–446.

Hoffmann, G. (2004): Postglacial to Holocene sedimentation history and palaeogeographical development of a barrier spit (Pudagla lowland, Usedom Island, SW Baltic coast). – Polish Geological Institute Special Papers, 11: 83–90.

Hoffmann, G. & Lampe, R. (2007): Sediment budget calculation to estimate Holocene coastal changes on the southwest Baltic Sea (Germany). – Marine Geology, 243: 143–156.

Hoffmann, G., Lampe, R. & Barnasch, J. (2005): Postglacial evolution of

barrier spits along the West Pomeranian coast (NE Germany). – Quaternary International, 133/134: 47–59.

Hurtig, T. (1954): Die mecklenburgische Boddenlandschaft und ihre entwicklungsgeschichtlichen Probleme. Ein Beitrag zur Küstengeschichte der Ostsee. – 148 S.; Berlin (Deutscher Verlag der Wissenschaften).

Jacob, H.-E. (1987): Die Fährinsel bei Hiddensee – Geomorphologie und Genese. – Petermanns Geographische Mitteilungen, 131: 85–92.

Kaiser, K. (2001): Die spätpleistozäne bis frühholozäne Beckenentwicklung in Mecklenburg-Vorpommern. Untersuchungen zur Stratigraphie, Geomorphologie und Geoarchäologie. – Greifswalder Geographische Arbeiten, 24: 176 S.

Kiden, P., Denys, L. & Johnston, P. (2002): Late Quaternary sea-level changes and isostatic and tectonic land movements along the Belgian-Dutch North Sea coast: geological data and model results. – Journal of Quaternary Science, 17: 535–546.

Kliewe, H. (1975): Spätglaziale Marginalzonen auf der Insel Rügen – Untersuchungsergebnisse und Anwendungsbereiche. – Petermanns Geographische Mitteilungen, 119: 261–269.

Kliewe, H. & Janke, W. (1978): Zur Stratigraphie und Entwicklung des nordöstlichen Küstenraumes der DDR. – Petermanns Geographische Mitteilungen, 122/2: 81–91.

Kliewe, H. & Janke, W. (1982): Der holozäne Wasserspiegelanstieg der Ostsee im nördlichen Küstengebiet der DDR. – Petermanns Geographische Mitteilungen, 126: 65–74.

Kliewe, H. & Janke, W. (1991): Holozäner Küstenausgleich im südlichen Ostseegebiet bei besonderer Berücksichtigung der Boddenausgleichsküste Vorpommerns. – Petermanns Geographische Mitteilungen, 135: 1–15.

Lampe, R. (2005a): Late-glacial and Holocene water-level variations along the NE German
Baltic Sea coast – review and new results. – Quaternary International, 133/134: 121–136.

Lampe, R. (2005b): Reliefgenese und Faziesdifferenzierung am mesolithischen Fundplatz von Lietzow-Buddelin auf Rügen. – Bodendenkmalpflege in Mecklenburg-Vorpommern. Jahrbuch 2004, 52: 185–195.

Lampe, R. & Janke, W. (2004): The Holocene sea-level rise in the Southern Baltic as reflected in coastal peat sequences. – Polish Geological Institute Special Papers, 11: 19–30.

Lemke, W. (1998): Sedimentation und paläogeographische Entwicklung im westlichen Ostseeraum (Mecklenburger Bucht bis Arkonabecken) vom Ende der Weichselvereisung bis zur Litorinatransgression. – 186 S.; Habilitationsschrift, Universität Greifswald,

Lemke, W., Jensen, J.B., Bennike, O., Endler, R., Witkowski, A. & Kuijpers, A. (2001): Hydrographic thresholds in the western Baltic Sea: Late Quarternary geology and the Dana River concept. – Marine Geology, 176: 191–201.

Lübke, H. (2005): Vorbericht zu den Sondierungen submariner steinzeitlicher Fundstellen in den nördlichen Boddengewässern Rügens. – Bodendenkmalpflege in Mecklenburg-Vorpommern, Jahrbuch 2004, 52: 211–220.

Ministerium für Bau, Landesentwicklung und Umwelt Mecklenburg-Vorpommern (1994): Generalplan Küsten- und Hochwasserschutz Mecklenburg-Vorpommern. – 108 S.; Schwerin.

Möbus, G. (2000): Geologie der Insel Hiddensee (südliche Ostsee) in Vergangenheit und Gegenwart – eine Monographie. – Greifswalder Geowissenschaftliche Beiträge, 8: 1–150.

Naumann, M. (2006): Faziesdifferenzierung und holozäne Küstenentwicklung der Halbinsel Bug /Rügen. – Thesis, Institut für Geographie und Geologie, Universität Greifswald, 83 S.

Peacock, J. D. (1993): Late quaternary marine mollusca as palaeoenvironmental proxies: A compilation and assessment of basic numerical data for NE Atlantic species found in shallow water. – Quaternary Science Reviews, 12: 263–275.

Rössler, D. (2006): Reconstruction of the Littorina Transgression in the Western Baltic Sea. - PhD thesis, Universität Greifswald, 135 S.

Roy, P. S., Cowell, P.J., Ferland, M.A. & Thom, B.G. (1994): Wave-dominated coasts. – In: Carter, R.W.G. & Woodroffe, C.D. (eds): Coastal evolution – Late Quaternary shoreline morphodynamics: 121–186.

Schwarzer, K., Diesing, M. & Trieschmann, B. (2000): Nearshore facies of the southern shore of the Baltic Ice Lake - example from Tromper Wiek (Rügen Island). – BALTICA, 13: 69-76.

Schütze, H. (1931): Die Haken und Nehrungen der Außenküste von Rügen. – Beiheft Jahrbuch der Pommerschen Geographischen Gesellschaft, 1931/32: 1–155.

Uscinowicz, S. (2006): A relative sea-level curve for the Polish Southern Baltic Sea. – Quaternary International, 145–146: 86–105.

Information on the new publication system

With no. 2 of volume 58 a distinctive further development of the *Quaternary Science Journal* performs. With this issue the tradition-rich journal is published with a new layout and for the first time as a hybrid publication: there is an online issue in addition to the printed journal. The online issue is *Open Access.*

The aims of these changes are the professionalisation of the journal and the adaptation to the current demands of the international scientific communication. These changes are important for the admission to the *Science Citation Index* too. With this modern form of publication we want to give additional impulses to the concern of our association: the promotion of quaternary scientific research. For that we have a new competent partner: the publisher *Geozon Science Media.*

New layout

The layout was converted to the larger DIN A4 format, to visualise the step from the yearbook to the journal. The print space amounts to 17.2 x 26 cm and the column width always 8.4 cm. So we have more flexible scopes for design and the process of production is more efficient. This process is resource-conserving and mostly carbon neutral. The future used paper is certified with the environmental test seal *Blauer Engel.*

Open Access

Prospectively, the PDF data files of the full issue and of the single articles are available on the internet. You can read it online, locally on your computer, e-reader or smartphone.

The digital publication is free for all users in the sense of a really *Open Access.* This publication-paradigm was formulated in 2003 in the *Berlin Declaration on Open Access to Knowledge in the Sciences and Humanities.* It is supported by all large German research institutions as well as by the *German Research Foundation* and the *Conference of University Presidents.*

The advantages of an *Open Access*-publication are the faster availability, wider distribution and higher citation rates, as studies document. For that purpose, all articles in the *Quaternary Science Journal* receive a DOI-number. This *Digital Object Identifier* enables the correct citation of an online-publication.

In addition, all articles are distributed under a *Creative-Commons-Licence.* This protects the rights of the authors and enables the free availability.

Webpage

At the URL *www.quaternary-science.net* you have access to the new journal page from September 2010. In addition to the download of PDF data files there are further productive features. E.g. you can see in a viewer all contents before you download the file and you can search the full text. Additional contents, e.g. basic data, interactive maps, photos, videos, lecture slides and other materials can be make available on the several publication page. Further there is a possibility for professional discussion or direct contact with the corresponding author via inbox system. By use of widgets – online function windows – every article is integratable into external webpages, e.g. your institutional webpage. This is possible without great programming effort. On these external webpages the main functions like viewer, download and order are directly available.

On the journal page you can format automatically the bibliographic data of an article into diverse citation styles. Special web technologies enable to transfer the publication data into one of the most important reference management software. Further it is possible to connect an article with bookmarking services and social networks.

If you want to submit a new article for the *Quaternary Science Journal* you can upload it directly in our submission system after you have login or create a first account. Afterwards you can look at your account the state of the peer review process. So it is no longer necessary to send articles by post.

In addition to the recent journal issues, you will find all back issues of the *Quaternary Science Journal* in an web archive and it is possible to use the full text free.

Geozon Science Media

The new publisher *Geozon Science Media* is a spin-off project of the *Department of Geography and Geology* of the *University of Greifswald*, Germany. The project was sponsored by the *European Union* and the *German Federal Ministry of Economics and Technology.* The aim of this sponsoring was to develop a modern *Open Access*-publication system for scientists.

This *Publication System for the Science* (PUBLISS) is a web-based application. It will enable an efficient multi-channel-publishing for scientific authors of the Earth Sciences and Environmental Sciences from September 2010. All essential services, e.g. proofreading, translation, layout, print, distribution and online archiving are bookable modularly according to requirements of the particular publication project. Furthermore a preview of the costs is available in real-time. In addition to hybrid books and journals it is possible to publish pure web documents via PUBLISS.

Holger Freund, Editor-in-chief E&G
Sascha Fricke, Geozon Science Media

Informationen zum neuen Publikationssystem

Mit der Ausgabe Nummer 2 des Jahrgangs 58 vollzieht sich eine markante Weiterentwicklung von *Eiszeitalter und Gegenwart.* Das traditionsreiche Wissenschaftsjournal erscheint mit dieser Ausgabe nicht nur im neuen Layout sondern erstmals als hybride Publikation – da neben der gedruckten auch eine elektronische Ausgabe veröffentlicht wird, welche unter dem *Open Access*-Paradigma steht.

Ziele dieser Veränderungen sind die weitere Professionalisierung des Journals und die Anpassung an die aktuellen Erfordernisse der internationalen Wissenschaftskommunikation. Damit sollen gleichzeitig auch die Anforderungen an eine Aufnahme in den *Science Citation Index* erfüllt werden. Dem Anliegen unserer Vereinigung, quartärwissenschaftliche Forschung zu fördern, möchten wir mit dieser modernen Publikationsform weitere Impulse geben. Dabei steht uns mit dem neuen Verlag *Geozon Science Media* ein innovativer und kompetenter Partner zur Seite.

Neues Layout

Das Layout wurde auf das größere DIN A4-Format umgestellt, um auch in der äußeren Form den Schritt vom Jahrbuch zum Journal sichtbar zu machen. Der Satzspiegel beträgt nun 17,2 x 26 cm und die Spaltenbreite jeweils 8,4 cm. Neben den flexibleren Gestaltungsmöglichkeiten bietet das neue Format auch einen effizienteren Produktionsprozess. Dieser wird ressourcenschonend und weitestgehend klimaneutral gestaltet. Das verwendete Papier ist mit dem Umweltsiegel *Blauer Engel* ausgezeichnet.

Open Access

Zukünftig stehen Ihnen die PDF-Dateien der Gesamtausgabe und darüber hinaus auch der einzelnen Artikel im Internet zur Verfügung. Sie können diese sowohl online als auch lokal auf Ihrem Computer, E-Reader oder Smartphone lesen.

Die digitale Publikation steht im Sinne eines echten *Open Access* kostenlos für alle Nutzer zur Verfügung. Dieses Publikations-Paradigma wurde bereits 2003 in der *Berliner Erklärung über offenen Zugang zu wissenschaftlichem Wissen* formuliert und wird mittlerweile von allen großen deutschen Forschungsinstitutionen sowie der *Deutschen Forschungsgemeinschaft* (DFG) und der *Hochschulrektorenkonferenz* (HRK) unterstützt.

Die Vorteile einer *Open Access*-Publikation liegen in der schnelleren Verfügbarkeit, größeren Verbreitung und – wie Studien belegen – höheren Zitationsrate. Zu diesem Zweck erhalten ab sofort alle Artikel in *Eiszeitalter und Gegenwart* eine eigene DOI-Nummer. Dieser *Digital Object Identifier* ermöglicht die korrekte Zitation einer Online-Publikation.

Weiterhin werden alle Beiträge unter einer *Creative Commons*-Lizenz vertrieben, was einerseits die Rechte der Autoren schützt und andererseits die freie Verfügbarkeit ermöglicht.

Online-Seite

Unter der URL *www.quaternary-science.net* haben Sie ab September 2010 Zugriff auf die neue Journal-Seite im Internet. Die Onlinepräsenz bietet neben dem Download der PDF-Dateien weitere produktive Features. So können Sie in einem Viewer alle Inhalte vor dem Download ansehen und den Volltext durchsuchen. Ergänzende Inhalte, wie z.B. umfangreiche Basisdaten oder interaktive Karten sowie Fotos, Videos, Vortragsfolien oder andere Materialien können direkt auf der jeweiligen Publikationsseite verfügbar gemacht werden. Ebenso besteht die Möglichkeit zur fachlichen Diskussion oder zum direkten Kontakt mit dem korrespondierenden Autor via Inbox-System. Über ein Widget – ein Online-Funktionsfenster – kann jeder Artikel ohne großen Programmieraufwand in externe Webseiten, z.B. Ihre Instituts- oder Projekt-Seite, eingebunden werden. Die Hauptfunktionen, wie Viewer, Download und Bestellung, sind durch diese technische Lösung dann dort direkt verfügbar.

Auf der Journal-Seite können Sie die bibliographischen Angaben eines Artikels automatisch in diverse Zitationsstile formatieren. Spezielle Webtechnologien ermöglichen es mit einem Klick die Publikationsdaten in eines der führenden Literaturverwaltungsprogramme zu übernehmen. Ebenso besteht die Möglichkeit, einen Artikel mit Bookmarking-Diensten oder Sozialen Netzwerken zu verknüpfen.

Wenn Sie einen neuen Artikel für *Eiszeitalter und Gegenwart* einreichen möchten, können Sie diesen, nach dem Login oder der erstmaligen Anlage eines Accounts, direkt in unser Submission System hochladen. Den Stand des Begutachtungsprozesses können Sie anschließend in Ihrem Account einsehen. Die postalische Einsendung von Ausdrucken entfällt somit.

Neben den aktuellen Journal-Ausgaben wird ein Online-Archiv nach und nach alle bisher erschienen Jahrgänge von *Eiszeitalter und Gegenwart* im Volltext erschließen und frei verfügbar machen.

Geozon Science Media

Der neue Verlagspartner *Geozon Science Media* ist ein Ausgründungsprojekt des *Institutes für Geographie und Geologie der Universität Greifswald.* Das Projekt wurde von der *Europäischen Union* und dem *Bundesministerium für Wirtschaft und Technologie* gefördert, mit dem Ziel ein modernes *Open Access*-Publikationssystem für Wissenschaftler zu entwickeln.

Dieses *Publication System for the Science* (PUBLISS) wird ab September 2010 als webbasierte Applikation wissenschaftlichen Autoren aus den Fachbereichen der Geo- und Umweltwissenschaften ein effizientes Multi-Channel-Publishing ermöglichen. Alle wesentlichen Services, wie z.B. Korrektorat, Übersetzung, Layout, Druck, Vertrieb und Online-Archivierung, können modular entsprechend den Anforderungen des jeweiligen Publikationsprojektes gebucht werden. Eine Kostenvorschau in Echtzeit sorgt dabei für die nötige Transparenz. Neben hybriden Büchern und Journals können via PUBLISS auch reine Web-Dokumente publiziert werden.

Holger Freund, Schriftleiter E&G
Sascha Fricke, Geozon Science Media

Instruction to Authors

Basically the manuscript shall be submitted in electronic form and has to include the name and the address of the first author. Please use a standard word processor in .rtf, .odt or .doc-format (LaTeX files on request). As character set please use the standard fonts Times Roman, Helvetica or Courier with 1.5 line spacing.

Please e-mail the manuscript to: *submission@quaternary-science.net*. If your manuscript files have more than 100 MB please contact the technical editor in advance. From September 2010 our Online Submission System is available at *www.quaternary.science.net* with comfortable upload function.

Manuscript style

The acceptable languages are English and German. Manuscripts in German have to contain an English subtitle, an abstract in English and English keywords. The rules of the new German spelling reform apply to German texts.

Manuscripts should be arranged in the following order:

I   Short but concise title
II Full names, full address and e-mail
III 5 to 10 keywords that describe the contents of your paper
VI An abstract of up to 200 words in German and English. The translated abstract should carry the translated titel in square brackets,
V   Clearly structured text. For chapter numbering use Arabic numerals.
VI The reference list has to be arranged alphabetically and should be conform to the examples given below.

References have to be insert in the text as brief quotations, the name of the author has to be set in small CAPITALS, the year of publication in brackets e.g. MÜLLER (2006). If more than one publication of the same author in the same year is cited, identify each citation as follows: MÜLLER (2006a, 2006b). Where three or more authors are listed in the reference list, please cite in the text as MÜLLER et al. (2006). Papers with up to three authors should be cited as MÜLLER & MEYER (2006) or MÜLLER, MEYER & SCHULZ (2006). If a special page or figure of a paper should be cited, use following citation style: MÜLLER (2006: 14) or MÜLLER (2006, Fig. 14).

Scientific names of flora and fauna (*gender, sub-gender, species, sub-species*) have to be written in *italics*. Use small CAPITALS for the author (*Armeria maritima* WILLD.)

Do not justify your text, use a ragged left alignment.
Do not use automatic hyphenation.
Do not use any automatic formatting.
Do not use pagination.

Do not insert images, tables and photos into the text, it should be added as separate files. Captions of figures and tables in German and English should be placed at the end of the manuscript.

Illustrations

Supply each figure as a separate file with the name of the author. Illustrations should be reducible to a column width (8.4 cm) or type area (17.2 x 26 cm). The lettering has to be easy readable after reduction. Where a key of symbols is required, include this in the figure, not in the caption of the figure. Avoid fine lines (hairlines) and grey-shading/halftones. All figures may be colored. There are no additional costs.

For printing all illustrations have to be supplied electronically. Please use for pixel-based images (photos) the .tif-format with a resolution of at least 450 dpi and for vector-based illustrations (graphs, maps, tables) the .eps-format. Greatly reduced .jpg-files or .pdf-files or figures included in word-documents are not accepted.

References (examples)

Papers:
SCHWARZBACH, M. (1968): Neue Eiszeithypothesen. – Eiszeitalter und Gegenwart, 19: 250–261.
EISSMANN, L. & MÜLLER, A. (1979): Leitlinien der Quartärentwicklung im norddeutschen Tiefland. – Zeitschrift für Geologische Wissenschaften, 7: 451–462.
ZAGWIJN, W.H. (1996): The Cromerian Complex Stage of the Netherlands and correlation with other areas in Europe. – In: TURNER, C. (ed.): The Middle Pleistocene in Europe: 145–172; Rotterdam (Balkema).
MAGNY, M. & HAAS, J.N. (2004): A major widespread climatic change around 5300 cal. yr BP at the time of the Alpine Iceman. – Journal of Quaternary Science, 19: 423–430. DOI: 10.1002/jqs.850

Books:
EHLERS, J. (1994): Allgemeine und historische Quartärgeologie. – 358 S.; Stuttgart (Enke).

Please do not use abbreviations of the journal names.

Specimen copies

Authors receive 2 printed specimen copies. The electronic version is available as download free.

For further questions about the submission of manuscripts please contact the production editor.

Autorenhinweise

Das Manuskript ist grundsätzlich in elektronischer Form einzureichen und muss mit Namen und Adresse des Erstautoren versehen sein. Bitte benutzen Sie eine Standard-Textverarbeitung im .rtf, .odt oder .doc-Format (LaTeX-Dateien auf Anfrage). Als Zeichensatz verwenden Sie bitte die Standard-Fonts Times Roman, Helvetica oder Courier mit einem 1,5-fachen Zeilenabstand.

Senden Sie das Manuskript per E-Mail an: *submission@quaternary-science.net* Bei einer Gesamtgröße der Manuskriptdateien über 100 MB kontaktieren Sie bitte vorab die technische Redaktion (s. Impressum). Ab September 2010 steht Ihnen auch unser Online Submission System unter *www.quaternary.science.net* mit einer komfortablen Upload-Funktion zur Verfügung.

Manuskriptform

Als Publikationssprachen sind Englisch und Deutsch zugelassen. Manuskripte in deutscher Sprache müssen einen englischen Untertitel tragen sowie eine englische Kurzfassung und englische Keywords beinhalten. Für die deutschen Texte gelten die Regeln der neuen Rechtschreibreform.

Die Manuskripte sollen folgendem Aufbau entsprechen:
I   Kurze, aber prägnante Überschrift
II Ausgeschriebener Vor- und Nachname, Post- und E-Mail-Adresse
III 5 bis 10 englische Keywords, die den Inhalt des Manuskriptes widerspiegeln.
IV Deutsche und englische Kurzfassung des Textes mit einer Länge von bis zu 200 Wörtern. Der englische Untertitel des Manuskriptes ist der englischen Kurzfassung in eckigen Klammern voranzustellen.
V   Klar gegliederter Text. Kapitelnummerierungen sind mit arabischen Ziffern zu versehen.
VI Alphabetisch geordnete Literaturliste. Die Zitierweise muss der unten angegebenen Form entsprechen.

Im fortlaufenden Text sind Literaturhinweise als Kurzzitate einzufügen, der oder die Autorennamen sind in Kapitälchen-Schrift zu setzen, das Erscheinungsjahr in Klammern, z. B. Müller (2006). Werden von einem Autor mehrere Arbeiten aus einem Jahr zitiert, so sind diese durch Buchstaben zu unterscheiden: Müller (2006a, 2006b). Bei mehr als drei Autoren kann et al. verwendet werden: Müller et al. (2006). Arbeiten mit bis zu drei Autoren werden folgendermaßen zitiert: Müller & Meyer (2006) oder Müller, Meyer & Schulz (2006). Sind mit der Zitierung bestimmte Seiten oder Abbildungen gemeint, müssen diese genau angegeben werden: Müller (2006: 14) oder Müller (2006: Fig. 14).

Die wissenschaftlichen Namen von Pflanzen und Tieren (*Gattungen, Untergattungen, Arten, Unterarten*) sind kursiv zu schreiben. Die den biologischen Namen folgenden Autoren werden in Kapitälchen gesetzt (*Armeria maritima* Willd.).

Bitte keinen Blocksatz verwenden, sondern einen linksbündigen Satz.
Bitte keine automatische Silbentrennung verwenden.

Bitte alle automatischen Formatierungen in Ihrer Textbearbeitung deaktivieren.
Bitte keine Seitenzählung.

Abbildungen, Tabellen und Fotos nicht in den Text einbauen, sondern separat als Datei beifügen. Abbildungsunterschriften in Deutsch und Englisch am Ende des Manuskripttextes platzieren.

Abbildungen

Bitte fügen Sie jede Abbildung als separate Datei mit einem eindeutigen Namen bei. Alle Grafiken müssen eine Verkleinerung auf Spaltenbreite (= 8,4 cm) oder Satzspiegel (= 17,2 x 26 cm) zulassen. Die Beschriftung muss nach der Verkleinerung noch gut lesbar sein. Sollte eine Legende nötig sein, so binden Sie diese in die Abbildung ein. Bitte vermeiden Sie Haarlinien oder Grauwerte. Alle Abbildungen können farbig sein. Es entstehen keine Mehrkosten.

Für die Drucklegung müssen alle Abbildungen in elektronischer Form eingereicht werden. Bitte verwenden Sie für pixelbasierte Abbildungen (Fotos) das .tif-Format mit einer Auflösung von mindestens 450 dpi und für vektorbasierte Abbildungen (Diagramme, Maps, Tabellen) das .eps-Format. Stark reduzierte .jpg oder .pdf-Dateien sowie in Text-Dokumente eingebundene Abbildungen werden nicht akzeptiert.

Zitierweise (Beispiele)

Aufsätze:
Schwarzbach, M. (1968): Neue Eiszeithypothesen. – Eiszeitalter und Gegenwart, 19: 250–261.
Eissmann, L. & Müller, A. (1979): Leitlinien der Quartärentwicklung im norddeutschen Tiefland. – Zeitschrift für Geologische Wissenschaften, 7: 451–462.
Zagwijn, W.H. (1996): The Cromerian Complex Stage of the Netherlands and correlation with other areas in Europe. – In: Turner, C. (ed.): The Middle Pleistocene in Europe: 145–172; Rotterdam (Balkema).
Magny, M. & Haas, J.N. (2004): A major widespread climatic change around 5300 cal. yr BP at the time of the Alpine Iceman. – Journal of Quaternary Science, 19: 423–430. DOI: 10.1002/jqs.850

Monographische Werke, Bücher:
Ehlers, J. (1994): Allgemeine und historische Quartärgeologie. – 358 S.; Stuttgart (Enke).

Bitte keine Abkürzungen der Zeitschriftentitel verwenden.

Belegexemplare

Autoren erhalten 2 gedruckte Belegexemplare. Die elektronische Version steht zum kostenlosen Download zur Verfügung.

Bei weiteren Fragen zur Manuskripteinreichung wenden Sie sich bitte an die technische Redaktion (s. Impressum).

DEUQUA

German Quaternary Association

The German Quaternary Association (DEUQUA) eV is an association of German-speaking Quaternary Scientists. The aim of the association is to promote the Quaternary Science, to represent it in public, to intensify the contact to applied science as well as to advice public and political boards in quatarnary issues.

Furthermore, the association has set itself the task of operating the contacts between the Quaternary Scientists and related organizations at home and abroad.

The DEUQUA published annually several editions of "E&G – Quaternary Science Journal". In that journal research results from the field of Quaternary Science are published. In addition, developments in the DEUQUA are announced in the "Geoscience messages" (GMIT). GMIT is published quarterly.

Every two years, the German Quaternary Association held the DEUQUA-Conference. At this conference the latest research results of the Quaternary Science are presented and discussed.

Deutsche Quartärvereinigung

Die Deutsche Quartärvereinigung (DEUQUA) e.V. ist ein Zusammenschluss deutschsprachiger Quartärwissenschaftler und wurde 1949 gegründet. Der Verein hat zum Ziel die Quartärwissenschaft zu fördern, sie in der Öffentlichkeit zu vertreten, den Kontakt zu angewandter Wissenschaft zu intensivieren sowie öffentliche und politische Gremien in quartärwissenschaftlichen Fragestellungen zu beraten. Desweiteren hat der Verein sich zur Aufgabe gemacht, die Kontaktpflege der Quartärforscher untereinander und zu verwandten Organisationen im In- und Ausland zu betreiben.

Die DEUQUA veröffentlicht jährlich mehrere Ausgaben von „Eiszeitalter und Gegenwart – Quaternary Science Journal". Dort werden Forschungserkenntnisse aus dem Bereich der Quartärwissenschaft publiziert. Zusätzlich werden Entwicklungen in der DEUQUA vierteljährlich in den Geowissenschaftlichen Mitteilungen (GMIT) bekannt gemacht.

Im zweijährigen Turnus veranstaltet die Deutsche Quartärvereinigung e.V. die DEUQUA-Tagung. Diese bietet ein Forum, in welchem aktuelle Forschungsergebnisse aus dem Bereich der Quartärwissenschaften vorgestellt und diskutiert werden.

Committee / Vorstand

PRESIDENT / PRÄSIDENTIN
PROF. DR. MARGOT BÖSE
Freie Universität Berlin
Malteserstr. 74–100
D-12249 Berlin, Germany
Tel.: +49 (0)30-838-70 37 3
E-Mail: m.boese [at] fu-berlin.de

VICE PRESIDENTS / VIZEPRÄSIDENTEN
PROF. DR. MARKUS FIEBIG
Department für Bautechnik und Naturgefahren
Institut für Angewandte Geologie
Universität für Bodenkultur
Peter Jordan Str. 70
A-1190 Wien, Austria
Tel.: +43-1-47654-54 02
E-Mail:markus.fiebig [at] boku.ac.at

PROF. DR. REINHARD LAMPE
Institut für Geographie und Geologie
Ernst-Moritz-Arndt-Universität Greifwald
Friedrich-Ludwig-Jahn-Strasse 16
17487 Greifswald, Germany
Tel: +49 (0)3834-86-45 21
E-Mail: lampe [at] uni-greifswald.de

TREASURER / SCHATZMEISTER
DR. JÖRG ELBRACHT
Landesamt für Bergbau, Energie und Geologie
Stilleweg 2
D-30655 Hannover, Germany
Tel.:+49 (0)511-643-36 13
E-Mail: Joerg.Elbracht [at] lbeg.niedersachsen.de

EDITOR-IN-CHIEF / SCHRIFTLEITUNG (E&G)
PD DR. HOLGER FREUND
ICBM – Geoecology
Carl-von-Ossietzky Universitaet Oldenburg
Schleusenstr 1
D-26382 Wilhelmshaven, Germany
Tel.: +49 (0)4421-94 42 00
E-Mail: holger.freund [at] icbm.terramare.de

ARCHIVIST / ARCHIVAR
DR. STEFAN WANSA
Landesamt für Geologie und Bergwesen
Sachsen-Anhalt
Postfach 156
D- 06035 Halle, Germany
Tel. +49 (0)345-5212-12 7
E-Mail: wansa [at] lagb.mw.sachsen-anhalt.de

ADVISORY BOARD / BEIRAT
DR. CHRISTIAN HOSELMANN
Hessisches Landesamt für Umwelt und Geologie
Postfach 3209
D-65022 Wiesbaden, Germany
Tel.: +49 (0)611-69 39 92 8
E-Mail: Christian.Hoselmann [at] hlug.hessen.de

DR. DANIELA SAUER
Institut für Bodenkunde und Standortslehre
Emil-Wolff-Str. 27
D-70593 Stuttgart, Germany
Tel.: +49 (0)711-459-22 93 5
E-Mail: d-sauer [at] uni-hohenheim.de

DR. FRANK PREUSSER
Geolog. Institut der Universität Bern
Baltzerstr. 1–3
CH-3012 Bern, Switzerland
Tel.: +41-31-631 87 70
E-Mail: preusser [at] geo.unibe.ch

DR. JÜRGEN REITNER
Geologische Bundesanstalt
Neulinggasse 38
A-1031 Wien, Austria
Tel.: +43-1-7125674-24 2
E-Mail: juergen.reitner [at] geologie.ac.at

PROF. DR. BIRGIT TERHORST
Geographisches Institut
der Universität Würzburg
Am Hubland
97074 Würzburg, Germany
Deutschland
Tel. +49 (0)931-88 85 58 5
E-Mail: birgit.terhorst [at] uni-wuerzburg.de

Reorder / Nachbestellung

The volumes 6–7, 11–17, 19–28 and 30–58 are currently available. All other volumes are sold out. A reduced special price of 10,– € per edition is up to and including volume 55. The regular retail price applies from vol. 56/1–2. A complete table of contents is downloadable at *www.deuqua.org*.

1951–2006

Vol. 6–7, 11–17, 19–28, 30–55	each volume 10,– €

2007	**Topics**	**Price**
Vol. 56 No 1–2	Special issue: Startigraphie von Deutschland – Quartär	54,– €
Vol. 56 No 3	Pfälzerwald, pollen types and taxa, Oberösterreich, Riß-Iller, Schatthausen	27,– €
Vol. 56 No 4	Nußloch, Rangsdorfer See, Lieth/Elmshorn, Gardno Endmoräne/Debina Cliff	27,– €

2008	**Topics**	**Price**
Vol. 57 No 1–2	Special issue: Recent progress in Quaternary dating methods	54,– €
Vol. 57 No 3–4	Special issue: The Heidelberg Basin Drilling Project	54,– €

2009	**Topics**	**Price**
Vol. 58 No 1	Surface Exposure Dating, Bodensee, Living Fossil, Hochgebirgsböden	27,– €
Vol. 58 No 2	Special issue: Changing environments – Yesterday, Today, Tomorrow	27,– €

The prices are understood plus shipping costs. VAT is included.

Contents